A PROTEOMIC INVESTIGATION OF BOTULINUM TOXIN SEROTYPE A PROTEIN-PROTEIN INTERACTIONS AT THE MAMMALIAN NEUROMUSCULAR JUNCTION

by

TONIA M. PARROTT

(Under the Direction of Julie A. Coffield)

ABSTRACT

Botulinum toxin is one of the most toxic substances known to man. Ironically, it is the toxin's specificity for cholinergic nerve terminals, its ubiquitous nature, and extremely low effective dose that has resulted in its use as a valuable therapeutic tool while at the same time earning it a place on the CDC's list of biological weapons. While early studies have developed a model regarding the toxin's mode of action, little is understood regarding intoxication involving cellular receptors at the physiological target, the mammalian neuromuscular junction. The first step toward identification of these receptors involves the ability to isolate a fraction rich in neuromuscular proteins. Earlier studies in our laboratory utilized a mouse diaphragm preparation to study substrate proteolysis. For receptor identification, it was important to determine whether this preparation would also serve as an adequate model of a "synaptosome." After demonstrating that this preparation contained proteins common to both pre- and post-synaptic machinery, it was utilized in an affinity precipitation with beads coated with botulinum toxin serotype A. Proteins from this precipitation were identified utilizing tandem mass spectrometry. Most of the identified proteins were intracellular proteins

that, while not serving as the toxin protein receptor, may be involved in intracellular toxin interactions. In the process, several peptides were also isolated that corresponded to conserved domains within growth factor receptors. Using antibodies to several growth factors, we were able to identify two growth factors in particular that demonstrated selective binding to toxin. These receptors were identified as Nogo-66 receptor isoform 2 (NGR2), and Fibroblast growth factor receptor III (FGFR3). Interestingly, both proteins have been shown to have roles in either neurogenesis or axonal development, which is a significant characteristic of botulinum toxin A intoxication. Both of these proteins have also been known to interact with complex gangliosides and to participate in lipid raft signaling. In these studies, we have identified two possible candidates in the binding of Botulinum toxin serotype A at the nerve cell terminal.

INDEX WORDS: Botulinum Toxin Serotype A, Neuromuscular Junction, Proteomics, Nogo-66 receptor (II), Fibroblast growth factor III.

A PROTEOMIC INVESTIGATION OF BOTULINUM TOXIN SEROTYPE A PROTEIN-PROTEIN INTERACTIONS AT THE MAMMALIAN NEUROMUSCULAR JUNCTION

by

TONIA M. PARROTT

B.S., University of Michigan-Flint, 1991

A Dissertation Submitted to the Graduate Faculty of The University of Georgia in Partial Fulfillment of the Requirements for the Degree

DOCTOR OF PHILOSOPHY

ATHENS, GEORGIA

2005

A PROTEOMIC INVESTIGATION OF BOTULINUM TOXIN SEROTYPE A PROTEIN-PROTEIN INTERACTIONS AT THE MAMMALIAN NEUROMUSCULAR JUNCTION

by

TONIA M. PARROTT

Major Professor: Julie Coffield

Committee: Phillip Greenspan
Arthur Grider
Cham Dallas

Electronic Version Approved:

Maureen Grasso
Dean of the Graduate School
The University of Georgia
December 2005

DEDICATION

This is dedicated to my parents who inspired me to dream bigger and strive for more; my husband Dominic, whose love and support helped me to make the dream a reality; and my sister Lisa and her family Phil, Vasa and Finn for their love and encouragement. I would like to thank all of my dear friends who could always make me laugh. Words cannot express how much I appreciate all of you.

ACKNOWLEDGEMENTS

I would like to acknowledge my professor and friend Dr. Julie Coffield for the support, knowledge, and inspiration that she has given to me. I would also like to thank Paula, Dee, Kimberly, Kristen, Ashwini, Neely, and Zane for their help, patience, and laughter. Finally, I would like to acknowledge my committee members Phillip Greenspan, Arthur Grider, and Cham Dallas for the guidance and knowledge that they have given me throughout my graduate career. It has been a wonderful “learning experience.”

TABLE OF CONTENTS

Page

ACKNOWLEDGEMENTS v

LIST OF TABLES vii

LIST OF FIGURES ix

CHAPTER

1 INTRODUCTION AND LITERATURE REVIEW 1

2 ISOLATION AND IDENTIFICATION OF SYNAPTIC PROTEINS IN A NEUROMUSCULAR ENRICHED MURINE DIAPHRAGM PREPARATION 39

3 THE USE OF PROTEOMIC TECHNIQUES TO ISOLATE AND IDENTIFY BOTULINUM TOXIN SEROTYPE A BINDING PROTEINS 79

4 IDENTIFICATION OF TWO GROWTH FACTOR RECEPTORS THAT DEMONSTRATE BINDING TO BOTULINUM TOXIN SEROTYPE A 131

5 CONCLUSION 163

LIST OF TABLES

Page

Table 2.1: MS/MS identification of spots enriched in either hydrophobic (H1) or hydrophilic (H3) fractions 57-58

Table 2.2: Proteins identified by LC-MS-MS 59-61

Table 2.3: Table of western blots: Antibodies & fractions tested 62-63

Table 2.4: Additional proteins identified by western blots 64

Table 3.1: Identification of spots selected from control precipitation of H_1 detergent fraction illustrated in Figure 3.3a 103

Table 3.2: Identification of spots selected from toxin precipitation of H_1 detergent fraction from Figure 3.3b and 3.4a 104

Table 3.3: Identification of selected spots from matched H_1 hydrophobic P_3 fraction illustrated in Figure 3.5 105

Table 3.4: Identification of selected spots from matched H_3 hydrophilic P_3 fraction illustrated in Figure 3.6 106

Table 3.5: Identification of selected spots from matched P_3 sample illustrated in Figure 3.7 107

Table 3.6: Identification of 1D bands of rabbit P_3 hydrophobic fraction precipitations as illustrated in Figure 3.8a and 3.8b 108-109

Table 3.7: Identification of 1D bands of rabbit P_3 hydrophilic fraction precipitations as illustrated in Figure 3.9a and 3.9b 110-111

Table 3.8: Proteins identified directly from toxin precipitations of mouse P_3 not subjected to electrophoresis 112

Table 4.1: Growth factor receptors tested for toxin binding 150

LIST OF FIGURES

Page

Figure 2.1: 65-66

Figure 2.2: 67-68

Figure 2.3A and 2.3B: 69-70

Figure 2.4: 71-72

Figure 2.5A and 2.5B: 73-74

Figure 2.6: 75-76

Figure 2.7: 77-78

Figure 3.1A, 3.1B, 3.1C: 113-114

Figure 3.2: 115-116

Figure 3.3A and 3.3B: 117-118

Figure 3.4A and 3.4B: 119-120

Figure 3.5: 121-122

Figure 3.6: 123-124

Figure 3.7: 125-126

Figure 3.8: 127-128

Figure 3.9: 129-130

Figure 4.1A and 4.1 B: 151-152

Figure 4.2: 153-154

Figure 4.3A and 4.3B: 155-156

Figure 4.4: 157-158

Figure 4.5A and 4.5B: 159-160

Figure 4.6: 161-162

CHAPTER 1

INTRODUCTION AND LITERATURE REVIEW

BACKGROUND

Botulinum toxin (BoNT), with a mouse oral LD_{50} of 1μg/kg body weight, is one of the most poisonous substances known to man (see review by Arnon, 2001). The symptoms of botulism, flaccid muscle paralysis, were first described by Justinus Kerner in people who had ingested spoiled sausage (Ergbuth et al., 1999). In the late 1800s, developments in microbiological techniques relevant to anaerobic bacterial isolation and culture allowed van Ermengem to identify the causative agent of Botulism as a gram positive rod now termed *Clostridium Botulinum* (van Ermengem, 1897). It was later demonstrated that like other anaerobic bacteria, *Clostridium* species were spore-forming, toxin producers, with the toxin being isolated and purified shortly after WWII (Schantz and Johnson, 1997). Later it was determined that the toxin is produced as seven distinct serotypes (termed A-G) and that, in addition to *C. botulinum*, C *butryicum* and *C. baratii* also produce BoNT serotypes E and F, respectively (see review by Collins and East, 1998). *C. botulinum* alone is capable of producing all seven serotypes of toxin and individual cultures may produce more than one serotype (Shapiro et al., 1998). Burgen, Dichens, and Zatman (1949) demonstrated that these neurotoxins exhibited a selective toxicity for cholinergic nerve terminals and blocked release of acetylcholine at the neuromuscular junction.

Since its discovery, BoNT has experienced a rapidly evolving role in regard to public health and clinical medicine. Even with improved food quality standards, intoxication following the accidental ingestion of either the toxin itself, or toxin-producing bacteria, is the leading cause of botulism. Infant botulism, in which the bacterium actually colonizes the gut epithelia, has been implicated in many infant deaths. The

most well known incident of this occurred in babies fed non-pasteurized honey (Arnon et al., 1979).

The unique ability of BoNT to selectively target cholinergic nerve activity led to the development of its use for the treatment of spasticity disorders. Botulinum serotype A (BoNT/A) was first tested in 1973 as a treatment for strabismus (Scott et al., 1973). In this study, extremely low doses of BoNT/A were injected into the extraocular muscles of affected monkeys and successfully inhibited involuntary eye movements. Serotype A (trade name BOTOX™) later went on to receive FDA approval for treatment of not only strabismus, but also a number of other debilitating and painful disorders including blepharospasm and hemifacial spasms (Brin et al., 1987; Binder et al., 2000).

Recognizing the pharmacological benefits of BoNT, physicians began using the toxin to treat a variety of conditions ranging from migraines and cerebral palsy to the relaxation of facial wrinkles (Jankovic and Brin, 1997). The FDA later approved the use of BOTOX™ for the treatment of wrinkles in 2002. Although relatively rare, the clinical use of botulinum can result in complications, including the development of immunoresistance and non-targeted muscle paralysis (Bhatia et al., 1997; Eleopra et al., 1996). More recently, four cases of botulism, stemming from the illegal injection of patients by physicians using research grade toxin (much more potent than BOTOX™) illustrates one of the concerns associated with the growing popularity of the clinical use of BoNT.

Research funded by the US government in the 1940s and 1950s demonstrated that, even then, there was worldwide recognition that BoNT could be used as a potential biological warfare agent. The United States, along with several other countries including

the then U.S.S.R., and later, other smaller countries such as Syria developed and produced BoNT as a biological weapon (Arnon et al., 2001; Bozheyeva et al., 1999). Individual groups have also attempted to utilize BoNT to incite terror, including the Aum Shinrikyo cult (sarin gas attack on Tokyo train) who attempted unsuccessfully to release BoNT in Tokyo (Shapiro et al., 1998).

There are several characteristics that make the toxin an attractive biological weapon: the toxin-producing bacteria occur naturally in the environment, the toxin is fairly easy to produce and isolate, and due to its extreme potency, only a small amount is needed thereby making it easy to transport. The discoveries that intoxication could occur through inhalation and that the extrapolated human inhalational LD_{50} was 0.7-0.9 μg/kg demonstrated that in the appropriate environment intentional dispersal of 1 g of purified toxin could kill at least one million people (Arnon et al., 2001).

There is no effective treatment for botulism, with death resulting from respiratory failure through paralysis. Anti-toxin therapy is available but is most efficacious when administered prior to symptoms onset. An unlicensed vaccine is available for military and laboratory workers, but its efficacy as measured by immunoglobulin titer is questionable, and it is considered impractical for general immunization. For these reasons, the Centers for Disease Control and Prevention has categorized the toxin as one of six select agents with the greatest potential of being used as a bio-terror weapon. In light of these factors, the identification of cellular pathways involved in toxin action is clearly an important research endeavor.

Regardless of its use, BoNT's mode of action requires that it crosses several cellular and intracellular membranes. The toxin itself is not directly cytotoxic. For

example, it does not kill cells upon contact. Instead, it is thought that the toxin utilizes existing cellular processes and proteins that are involved in normal cellular activities such as transcytosis and endocytosis in order to reach its sight of action (Simpson, 2004). This introduction focuses on what is known about BoNT action and its protein interactions, as well as, brings to the readers' attention areas where research is limited. This introduction also explores the field of proteomics, the newest frontier for the study of protein-protein interactions, and the promise it holds for identification of unknown protein partners. Finally, a number of issues associated with this emerging field in regard to identifying protein-protein interactions at the cellular membrane are discussed.

BOTULINUM TOXIN STRUCTURE AND FUNCTION

BoNT is initially produced by bacterial strains as a 300-900 kDa protein complex. This complex, or progenitor toxin, is made up of a 150 kDa holotoxin as well as serotype specific hemagglutinin and non-hemagglutinin components (Dasgupta and Sugiyama, 1972). These non-toxic components are thought to protect the holotoxin from the harsh acidic, proteolytic environment in the stomach. Oral toxicity studies have demonstrated that there is a large increase in toxicity between the pure holotoxin and the 900 kDA progenitor toxin (Oshishi et al., 1977). However, discrepancies regarding the role of the non-toxin components in binding and GI adhesion remain unresolved. Research has suggested that the intestinal binding domain for BoNT is present in the non-toxic hemagglutinin components (Fujinaga et al., 1997). In contrast, other studies demonstrate that the non-toxin complexes are not required for absorption of the toxin from the small intestine. These latter studies demonstrated that at low toxin concentrations the toxicity of pure toxin was slightly decreased from that of the

complexed toxin; however, at higher doses this difference in toxicity disappeared. This suggests that at lower concentrations the non-toxic components act to protect the toxin, allowing for enough toxin to be absorbed and transported to its site of action; as the exposure dose increases this protection is no longer necessary to ensure that enough toxin survives the gut to produce symptoms (Maksymowych et al., 1999).

The holotoxin is initially produced as a single chain 150 kDa protein. This chain is usually nicked by proteases within the bacteria into a 100 kDa heavy chain connected by disulfide bond to a 50 kDa light chain (Lacy et al., 1998). The heavy chain is further divided into an n-terminal domain (H_N) and a c-terminal domain (H_C). The H_N domain has a coiled coil domain similar to those found in other pore-forming viruses such as influenza (Lacy et al., 1998; Bullough et al., 1994). It is thought that this domain is responsible for channel formation within endosomes that allow the light chain to move into the cytosol. Evidence suggests that this channel formation is pH-dependent, with channel formation occurring at low pH and more likely to form across a pH gradient. There is also evidence that these channels are charge-dependent, with differences in the charges required between gradient and non-gradient environments (Hoch et al., 1985). Research involving the mammalian neuromuscular junction also demonstrated that endosomal neutralization with methylamine hydrocholoride decreased both paralysis and substrate proteolysis by botulinum toxin serotype A (Kalandakanond and Coffield, 2001). These findings support the theory that toxin translocation requires acidification of endosomes, and that the resultant pH gradient is an important factor for channel formation.

The H_C domain is thought to function as the plasma membrane targeting domain. It consists of two subdomains known as the heavy chain n-terminal domain (Hc_n), and the heavy chain c-terminal domain (Hc_c). These domains may be referred to by their structural characteristics to avoid confusion. For example, the Hc_n domain exhibits a jelly roll motif found in lectins and is called the lectin-like domain, while the Hc_c region exhibits a β-trefoil motif common to proteins such as interleukin 1 and fibroblast growth factor (See review by Schiavo, 2000). Characterization of these subdomains provided support to the dual receptor theory proposed by Montecucco (1986). In this theory, it is hypothesized that the toxin would first bind to a low affinity receptor, initiating an alteration of the toxin structure that would promote binding to serotype specific high affinity protein receptors. Further investigation has led to the identity of the low affinity receptor which will be discussed in more detail later. The β-trefoil fold subdomain appears to be non-conserved among the BoNT serotypes; however, utilizing x-ray crystallography this subdomain has been shown to contain a highly conserved ganglioside binding pocket that is lined at the bottom with hydrophilic amino acids. The interdomain cleft formed between the lectin-like subdomain and the β-trefoil fold subdomain demonstrates less similarity in shape and electrostatic properties between the botulinum serotypes and therefore, has been hypothesized to contain the higher affinity receptor (Lacy et al., 1998; Ginalski et al., 1999; Swaminathan and Eswaramoorthy, 2000).

The toxin light chain is a 50 kDa domain that contains a zinc binding site characterized by the HExxH+E protein-protein interaction motif common to metalloproteases (Morante et al., 1996). Indeed, the light chains act as zinc

metalloproteases that exhibit substrate serotype specificity. The role of zinc in this activity has been hypothesized to be either structural, in which the zinc acts to maintain the structural conformation; or catalytic, in which the zinc atom is involved in the catalytic activity. In functional studies utilizing serotype B, zinc was able to be removed and reintroduced with corresponding changes in activity. These findings suggested that significant conformational changes in the toxin structure did not occur upon removal of zinc (Fillippis et al., 1995). X-ray crystallography studies support this finding, demonstrating that zinc removal has little impact on toxin structure (Eswaramoorthy et al., 2004).

SYNAPTIC VESICLE EXOCYTOSIS AND BOTULINUM TOXIN MECHANISM OF ACTION

Synaptic vesicles are formed from lipids and membrane proteins within the endoplasmic reticulum, and later modified within the Golgi of the neuronal somata. The vesicles are filled with neurotransmitter or precursors taken up at the nerve terminal (Lin and Scheller, 2000). Synaptic vesicles are thought to exist in three functional pools: the resting (storage) pool consisting of vesicles that are located away from the active zone attached to cytoskeletal elements, the readily releasable pool consisting of vesicles that are ‘docked’ at the active zone (Neher and Zucker, 1993; Xu et al., 1998) and a reserve pool that serves to replenish the ready releasable pool during prolonged activation (see review by Sudhof, 2004)

There are at least five steps for the release of transmitter to occur from vesicles recruited from the resting pool. The first step involves mobilization of the vesicle from the actin cytoskeleton. This process requires phosphorylation of proteins synapsin I

and myosin II by ATP, calcium calmodulin kinase II, and myosin light chain kinase. Other proteins such as microtubule-related proteins rab6 and kinesin motor proteins may also be involved (Kukamura et al., 1994; Mochida et al., 1994; Ryan 1999). Vesicles are then targeted to the active zone membrane through unknown proteins, possibly involving the Sec 6/8 complex, and other associated proteins including the septins. This complex, however, seems to be more highly concentrated in regions undergoing synaptogenesis (Guo, et al., 1999; Hazuka et al., 1999). Docking of the vesicles is then thought to occur through the Rab G-proteins and associated RIMs (Rab interacting molecule). This process involves the reversible attachment of the vesicle to the membrane, and precedes the involvement of SNARE [soluble NSF (n-ethylmaleimide sensitive factor) attachment protein receptor] proteins (Wang et al., 1997; see review by Südhof, 2001).

Other proteins that have been implicated in having potential roles in vesicle docking are the large scaffolding proteins, aczonin, and CASK. These proteins share similar features in that they are large proteins that consist of multiple functional domains all capable of protein-protein interactions (tom Dieck et al., 1998; Wang et al., 1999). For example CASK, a MAGUK protein, contains PDZ, SH3, and calcium calmodulin domains, as well as a guanylate kinase domain, which have been shown to interact not only with presynaptic voltage-gated calcium channels, but also with Rabphilin 3a, and junctional adhesion molecules (Martinez-Estrada et al.,2001; Zhang et al., 2001). These different protein binding domains suggest a role in active zone organization. The protein scaffolding characteristics of these proteins could initiate docking, bringing the vesicle close enough to the membrane for SNARE interactions to occur.

The SNARE proteins consist of proteins known as t-SNAREs (target membrane) and v-SNAREs (vesicular membrane). Syntaxin I and SNAP-25 (synaptosomal protein of 25 kDa) are t-SNAREs. Both are found at the active zone membrane; syntaxin I has a c-terminal integral membrane domain, while SNAP-25 is membrane associated (Bennett et al., 1992; Oyler et al., 1989). The v-SNARE is synaptobrevin or VAMP (vesicle associated membrane protein) (Söllner et al., 1993b). VAMP has a c-terminal single transmembrane domain that anchors it to the vesicle membrane (Söllner et al., 1993b). At the active zone, these three proteins form the core fusion complex (the SNARE complex), an α-helical bundle consisting of four coiled-coil domains, one each contributed by syntaxin and VAMP and two from SNAP-25 (Sutton et al., 1998). This core complex mediates the fusion of the vesicular and active zone membranes in response to a Ca^{2+} signal, leading to the release of transmitter.

Priming of the SNARE complex involves ATP-dependent rearrangement of the SNARE complex to ensure that it is ready for Ca^{2+} dependent fusion. For example, while syntaxin and SNAP-25 are usually associated with the neuronal membrane, there are small amounts that are located on the vesicle membrane. These vesicular t-SNARE proteins can interact with each other forming a non-fusion competent *cis*-complex (Walch et al., 1995). Priming is thought to occur when ATP and NSF unwrap these *cis*-complexes and arrange them in a fusion competent *trans*-complex where SNAP-25 and syntaxin are both associated with the active zone membrane (Otto et al., 1997; Klenchin and Martin, 2000).

Membrane fusion occurs when calcium signaling initiates ‘zippering’ of the SNARE protein α-helices forming the core complex. Formation of this

thermodynamically more stable complex provides the energy that drives fusion of the two membranes (Sollner et al., 1993a). There are differing theories as to how these membranes fuse and reform, with most of the data coming from non-synaptic cells. In the first theory, known as “kiss and run”, the membranes do not fully fuse, instead, a fusion pore is generated and a small amount of material is released. The pore is then closed and the vesicle undocks from the membrane (Ceccarelli et al., 1973; Schneider, 2001). In the ‘full fusion’ model the membranes of the vesicle and active zone fuse completely, and the vesicular contents are fully expelled. The vesicle membrane is then recycled through endocytosis by clathrin-coated pits at sites that are distant from the exocytotic sites. The vesicles are then mixed with the existing pools (Heuser et al., 1973, Betz et al., 1992, Landis et al., 1988, Krazewski et al., 1996).

BoNTs have been useful tools in the study of vesicular exocytosis. The discovery that poisoned motor endplates still bound exogenously applied acetylcholine, and that muscle cells were still able to generate action potentials, demonstrated that the toxins were actually preventing neurotransmitter release (Burgen et al., 1949). It was not until several decades later when it was discovered that the toxin acts to inhibit the vesicular fusion machinery in a serotype specific manner. Serotypes B, D, F, and G all cleave the vesicular SNARE protein VAMP, although each serotype recognizes and cleaves at a specific site (Schiavo et al., 1992; 1993a; 1993c; 1994a; 1994b; Yamasaki et al., 1994a; 1994b; 1994c). Serotypes A and E cleave SNAP-25, and again each substrate cleavage site is serotype specific (Blasi et al., 1993a; Schiavo 1993a; 1993b). Serotype C is interesting in that it cleaves both SNAP-25 and syntaxin in the CNS, while at the

peripheral nerve terminal it cleaves syntaxin (Schiavo et al., 1994; Blasi et al., 1993b; Kalandakanond et al., 2001).

Once cleaved the SNARE proteins are either unable to form complexes or they form non-functional complexes. How long the active toxin exists in the cytosol is still debatable and may be dependent on the serotype. However, our laboratory found that there was little temporal correlation between paralysis and detectable substrate proteolysis, suggesting that only a small amount of SNARE cleavage is required to disrupt exocytotic function (Kalandakanond et al., 2001).

FROM EXPOSURE TO INTOXICATION: THE JOURNEY OF BOTUINUM TOXINS

Absorption from the gastrointestinal system and respiratory system

Toxin exposure can occur through three routes: ingestion, inhalation, and wound. Exposure is usually to the progenitor toxin and it is thought that these components act to protect the toxin against the harsh conditions of the stomach. Absorption of toxin in the alimentary tract occurs in increasing amounts as it moves through the tract with minute to small amounts being absorbed from the mouth and stomach (Bonventre, 1979). The majority of toxin absorption is thought to occur in the duodenum of the small intestine.

Early sedimentation studies suggested that the toxin is mainly absorbed into the lymph as a smaller fragment then the progenitor toxin (Heckly et al., 1960). Later studies have disagreed on whether or not the hemagglutinin portions actually bind and transcytose into the lymph. Studies utilizing rat and guinea pig intestinal epithelia suggest that the entire progenitor toxin is required to bind to the epithelial cells, and that disassociation occurs at pH greater than 7 (Suggi et al., 1977a; 1977b; Fuginaga et

al.,1997). Studies involving intestinal epithelial cells in vitro, however, demonstrate that pure toxin (no hemagglutinin) is able to bind, endocytose, transcytose, and still demonstrate toxicity (Maksymowych and Simpson, 1998). In these studies, the non-hemagglutinin non-toxic portion also appeared to be endocytosed, but remained in the cytosol of the cells suggesting little transcytosis of this fraction occurred.

Studies to determine the actual intestinal cell types responsible for toxin transport have yet to be published; however, it has been suggested that absorptive enterocytes rather than M cells are required (Simpson, 2004). An interesting feature of absorptive enterocytes that may prove important when studying BoNT binding is the fact that their apical brush border is composed of two different types of lipid raft domains. Lipid rafts are specialized membrane components with increased sphingolipid content that are enriched with GPI-anchored proteins. Lipid rafts have been implicated in many functions including vesicular sorting, membrane targeting, and cell signaling (Danielson, 2003).

Toxin movement across endothelial cells of the vasculature

Studies suggest that once the toxin crosses the intestinal epithelia it is concentrated in the lymph with only small amounts initially entering the bloodstream (Suggi et al., 1977b). The mechanism by which the toxin crosses from the bloodstream to the target tissue has not been studied. Macromolecular permeability of the endothelial microvasculature has been explained by several different mechanisms including passive diffusion through large pores, vesicular transport, and the creation of leaks by receptor-mediated activation of actin cytoskeleton rearrangement (Frokjaer-Jensin, 1984; Crone, 1986).

Toxin binding at the neuromuscular junction

In 1986, Simpson proposed a four step mechanism of action for BoNT. The toxin first binds to a serotype specific receptor; the toxin is then internalized through receptor-mediated endocytosis. Once in the endosome internal acidic conditions cause structural changes to the Hc_n portion of the toxin resulting in pore formation. The disulfide bond between the heavy and light chain is reduced and the light chain moves through the pore and into the cytosol, possibly chaperoned by the heavy chain. Once in the cytosol, the toxin binds and cleaves its substrate (Simpson, 1981). There are several studies supporting each of these postulated steps.

Seminal studies by Black & Dolly (1986) in which murine neuromuscular junctions were exposed to ^{125}I radiolabeled BoNT, demonstrated that receptors for BoNT were selectively located at the unmyelinated nerve terminal. It was also determined that the receptors were of low density, and that the density of binding was unique between serotypes, suggesting serotype specificity. Further, internalized radiolabeled toxin appeared to concentrate into endosomes supporting the theory of receptor-mediated endocytosis. Further studies using competitive binding of serotypes A, B, and E, demonstrated that binding of one serotype did not preclude binding of another, thereby supporting the hypothesis that each serotype has a specific high affinity receptor.

The first membrane constituents shown to bind BoNT were polysialogangliosides (van Heyningen, 1974). Early research demonstrated that these glycosphingolipid entities bound BoNTs, and that pre-incubation of toxin with gangliosides reduced toxicity of BoNT (Kitamura et al., 1980). Further, by pre-treating neural membranes with

ganglioside-binding lectins from Triticum Vulgaris or Limax flavus, Bakry and colleagues found that the binding of all serotypes of BoNT was reduced (1991). Gangliosides, however, are not likely to be the sole receptor, since they are ubiquitously expressed throughout the nervous system, and their binding toxin is reported to be of low affinity. This binding, however, may act to increase or facilitate the toxins exposure to the high affinity protein receptor site.

Several studies utilizing brain synaptosomes have identified a few different proteins that seemed to demonstrate binding to BoNTs. Initial binding experiments utilizing SDS-PAGE, identified a pair of doublets, one at ~80 kDa and the other at ~116 kDa that demonstrated ganglioside dependent binding. These proteins were later identified as adducin and synapsin (Schengrund et al., 1993; 1996). Adducin is a cytoskeletal protein that functions to recruit spectrin to bind to actin. Synapsin is a vesicular protein that interacts with actin, and is thought to help sequester the storage pool of synaptic vesicles to the cytoskeletal compartment; although synapsin may also play a role in later steps involving vesicular docking. However, neither of these proteins have extracellular domains, making them unlikely candidates for toxin receptors.

In 1992, binding of ^{125}I labeled toxin gold complexes to a 140 kDa protein at the plasma membrane was demonstrated in the torpedo electric organ, a concentrated source of cholinergic nerve terminals. This protein was not identified (Blasi et al., 1992). More recently, evidence using non-target tissue assays suggested that the vesicular proteins synaptotagmins may act as binding proteins for BoNT. Interestingly, the n-terminus of synaptotagmin has been shown to be presented extracellularly during exocytosis (Angaut-Petit et al., 1995; 1998). Other studies demonstrated that

synaptotagmin II bound botulinum toxin serotype B (BoNT/B) with high affinity (Nikishi et al., 1994, 1996a; 1996b; Kozaki et al., 1998). It was proposed that this high affinity binding was achieved through binding of the n-terminus of synaptotagmin II to complex gangliosides, particularly GT1b or GD1a, to form a high affinity binding site for BoNT/B (Nikishi et al., 1996a; 1996b).

Two recent studies, that utilized both an in vivo model and an ex vivo mouse diaphragm preparation, support synaptotagmin II as a functional receptor for BoNT/B. The first study demonstrated that pre-incubation of BoNT/B with synaptotagmin II peptides decreased in vivo toxicity when injected into mice. Secondly, pre-incubation of the toxin with peptides corresponding to amino acids 31-60, the proposed binding site, delayed paralysis when added to a mouse hemidiaphragm (Wang et al., 2004). Interestingly, studies utilizing brain synaptosomes reported that both serotypes A and E bound synaptotagmin I (Li and Singh, 1998). These findings are inconsistent with previous reports suggesting that the toxin receptors are serotype specific and non-competitive (Kozaki, 1979). Recent work in our lab has demonstrated that BoNT/A binding to synaptotagmin I was inconsistent, and that pre-incubation of the toxin with peptides to synaptotagmin I did not inhibit toxin activity. This suggests that synaptotagmin I is not a functional receptor for BoNT/A.

Recently, a 15 kDa protein Glycosylphosphotydylinositol-anchored (GPI) lipid raft associated protein THY1 was shown to bind tetanus toxin, a related clostridial toxin that cleaves VAMP (Herreros et al., 2000; Herreros et al., 2001). This binding, and the apparent inability to completely inhibit toxin action by blocking synaptotagmin, led to the provocative proposal that the Clostridial toxins may actually bind to an ‘array’ of proteins

that are concentrated in segments of lipid rafts. It was postulated that the synaptotagmins may not be 'the receptor', but rather, they may act in concert with gangliosides, GPI-anchored proteins, Src kinases, and other lipid raft associated proteins to bind and mediate endocytosis of the clostridial toxins (Montecucco et al., 2004).

To further support the involvement of lipid rafts in clostridial toxin binding, studies in which cells underwent cholesterol depletion by methyl- 3-cyclodextrin (MCDX) demonstrated reduced internalization of tetanus toxin, and a dose dependent decrease in toxin activity as measured by VAMP cleavage (Herreros et al., 2001). Lipid raft binding would not be a unique phenomenon; a wide variety of pathogens including viruses such as the simian forest virus and bacterial toxins such as cholera and shiga toxin may be internalized through lipid rafts.

Endosomal proteins and translocation

The mechanism by which the toxin light chain is released from the endosome has yet to be identified. As stated previously, it appears that agents that neutralize the pH of the endosome (methylamine hydrochloride) or inhibit the proton pump (bafilomycin) also inhibit toxicity, suggesting that the mechanism is pH induced translocation (Coffield et al., 1999; Simpson, 1983,).

Research involving A-B toxins, (toxins in which the parent toxin, a single peptide chain, is enzymatically cleaved into two chains, only one of which is intracellularly active), demonstrates two potential ways in which the active chain is released from endosomes. In the first group of A-B toxins, the heavy chain does not demonstrate the ability to form channels, and the toxin requires activation within the endoplasmic

reticulum (ER) by protein disulfide isomerase (Orlandi, 1997). It is thought that these protein toxins are targeted to the ER through retrograde transport involving the KDEL receptor a transmembrane protein localized predominantly to the ER that recognizes proteins containing the KDEL targeting motif. In the ER, these toxins take advantage of the ubiquitin-proteosome sec61p complex. This complex moves misfolded proteins through the ER translocon. Once through the membrane and into the cytosol the toxins escape ubiquination due to their lack of lysine residues (Lord et al., 2003; Hazes and Read, 1997).

The second group of A-B toxins includes botulinum, tetanus, and diphtheria toxins. It has been shown that the heavy chain possesses the ability to form channels within the endosome membrane, which may allow for the light chain to escape. One hypothesis is that the toxin contains a signal peptide that recruits other proteins to form a transmembrane channel. Membrane conductance tests suggest that these channels are large enough for passage of the light chain (Hoch et al., 1985). A second hypothesis is that the two chains act together to form a cleft in which the hydrophobic residues from both chains interact with membrane lipids. Once the light chain is extruded, the disulfide bond connecting it to the heavy chain is cleaved and the light chain is released into the cytosol. The possibility also exists that the light chain is assisted out of the endosome and refolded utilizing chaperone proteins (see review by Schiavo et al., 2000).

THE USE OF PROTEOMICS TO IDENTIFY TOXIN-PROTEIN INTERACTIONS

Proteomics is the study and methodology involved in the identification of all proteins expressed by a cell, tissue, organ or organism. The field of proteomics is in its

infancy and as such, while demonstrating amazing possibilities in deriving cellular function, including insight into cell-cell signaling, posttranslational modifications, protein targeting, and cellular responses to chemicals and drugs, it is important to recognize it also has significant limitations. In this section, important methodologies involved in proteomics will be reviewed and, more importantly, the limitations of the technology will be recognized.

It is important to realize that under the best of circumstances shotgun proteomics, in which a sample (e.g., cell lysate, tissue homogenate) is solubilized, trypsin-digested, and run through an LC-MS (liquid chromatography mass spectrometer) will only identify 1000-2000 proteins of a possible 10-100 thousand proteins. Further, proteins do not exist in equal abundance; therefore, it is more likely that higher abundant proteins will be identified more frequently than lower abundant proteins. This implies that the major step in protein identification is the ability to extract and enrich proteins of interest in test samples.

Particularly problematic are membrane proteins; several studies have been aimed at developing protocols to enhance resolution of membrane proteins (Lehner et al., 2003; Babu et al., 2004; le Maire et al., 2000; Henningson et al., 2002; Bordier 1981). These involve modifications at all steps of protein isolation including: extraction, solubilization, and enrichment. Extraction of proteins can occur through gentle methods such as freeze thaw, or osmotic lysis; moderate methods such as polytron homogenization; and vigorous methods such as sonication. Detergents such as SDS and Triton X-100 may be used to lyse cells; still others have described the use of high pH buffers (pH 11) to extract membrane proteins (Zamorano and Garner, 2001).

Several different enrichment methods have been utilized including differential centrifugation, detergent/sucrose fractionation, immunoprecipitation, and chromatography. Membrane solubilization techniques involving detergent phase partitioning and detergent solubilization have been employed with mixed results. Each of these methods must be evaluated for the specific sample used and the target proteins to be identified.

After enrichment, proteins may be further separated utilizing one or two–dimensional gel electrophoresis. In SDS-PAGE, SDS coats the proteins neutralizing their charge, thereby allowing them to separate by size. This method also proves useful for the removal of detergents or salts that may interfere with mass spectrometers and, therefore, has been used to clean up samples prior to mass spectrometry. A drawback to SDS-PAGE separation is that it can only separate proteins by relative size; with so many proteins exhibiting masses between 25-100 kDa it becomes extremely difficult to separate proteins from highly complex mixtures.

Two-dimensional electrophoresis utilizes immobilized pH gradients to separate proteins not only by size, but also by their relative pIs. In this method, as reviewed by Malloy (2000), several different reagents are utilized to isolate proteins. Initially the proteins are rehydrated in a buffer containing chaotropes that are used to disrupt hydrogen bonding within the proteins, thereby causing denaturation and unfolding. A combination of urea and thiourea works well for most proteins. The unfolding of these proteins leads to exposure of their hydrophobic domains which may interact and aggregate within the acrylamide gel. In order to prevent this, surfactants are added to inhibit these hydrophobic interactions; there are a number of detergents that are used

including CHAPS, Triton X-100, and the sulfobetaines. The third reagent added to disrupt protein structure and promote migration is a reducing agent such as dithiothreitol (DTT) or Tri-butyl phospheines (TBP). Proteins are then rehdyrated into the immobilized pH gradient (IPG) strips either through passive or active rehydration.

Active rehydration utilizes a low voltage to force proteins into the strip, thereby aiding the insertion of large proteins. After rehydration, an incremental increase of voltage is applied and the proteins are focused along the strip until they reach their respective pIs. The strips are then equilibrated, inserted into gels and the proteins separated by size through SDS-PAGE. Gels can then be stained with a variety of stains including Coomassie, Sypro, or silver nitrate, each displaying differing sensitivities. Spots can then be analyzed and picked for further testing by LC-MS-MS.

This introduction will not go into the specifics of tandem mass spectrometry analyzers, except to point out that there are several different types of analyzers that differ by their injection source (chips, electrospray, and nanospray) and their ionization sources (ie.quadropole, ion-trap, FTCR). Again each mass analyzer should be evaluated as to the level of sensitivity needed relative to protein abundance, size, and ability to detect posttranslational modifications. One relative note regarding mass spectrometers is that for LC-MS, proteins are separated by reverse phase chromatography, which separates by hydrophobicity. This may be problematic with extremely hydrophobic proteins in that they can be retained by the column. Recently mass spectrometers utilizing hydrophilic interaction liquid chromatography (HILIC) have been developed. In the past HILIC separation followed by gel analysis had been proposed for isolation of small polar groups and membrane proteins (Alpert, 1990).

There is little research yet to suggest whether this column coupled to a mass spectrometer can be utilized successfully to increase identification of inner membrane proteins.

By far, the greatest challenge in proteomics is working with membrane proteins. Membrane proteins tend to be extremely hydrophobic resulting in their loss in either the column, or the gel. They are difficult to solubilize into single polypeptides leading to difficulty in isolation, enrichment and gel mobilization. They tend to have very low abundance leading to an inability to detect or identify with LC-MS. Membrane proteins also tend to precipitate at their pIs resulting in loss when transferred from the IPG strips to the gel. Integral membrane proteins may also have domains that are not exposed to trypsin resulting in large non-fragmented peptides that are unable to be identified by MS. In addition to these physical limitations, several proteins may be localized to both cytoplasmic and membrane compartments. Their function and localization is determined by their posttranslational glycosylation patterns. These modifications along with modification of selected amino acids can make it difficult to isolate and identify these proteins utilizing routine MS (reviewed by Hancock et al., 2002). Thus, these characteristics when compared with the available technology ensure that membrane proteins remain the least characterized and represented proteins in proteome analysis.

This dissertation discusses the protocols, limitations, and advances made in the effort to identify the receptor of BoNT/A at the motor nerve terminal. Although there were unforeseen technical limitations, the ability to utilize these methodologies to analyze and identify possible protein-protein interactions between BoNTs and the

cellular proteins involved at each of the identified stages of intoxication remains a viable research tool to elucidate the journey of BoNT.

REFERENCES

Alpert A. Hydrophilic-interaction chromatography for the seperation of peptides, nucleic acids, and other polar compounds. Journal of Chromatography 1990; 499: 177-196.

Angaut-Petit D, Molgo J, Faille L, Juzans P, Seager MJ, Takahashi M. Mouse motor nerver terminal immunoreactivity to synaptotagmin II during sustained quantal transmitter release. Brain Res 1995; 681: 213-217.

Angaut-Petit D, Molgo J, Faille L, Juzans P, Takahashi M. Incorporation of synaptotagmin II to the axolemma of botulinum type A-poisoned mouse motor endings during enhanced quantal acetylcholine release. Brain Res 1998; 797: 357-360.

Arnon SS, Schechter R, Inglesby TV, Henderson DA, Bartlett JG, Ascher MS, Eitzen E, Fine AD, Hauer J, Layton M, Lilibridge S, Osterholm MT, O'Toole T, Parker G, Perl TM, Russell PK, Swerdlow DL, Tonat K. Botulinum toxin as a biological weapon: Medical and public health management. JAMA 2001; 285: 1059-1070.

Babu GJ, Wheeler D, Alzate O. Periasamy M. Solubilization of membrane proteins for two-dimensional electrophoresis: Identification of sarcoplasmic reticulum membrane proteins. Analytical Biochemistry 2004; 325: 121-125.

Bakry N, Kamata Y, Simpson LL. Lectins from Triticum Vulgaris and Limax Flavus are universal antagonists of botulinum toxin and tetanus toxin. J Pharmacol Exp Ther 1991; 258: 830-836.

Bennett MK, Calakos N, Scheller RH. Syntaxin: A synaptic protein implicated in docking of synaptic vesicles at presynaptic active zones. Science 1992; 257: 255-259.

Betz WJ, Bewick GS. Optical analysis of synaptic vesicle recycling at the frog neuromuscular junction. Science 1992; 255: 200-203.

Bhatia KP, Münchau A, Thompson PD, Houser M, Chauhan VS, Hutchinson M, Shapira AHV, Marsden CD. Generalized muscular weakness after botulinum toxin injections for dystonia: a report of three cases. J Neurol Neurosurg Psychiatry 1999; 67: 90-93.

Binder WJ, Brin MF, Blitzer A, Schoenrock LD, Pagoda JM. Botulinum toxin type A (BOTOX) for treatment of migraine headaches: An open-label study. Otolaryngol Head Neck Surg 2000; 123(6): 669-676.

Black JD, Dolly O. Interaction of ^{125}I-labeled botlinum neurotoxins with nerve terminals. II. Autoradiographic evidence for its uptake into motor nerves by acceptor mediated endocytosis. J Cell Biol 1996b; 103: 535-544.

Black JD, Dolly O. Interaction of ^{125}I-labeled botlinum neurotoxins with nerve terminals. I. Ultrastructural autoradiographic localization and quantitation of distinct membrane acceptors for types A and B on motor nerves. J Cell Biol 1986a; 103: 521-34.

Blasi J, Chapman ER, Link E, Binz T, Yamasaki S, De Camilli P, Sudhof TC, Niemann H, Jahn R. Botulinum neurotoxin A selectively cleaves the synaptic protein SNAP-25. Nature 1993a; 365: 160-163.

Blasi J, Chapman ER, Yamasaki S, Binz T, Niemann H, Jahn R. Botulinum toxin C1 blocks neurotransmitter release by means of cleaving HPC1/syntaxin. Embo J 1993b; 12: 4821-4828.

Blasi J, Egea G, Castiella MJ, Arribas M, Solsona C, Richardson PJ, Marsal J. Binding of Botulinum neurotoxin to pure cholinergic nerve terminals isolated from the electric organ of Torpedo. J Neural Transm Gen Sect 1992; 90: 87-102.

Bonventre PF. Adsorbtion of botulinal toxin from the gastrointestinal tract. Rev Infect Dis 1979; 1(4): 663-667.

Bordier C. Phase seperation of Integral membrane protein in Triton X-114 solution. J Biol Chem 1981; 256(4): 1604-1607.

Bozheyeva G, Kunakbayev Y, Yeleukenov, D. Former soviet biological weapons facilities in Kazakhstan: Past, present, and future. Monteray, Calif. Center for Nonprolifereration Studies, Monteray Institute of International Studies. 1999; June: 1-20.

Brin MF. Botulinum toxin: Chemistry, pharmacology, toxicity, and immunology. Muscle Nerve 1997; Suppl 6: S146-168.

Brin MF, Fahn S, Moskowitz C, Friedman A, Shale HM, Greene PE, Blitzer A, List T, Lange D, Lovelace RE, McMahon D. Localized injections of botulinum toxin for the treatment of focal dystonia and hemifacial spasm. Mov Disord 1987; 2: 237-254.

Bullough PA, Hughson FM, Skehel JL, Wiley DC. Structure of Influenza haemagglutinin at the pH of membrane fusion. Nature 1994; 371: 37-43.

Burgen ASV, Dickens F, Zatman LJ. The action of botulinum toxin on neuromuscular junction. J Physiol 1949; 109: 10-24.

Cases-Langhoff C, Voss B, Garner AM, Appeltauer U, Takei K, Kindler S, Veh RW, De Camilli P, Gundelfinger ED, Garner CC**.** Piccolo, a novel 420 kDa protein associated with the presynaptic cytomatrix. Eur J Cell Biol 1996; 69: 214-223.

Ceccarelli B, Hurlbut, WP, Mauro A. Turnover of transmitter and synaptic vesicles at the frog neuromuscular junction. J Cell Biol 1973; 57: 499-524.

Coffield JA, Bakry NM, Maksymowych AB, Simpson LL. Characterization of a vertebrate neuromuscular junction that demonstrates selective resistance to botulinum toxin. J Pharmacol Exp Ther 1999; 289: 1509-1516.

Collins MD, East AK. Phylogeny and taxonomy of the food borne pathogen Clostridium Botulinum and its neurotoxins. J Appl Microbiol 1998; 84: 5-17.

Crone C. Modulation of solute permeability in microvasculature endothelium. Fed Proc 1986; 45(2): 77-83.

Danielson EM, Hansen GH. Lipid rafts in epithelial brush borders: atypical microdomains with specialized functions. Biochimica et Biophsyica Acta (BBA)-Biomembranes 2003; 1617(1-2): 1-9.

Dasgupta BR, Sugiyama HA. A common subunit structure in Clostridium botulinum type A, B, and E toxins. Biophys Res Comm 1972; 48: 108-112.

Dong M, Richards DA, Goodnough MC, Tepp WH, Johnson EA, Chapman ER. Synaptotagmins I and II mediate entry of botulinum neurotoxin B into cells. J Cell Biol 2003; 162(7): 1293-1303.

Eleopra R, Tugnoli V, Caniatti L, De Grandis D. Botulinum toxin treatment in the facial muscles of humans: Evidence of an action in untreated near muscles by peripheral local diffusion. Neurology 1996; 46: 1158-1160.

Ergbuth FJ, Naumann M. Historical aspects of botulinum toxin: Justinus Kerner (1786-1862) and “sausage poison.” Neurobiology 1999; 53: 1850-1853.

Eswaramoorthy S, Kumaran D, Keller J, Swaminathan S. Role of metals in the biological activity of Clostridium Botulinum neurotoxins. Biochemistry 2004; 43: 2209-2116.

Fillippis VD, Vangelista L, Schiavo G, Tonello F, Montecucco C. Structural studies on the zinc-endopeptidase light chain of tetanus neurotoxin. Eur J Biochem 1995; 229: 61-69.

Frokjaer-Jensen J. The plasmalemmel vesicular system in striated muscle capillaries and pericytes. Tissue Cell 1984; 16(1): 31-42.

Fuginaga Y, Inoue K, Watanabe S, Yakota K,Hirai Y, Nagamachi E, Oguma K. The haemagglutinin of Clostridium Botlulinum type C progenitor toxin plays an essential role in binding of toxin to the epithelial cells of guinea pig small intestine, leading to the efficient absorption of the toxin. Microbiology 1997; 143: 3841-3847.

Fujinaga Y, Inoue K, Watanabe S, Yokota K, Hirai Y, Nagamachi E, Oguma K. The haemagglutinin of Clostridium botulinum type C progenitor toxin plays an essential role in binding of toxin to the epithelial cells of guinea pig small intestine, leading to the efficient absorption of the toxin. Microbiology 1997; 143 (part 12): 3841-3847.

Ginalski K, Venclovas Č, Lesyng B, Fidelis K. Structure-based sequence alignment for the β-trefoil subdomain of the clostridial neurotoxin family provides residue level

information about the putative ganglioside binding site. FEBS Letters 2000; 482: 119-124.

Guo W, Roth R, Walch-Solimena C, Novick P. The exocyst is an effector for sec4p targeting secretory vesicles to sites of exocytosis. EMBO J 1999; 18: 1071-1080.

Hancock WS, Wu SL, Shieh P. The challenges of developing a sound proteomics strategy. Proteomics 2002; 2: 252-359.

Hazuka CD, Foletti DL, Hsu SC, Kee Y, Hopf FW, Scheller RH. The sec 6/8 complex is located at neurite outgrowth and axonal syanpse assembly domain. J Neurosci 1999; 19: 1324-1334.

Heckly RJ, Hildebrand GJ, Lammana C. On the size of the toxic particle passing the intestinal barrier in botulism. J Exp Med 1960; 111: 745–759.

Henningson R, Gale B, Straub KM, DeNagel DC. Application of zwitterionic detergents to the solubilization of intergral membrane proteins for two dimensional gel electrophoresis and mass spectrometry. Proteomics 2002; 2: 1479-1488.

Herreros J, Lalli G, Montecucco C, Schiavo G. Tetanus toxin fragment C binds to a protein present in neuronal cell lines and motorneurons. J Neurochem 2000; 74: 1941-1950.

Herreros J, Ng T, Schiavo G. Lipid rafts act as specialized domains for tetanus binding and internalization into neurons. Mol Biol Cell 2001; 12: 2947-2960.

Heuser JE, Reese TS. Evidence for recycling of synaptic vesicle membrane during transmitter release at the frog neuromuscular junction. J Cell Biol 1973; 57: 314-344.

Hoch DH, Romera-Mira M, Ehrlich BE, Finkelstein A, DasGupta BR, Simpson LL. Channels formed by botulinum, tetanus, and diphtheria toxins in planar lipid bilayers: Relevance to to translocation of proteins across membranes. Proc Natl Aca Sci USA 1985; 82: 1692-1696.

Hsu SC, Hazuka CD, Foletti DL, Scheller RH. Targeting vesicles to specific sites on the plasma membrane: The role of sec6/8complex. Trends Cell Biol 1999; 9: 150-53.

Jankovic J, Brin MF. Botulinum toxin: Historical perspective and potential new indications. Muscle Nerve 1997; Suppl 6: S129-145.

Kalandakanond S, Coffield JA. Cleavage of intracellular substrates of botulinum toxin A, C, and D in a mammalian target tissue. J Pharmacol Exp Ther 2001; 296: 749-755.

Kitamura M, Iwamori M, Nagai Y. Interaction between clostridium botulinum neurotoxin and gangliosides. Biochem Biophys Acta 1980; 62: 328-335.

Klenchin VA, Martin T. Priming in exocytosis: Attaining fusion-competence after vesicle docking. Biochimie 2000; 82: 399-407.

Kozaki S, Kamata Y, Watari S, Nishiki T, Mochida S. Ganglioside Gt1b as a complementary receptor component for clostridium botulinum neurotoxins. Microbial Pathogenesis 1998; 25: 91-99.

Kozaki S. Interactions of botulinum toxin A, B, and E derivative toxins with synaptosomes of rat brain. Naunyn-Scmiedebergs Arch Pharmacol 1979; 308: 67-70.

Kraszewski K, Daniell L, Mundigl O, DeCamilli P. Mobility of synaptic vesicles in nerve ending monitored by photobleaching of synaptic vesicle-associated fluorescence. J Neurosci 1996; 16: 5905-5913.

Kumakura K, Sasaki K, Sakurai T, Ohara-Imaizumi M, Misonou H. Essential role of myosin light chain kinase in the mechanism for Mg-ATP dependent priming of exocytosis in adrenal chromaffin cells. J Neurosci 1994; 14: 7695-7703.

Lacy BD, Tepp W, DasGupta BR, Stevens RC. Crystal structure of botulinum neurotoxin type A and implications for toxicity. Nat Struct Biol 1998; 5: 898-902.

Landis DM, Hall AK, Weinstein LA, Reese TS. The organization of the cytoplasm at the presynaptic zone of a central nervous system synapse. Neuron 1988; 1: 201-209.

Lehner I, Niehof M, Brolak J. An optimized mehod for the isolation and identification of membrane proteins. Electrophoresis 2003; 24: 1795-1808.

Lencer WI, Hirst TR, Holmes RK. Membrane traffic and the cellular uptake of cholera toxin. Biochimica et Biophysica Acta 1999; 1450: 177-190.

Li L, Singh BR. Isolation of synaptotagmin as a receptor for types A and E botulinum neurotoxin and analysis of their comparative binding using a new microtiter plate assay. J Nat Toxins 1998; 7: 215-226.

Lin RC, Scheller RH. Mechanisms of synaptic vesicle exocytosis. Ann Rev Cell Dev Biol 2000; 16:19-49.

Link E, Blasi J, Chapman ER, Edelmann L, Baumeister A, Binz T, Yamasaki S, Neimann H, Jahn R. Tetanus and botulinal neurotoxins: tools to understand

exocytosis in neurons. Adv Second Messenger Phosphoprotein Res 1994; 29: 47-58.

Lord JM, Deeks CJ, Marsden K, Moore C, Pateman C, Smith DC, Spooner RA, Watson P, Roberts LM. Retrograde transport of toxins across the endoplasmic reticulum membrane. Biochemical Society Transactions 2003; 31(6): 1260-1262.

Lubec G, Krapfenbauer, K, Fountoulakis M.. Proteomics in brain research:potentials and limitations. Progress in Neurobiology 2003; 69: 193-211.

Maksymowych A, Simpson LL. Binding and Transcytosis of Botulinum Neurotoxin by Polarized Human Colon Carcinoma Cells. J Biol Chem 1998; 273 (24): 21950-21957.

Maksymowych AB, Reinhard M, Malizio CJ, Goodnough MC, Johnson E, Simson LL. Pure botulinum toxin is absorbed from the stomach and small intestine and produces peripheral neuromuscular blockade. Infection and Immunity 1999; 67(9): 4708-4712.

Malloy MP, Two-dimensional Electrophoresis of Membrane proteins using immolbilized pH gradients. Analytical Biochemistry 2000; 280: 1-10.

Martinez-Estrada OM, Villla A, Breviario F, Orsenigo F, Dejana E, Bazzoni G. Association of junctional adhesion molecule with calcium/calmodulin dependent serine protein kinase (CASK/ LIN-2) in human epithelial caco-2 cells. J Biol Chem 2001; 276: 9291-9296.

Mochida S, Kobayashi H, Matsuda Y, Yuda Y, Muramoto K, Nonomura Y. Myosin II is involved in transmitter release in synapses formed between rat sympathetic neurons in culture. Neuron 1994; 13: 1131-1142.

Montecucco C, Rossetto O, Schiavo, G. Presynaptic receptor arrays for clostridial neurotoxins. Trends in Microbiol 2004; 12(10): 442-446.

Montecucco C. How do tetanus and botulinum toxins bind to neuronal membranes? TIBS 1986; 11: 314-317.

Morante S, Furenlid L, Schiavo G, Tonello F, Zwilling R, Montecucco C. X-ray adsorption spectrosropy of zinc coordination in tetanus neurotoxin, astacin, alkaline protease, and thermolysin. Eur J Biochem 1996; 235: 606-612.

Neher E, Zucker RS. Multiple calcium-dependent processes related to secretion in bovine chromaffin cells. Neuron 1993; 10: 21-30.

Nickell W, Weber T, McNew A, Parlati F, Sollner TH, Rothman JE. Content mixing and membrane integrity during membrane fusion driven by pairing of isolated v-SNARE's and t-SNARE's. Proc Natl Acad Sci 1999; 96: 12571-1276.

Nikishi T, Kamata Y, Nemoto Y, Omori A, Ito T, Takashi M, Kozaki S. Identification of the protein receptor for clostridium botulinum type B neurotoxin in rat brain synaptosomes. J Biol Chem 1994; 269: 10498-10503.

Nikishi T, Tokuyama Y, Kamata Y, Nemoto T, Yoshida A, Sekiguchi M, Takahashi M, Kozaki S. Binding of botulinum type B neurotoxin to chinese hamster ovary cells transfected with rat synaptotagmin I cDNA. Neurosci Lett 1996b; 208: 105-108.

Nikishi T, Tokuyama Y, Kamata Y, Nemoto Y, Yoshida A, Sato K, Sekiguchi M, Takahashi M, Kozaki S. The high affinity binding of clostridium botulinum type B neurotoxin to synaptotagmin I associated with gangliosides Gt1b/Gd1a. FEBS Lett 1996a; 378: 253-257.

Orlandi PA, Protein-disulfide isomerase-mediated reduction of the A subunit of cholera toxin in a human intestinal cell line. J Biol Chem 1997; 272: 4591-4599**.**

Oshishi I, Sugii S, Sakaguchi. Oral toxicities of clostridium botulinum toxins in response to molecular size. Infect Immun 1977; 16: 107-109.

Otto H, Hanson PI, Jahn R. Assembly and disassembly of a ternary complex of synaptobrevin, syntaxin, and SNAP-25 in the membrane of synaptic vesicles. Proc Natl Acad Sci USA 1997; 242: 6197-6201.

Oyler GA, Higgins GA, Hart RA, Battenberg E, Billingsly M. The identification of a novel synaptosomal associateed protein Snap-25, differentially expressed by neuronal subpopulations. J Cell Biol 1989; 109: 3039-3052.

Ryan, TA. Inhibitors of myosin light chain kinase block synaptic vesicle pool mobilization during action potential firing. J Neurosci 1999; 19: 1317-1323.

Schantz E, Johnson E. Botulinum toxin: the story of its development for the treatment of human disease. Perspect Biol Med 1997; 40(3): 317-327.

Schengrund CL, DasGupta B, Hughes CA, Ringler NJ. Ganglioside-induced adherence of botulinum and tetanus neurotoxins to adducin. J Neurochem 1996; 66(6): 2556-2561.

Schengrund CL, DasGupta BR, Ringler NJ. Ganglioside GD3 enhances adherence of botulinum and tetanus neurotoxins to bovine brain synapsin. Neurosci Letters 1993; 158: 159-162.

Schiavo G , Shone CC, Bennett MK, Scheller RH, Montecucco C. Botulinum neurotoxin type C cleaves a single Lys-Ala bond within the carboxyl terminal of syntaxins. J Biol Chem 1995; 270: 10566-10570.

Schiavo G, Benefenati F, Poulain B, Rossetto O, Polverino De Laureto P, DasGupta BR, Montecucco C. Tetanus and botulium-B neurotoxins block neurotransmitter release by proteolytic cleavage of synaptobrevin. Nature 1992; 359: 832-835.

Schiavo G, Malizio C, Trimble WS, Polverino De Laureto P, Milan G, Sugiyama H, Johnson EA, Montecucco C. Botulinum G neurotoxin cleaves VAMP/synaptobrevin at a single Ala/Ala peptide bond. J Biol Chem 1994a; 269: 20213-20216.

Schiavo G, Matteoli M, Montecucco C. Neurotoxins affecting neuroexocytosis. Pharmacological reviews 2000; 80(2): 717-766.

Schiavo G, Rosseto O, Benefati F, Poulain B, Montecucco C. Tetanus and botulinum neurotoxins are zinc proteases specific for components of the neuroexocytosis apparatus. Ann NY Acad Sci 1994b; 710: 65-67.

Schiavo G, Rosseto O, Catsicas S, Delaureto PP, DasGupta BR, Benefenati F, Montecucco C. Identification of the nerve terminal targets of botulinum toxin serotype A, serotype D, and serotype E. J Biol Chem 1993a; 268: 23784-23787.

Schiavo G, Rossetto O, Santucci A, DasGupta BR, Monteucco C. Botulinum neurotoxins are zinc proteins. J Biol Chem 1992a; 267: 23479-27483.

Schiavo G, Santucci A, Dasgupta BR, Mehta PP, Jontes J, Benfanati F, Wilson MC, Montecucco C. Botulinum neurotoxins A and E cleave SNAP-25 at distinct COOH terminal peptide bonds. FEBS Lett 1993b; 335: 99-103.

Schiavo G, Shone CC, Bennett MK, Scheller RH, Montecucco C. Botulinum neurotoxin type C cleaves a single Lys-Ala bond within the carboxyl terminal region of syntaxins. J Biol Chem 1995; 270: 10566-10570.

Schiavo G, Shone DD, Rossetto O, Alexander FCG, Montecucco CL. Botulinum neurotoxin serotype-F is a zinc endopeptidase specific for VAMP/synaptobrevin. J Biol Chem 1993c; 268: 11516-11519.

Schnieder SW. Kiss and run mechanism in exocytosis. J Membrane Biol 2001; 181: 67-76.

Scott AB, Rosenbaum A, Collins CC. Pharmacologic weakening of extraocular muscles. Invest Opthalmol Vis Sci 1973; 12: 924-927.

Shapiro RL, Hatheway C, Swerdlow DL. Botulism in the United States: a clinical and epidemiologic review. Ann Inter Med 1998; 129: 221-228.

Simpson LL, Rappaport MM. The binding of botulinum toxin to membrane lipids; sphingolipids, steroids, and fatty acids. J Neurochem 1971; 18: 1751-1759.

Simpson LL. The origin, structure, and pharmacological activity of botulinum toxin. Pharmacol Rev 1981; 33: 155-188.

Simpson LL. Ammonium Chloride and methylamine hydrochloride antagonize clostridial neurotoxins. J Pharmacol Exp Ther 1983; 225: 546-552.

Simpson LL. The origin, structure, and pharmacological activity of botulinum toxin. Pharmacol Rev 1981; 33: 155-188.

Simpson, LL. Identification of the major steps in botulinum toxin action. Annu Rev. Pharmacol Toxicol 2004; 44: 167-193.

Sollner T, Whiteheart SW, Brunner M, Erdjument-Bromage H, Geromonas. SNAP receptors implicated in vesicle targeting and fusion. Nature 1993b; 362: 318-324.

Sollner T, Whiteheart SW, Scheller RH, Rothman JE. A protein assembly-disassembly pathway in vitro that may correspond to sequential steps of synaptic vesicle docking, activation, and fusion. Cell 1993a; 75: 409-418.

Südhof TC. The synaptic vesicle cycle. Annu Rev Neurosci 2004: 27: 509-47.

Suggi S, Oshishi, I, Sakaguchi G. Correlation between oral toxicity and invitro stability of Clostridium botulinum type A and B toxins of different molecular sizes. Infect Immun 1977a; 16: 910-914.

Suggi S, Oshishi, I, Sakaguchi G. Intestinal Absorption of Botulinum Toxins of Different Molecular Sizes in Rats. Infect. Immun. 1977b; 17(3): 491-496.

Sutton RB, Fasshauer D, Jahn R, Brunger AT, Crystal structure of a SNARE complex involved in synaptic exocytosis at 2.4 Å resolution. Nature 1998; 395: 347-353.

Swaminathan S and Eswaramoorthy S. Stuctural analysis of the catalytic and binding sites of Clostridium botulinum neurotoxin B. Nat Struct. Biol. 2000; 7: 693-699.

tom Dieck S, Sanmarti-Vila L, Langanese K, Richter K, Kindler S et al. Bassoon, a novel zinc finger CAG/Glutamine-repeat protein selectively localized at the active zone of presynaptic nerve terminals. J Cell Biol 1998; 142: 499-509.

van Ermengem E. Uber einem neuen anaeroben Bacillus und seine Beziehungen zum. (English translation) A new anaerobic bacillus and its relation to botulism. Rev Infect Dis 1979; 1701-1719. Z Hyg Infetionskranskh 1897; 26(1-56): 701-719.

van Heynigan WE, Miller PA. The fixation of tetanus toxin by ganglioside. J Gen Microbiol 1974a; 24: 107-119.

van Heynigan WE. Gangliosides as membrane receptors for tetanus toxin, cholera toxin and serotonin. Nature 1974b; 249: 415-417.

Walch-Solimena C, Blasi J, Endelmann L, Chapman ER, vonMollard GF, Jahn R. The t-SNARES syntaxin I and SNAP-25 are present on organelles that participate in synaptic vesicle recycling. J Cell Biol 1995; 128: 637-645.

Wang X, Kibschull M, Laue MM, Lichte B, Petrasch-Parwez E, Kilimann MW. Aczonin a 550 kD putative scaffolding protein of presynaptic active zones, shares homology regions with Rim and Bassoon and binds profilin. J Cell Biol 1999; 147: 151-162.

Wang Y, Okamoto M, Schmitz F, Hufman K. Südhof TC. Rim is a putative Rab3 effector in regulating synaptic vesicle fusion. Nature 1997; 388: 593-598.

Xu T, Binz T, Niemann H, Neher E. Multiple kinetic components of exocytosis distinguished by neurotoxin sensitivity. Nature Neuroscience 1998; 1(3): 192-200.

Yamasaki S, Baumeister A, Binz T, Blasi J, Link E, Cornille F, Roques B, Fykse EM, Sudhof TC, Jahn R. Cleavage of members of the synaptobrevin/VAMP family by types D and F botulinum neurotoxins and tetanus toxin. J. Biol Chem 1994a; 269: 12764-12772.

Yamasaki S, Binz T, Hayashi T, Szabo E, Yamasaki N, Eklund M, Jahn R, Niemann H. Botulinum neurotoxin G proteolyses the Ala81-Ala82 bond of rat synaptobrevin 2. Biochme Biophys Res Commun 1994b; 200: 829-835.

Zamorano PL, Garner CG. Unwebbing the presynaptic web. Neuron 2001; 32(1): 3-6.

Zhang Y, Luan Z, Liu A, Hu G. The scaffolding protein CASK mediates the interaction between rabphilin 3a. and beta neurexins. FEBS Lett 2001; 497: 99-102.

CHAPTER 2

ISOLATION AND IDENTIFICATION OF SYNAPTIC PROTEINS IN A NEUROMUSCULAR ENRICHED MURINE DIAPHRAGM PREPARATION[1]

[1] Parrott TM, Brooks PM, Hoyt N, Baxter VZ, Coffield JA. Manuscript to be submitted.

ABSTRACT

The objective of this study was to identify neuronal proteins from a neuromuscular junction-enriched preparation obtained from murine diaphragm. This synaptosomal-like preparation has been utilized in previous studies in our laboratory and has demonstrated an enrichment of SNARE complex proteins. To further characterize this synaptosomal-like preparation in regard to its composition of junctional plasma membrane proteins, we have combined differential centrifugation with non-ionic detergent solubilization to isolate membrane fractions that are enriched in integral and membrane associated proteins. Using this protocol, several proteins from both the pre- and postsynaptic regions of the neuromuscular junction were identified through a combination of LC-MS-MS and western blot. LC-MS-MS alone was unable to generate a reportable identification of neuronal specific membrane proteins; instead, most of the MS identified proteins were generally compartmentalized to the cytoplasm and mitochondria. Detergent partitioning of the more highly abundant cytoplasmic proteins into the hydrophilic fraction did offer some improvement in the isolation and identification of low abundant membrane proteins by two-dimensional electrophoresis. However, further refinement in these methodologies will be needed for complete characterization of membrane proteins that comprise complex neuronal structures such as those found at the neuromuscular junction.

INTRODUCTION

Recent evidence suggests that the protein components of the pre- and postsynaptic membranes of the CNS synapse are highly specialized and form a rigorous structural relationship of orthogonal projections. These orthogonal projections consist of electron dense pegs caused by thickening of the pre- and postsynaptic membranes which project into the synaptic cleft (Ichimura and Hashimoto, 1988). The pre- and postsynaptic membranes differ in how these thickenings are arranged. The postsynaptic side of the membrane, known as the postsynaptic density, is uniformly thickened; while the presynaptic side, known as the active zone, demonstrates a grid-like pattern that has been described as a particle web (Phillips et al., 2001). This highly organized structuring of the synapse is required to ensure reliability of synaptic transmission. Peripheral synapses such as the neuromuscular junction would seem to share this structural rigidity. Neurotransmitter release, a specialized form of calcium regulated exocytosis, has been shown to occur at active zones (Harlow et al., 2001). Active zones are characterized by certain proteins that demonstrate specialized domains which interact with calcium channels (Leveque et al., 1992; O'Conner et al., 1993). This association is thought to modulate the calcium sensitivity of neurotransmitter release in several ways, including organizational structuring that ensures rapid response and reliability of synaptic vesicle exocytosis (Stanley 1992; Mochida et al., 1996; Cooper et al., 1996).

Each synaptic membrane structure contains the proteins associated with that particular membrane's physiological function. Since the presynaptic side is responsible for neurotransmitter release it is expected to contain proteins associated with vesicular

recruitment, exocytosis, and endocytosis. The post-synaptic side would include neurotransmitter receptors, and proteins involved in signaling pathways. Arranged within the lipid bilayer of both synaptic membranes are many integral membrane proteins. These proteins exhibit a variety of activities including functioning as receptors, transporters, or ion channels. Although they may differ in function, they share similar structural characteristics. Their trans-membrane regions consist of alpha-helical domains with exposed hydrophobic side chains. These side chains strongly interact with membrane lipids to form highly insoluble membrane protein complexes (Lehner et al., 2003). In addition to membrane lipids and integral proteins, these insoluble complexes may contain extracellular glycoproteins, cofactors, and sialogangliosides.

Since neurotransmission is the major function of the nervous system, the identification and characterization of the individual proteins within these complexes is an important area of neuroscience research. One method for protein isolation involves the formation of synaptosomes. Synaptosomes, originally obtained from CNS preparations, were initially isolated through differential centrifugation with or without sucrose gradients, with most synaptic vesicle proteins being found in microsomal fractions (Levitan et al., 1972; Szutowicz, 1976). However, complete isolation of individual synaptic membrane proteins can prove quite challenging due to the nature of their interactions within insoluble complexes.

Non–ionic detergents have been used successfully to solubilize membrane complexes while retaining protein functionality. The detergents act to replace the lipids that interact with the hydrophobic domains of these proteins, and form mixed micelles (Bordier, 1981). These mixed micelles, when warmed, turn cloudy and separate into two

phases, one of which is selectively enriched in detergent and mixed micelles. To date, these detergent-based separation techniques have been developed and used primarily in cell systems. However, in the emerging field of proteomics, the ability to extrapolate these purification and enrichment techniques to whole tissues has become increasingly important.

In our continuing efforts to identify and characterize botulinum toxin receptors at the neuromuscular junction, it was first necessary to modify our protocol for optimal isolation of membrane proteins. Using this optimized protocol we were able to further characterize the neuromuscular junction-enriched murine diaphragm preparation originally developed in our laboratory. To achieve this, differential centrifugation was combined with non-ionic detergent solubilization to isolate hydrophobic membrane fractions enriched with integral and membrane associated proteins. Highly abundant cytoplasmic proteins were partitioned into the hydrophilic fraction, increasing the likelihood of isolation and identification of low abundant membrane proteins. Following isolation, several proteins from both the pre- and postsynaptic regions of the neuromuscular junction were identified through a combination of two dimensional electrophoresis (2-DE), tandem mass spectrometry (LC-MS-MS) and western blot.

MATERIALS AND METHODS

Tissue isolation

Phrenic nerve-hemidiaphragm tissue were removed from adult male NIH Swiss mice (n=120) following decapitation as approved by the University's Institutional Animal Care and Use Committee.

Synaptic membrane preparation

Neuromuscular tissue was prepared on ice according to our previously published procedures (Kalandakanond & Coffield, 2001a). Briefly, diaphragm tissues were minced in homogenization buffer containing 250 mM sucrose, 1 mM EDTA, protease inhibitor cocktail (Sigma-Aldrich; St. Louis, MO) and 20 mM HEPES (pH 7.4). The resulting suspension was homogenized with a handheld electronic homogenizer (Omni 1000) at 15,000 rpm for 1 min. The homogenate was fractionated by centrifugation. Homogenates were initially spun at 1,000 X g for 5 min using a tabletop centrifuge. The resulting supernatant (S_1) was then centrifuged at 10,000 X g for 10 min. The supernatant (S_2) was removed from the pellet (P_2) and centrifuged at 250,000 X g for 1 hr in an Optima ultracentrifuge (Beckman Coulter; Fullerton, CA). The final resulting supernatant (S_3) was then separated from the pellet (P_3).

Detergent fractionation and enrichment

The resulting P_2 and P_3 synaptic membrane preparations were further fractionated using the Mem-Per Kit (Pierce Biochemical; Rockford, IL). Briefly, the P_2 and P_3 samples were incubated in the Pierce lysis buffer (Reagent A) for 30 min at room temperature followed by a 45 min incubation on ice, and then frozen overnight. Sample protein concentration was determined by the modified Lowry method (BioRad; Hercules, CA). To solubilize and separate proteins into hydrophobic and hydrophilic fractions, 500 µg each of P_2 and P_3 were mixed in a 1:4 ratio with a dilute Pierce Reagent C detergent (diluted in a 2:1 ratio with Reagent B). This mixture was vortexed and placed on ice for 45 min, with vortexing every 5 min. At the end of this incubation the mixture was placed in a 37^{o}C incubator for 20 min. The sample was then spun at 10,000 X g for 3 min to

separate the sample into an upper aqueous and a lower detergent rich layer. To prevent remixing, the upper hydrophilic layer was rapidly separated from the lower hydrophobic (H_1) layer. To enhance recovery of integral membrane proteins, the upper hydrophilic layer was subjected to a second extraction by the addition at 1:1 per volume of concentrated Reagent C detergent according to manufacturer's instructions. The (H_3) hydrophilic upper layer was again separated from the lower (H_2) hydrophobic layer (See Figure 2.1). The H_1 and H_2 hydrophobic layers were then pooled into a single hydrophobic fraction (H_1/H_2). The hydrophilic fraction and the pooled hydrophobic fractions were subjected to 2DE or SDS polyacrylamide gel electrophoresis.

2-dimensional electrophoresis

Both unfractionated P_3 and P_2 samples as well as the detergent-enriched P_3 and P_2 fractions were treated with cold acetone to precipitate proteins. The protein concentrated pellets were reconstituted in one of the following 2-DE rehydration buffers and incubated for 1 h. Buffer 1 consisted of 7M Urea, 2M Thiourea, 4% CHAPS and 25 mM DTT, 0.5% ampholytes (pH 3-10), 1% Triton X-100, and 1% TBP; buffer 2 consisted of 6M Urea, 2M Thiourea, 25mM DTT, 1% CHAPs, 1% ASB-14, 1% Triton X-100, 0.5% ampholytes (pH 3-10) plus 1% TBP. The rehydrated sample containing solution was then added to Bio-Rad immobilized pH gradient (IPG) strips (3-10) and incubated for 1 h at which time they were overlayed with mineral oil in preparation for active rehydration.

Sample loaded strips were then placed in the PROTEAN IEF Cell (Bio-Rad; Hercules, CA) for active rehydration for 12 h. Following rehydration, proteins were focused up to 35,000 Vh at 15^{o}C and separated by pI. Salt contamination was

collected on wicks to avoid altering the gradient. To prepare the strips for the second dimension, focused strips were placed in equilibration buffer consisting of 6M UREA; 2% SDS; 0.375% Tris-HCl; 20% glycerol, and 2 mM TBP for 40 min. The equilibrated strips were then embedded in Criterion 10-20% Tris-HCl (Bio-Rad) and proteins separated by mass using SDS-PAGE. Gels were either stained with Colloidal Coomassie or processed further for immunoblot detection. Coomassie stained gels underwent spot comparison and extraction and were sent for MS-MS identification by either electrospray ionization quadropole tandem mass spectrometer, or a nanospray LCQ XP ion-trap mass spectrometer (Ohio State Proteomics facility; Columbus, OH, and Michigan State Proteomics Facility; East Lansing, MI).

Immunoblot

Following SDS page electrophoresis for either 1 dimension or 2 dimension analysis, proteins were transferred to PVDF membranes. Membranes were blocked in 3% milk-TBS for either 2 h at room temp (all antibodies other than Santa Cruz) or overnight cold (Santa Cruz). Blots were probed for the following pre- and postsynaptic proteins using rabbit polyclonal antibodies: synaptotagmin I 1:5000, NGFp75 1:8000 (Sigma-Aldrich; St Louis, MO); alpha 7 nicotinic acetylcholine receptor 1:100 (Research & Diagnostic Antibodies; Concord, MA); MuSK 1:250 (Affinity Bioreagents; Golden CO); VAMP 1:4000 (Wako Chemicals; Richmond, VA); Syntaxin 1A,1b, 1:1000, ERC-2 1:500, Dynamin 1:1000 (Synaptic Systems; Goettingen, Germany); synaptophysin 1:300, LAR 1:400,CASK 1:400, ERB-B2 1:400, ERB-B4 1:300,ACHE, TrkB 1:800 (Santa Cruz; Santa Cruz ,CA); Ngr2 1:200, Ngr3 1:200 (Alpha Diagnostic; San Antonio, TX); P2X2 1:600, Neuregulin 1:200 (Chemicon; Temecula, CA) α-beta crystallin 1:2000,

AP2 (Stressgen; Victoria, British Columbia, Canada). All primary antibodies were diluted in 1% milk-TBS. After removal of primary antibody, blots were washed 4 times in TBS and probed with an HRP- labeled goat anti-rabbit antibody (BioSource; Camarillo, CA; 1:5000) for 1 h at room temperature. Membranes were then washed 6 times in TBS, and the immunoreactive bands were visualized using ECL^+ Chemiluminescence Detection System (Amersham Life Science; Piscataway, NJ). Band strength was evaluated qualitatively by visual inspection.

RESULTS

Isolation and fractionation of proteins

In contrast to a whole cell lysate in which the proteins are reported to be focused predominantly within the acidic region (pI 4-6), the majority of the proteins from our unfractionated synaptic membrane enriched sample (P_3) shown in Figure 2.2, were isolated between pI 6-10, with large clusters of protein spots found in the 50-75 kDa mass range. However, the ability to resolve individual protein spots for further identification or to measure quantifiable differences between fractions was limited due to the complexity of the neuromuscular tissue preparation.

Detergent fractionation of the P_3 sample (500 µg total protein) permitted greater resolution of protein spots within this mass range. Further, the fractionation protocol shown in Figure 2.1 also permitted the isolation and 2-D separation of several proteins that were selectively enriched in either the hydrophobic fraction (Figure 2.3A) or the hydrophilic fraction (Figure 2.3B). Seven of these spots were sent for identification by mass spectrometry. The hydrophobic fraction returned identifications for all spots including heat shock proteins, glyceraldehyde-3-phosphate dehydrogenase and

cytoskeletal protein Desmin, while the hydrophilic protein spots were identified as alpha beta crystallin.

On average unique peptides were isolated that matched to several proteins including Rab (membrane associated), actin gamma, glial fibrillary acidic proteins (cytoskeletal) and vitamin D binding protein. Initial analyses of these MS-MS results revealed a lack of plasma membrane protein identifications. One potential explanation for this was that incompletely solubilized membrane protein complexes were being captured in the earlier pelleted fraction (P_2). Figure 2.4 displays a gel of P_2 samples resolved by 2DE. Interestingly, it was necessary to decrease the initial amount of protein to 400 µg due to the high resistance generated from the sample which resulted in burning of the IPG strip. This illustrated the benefit of additional fractionation of the complex sample with detergents in order to increase the total amount of protein analyzed. These detergent fractions were separated by 2-DE and are shown in Figure 2.5A (hydrophobic fraction) and 2.5B (hydrophilic fraction).

Identification of proteins in P_2 and P_3 fractions by LC-MS-MS

In an attempt to further identify proteins that were in the P_2 and P_3 fractions, acetone precipitated samples of each were sent for LC-MS-MS (Michigan State Proteomics Facility). Proteins that were identified are listed in Table 2.2, with proteins grouped by cellular location. The results of MS-MS identified a majority of ubiquitously expressed proteins generally compartmentalized in either the mitochondria or the cytosol with relatively few documented at the plasma membrane. Since only a few synapse associated proteins were identified by tandem MS-MS, P_2 and P_3 detergent

fractions were further analyzed by western blot to determine whether fractions where enriched in additional synaptic proteins.

Presynaptic membrane complexes isolated through differential centrifugation

To demonstrate that the synaptic membrane enriched P_3 preparation was a synaptosomal-like preparation (i.e., containing both pre- and postsynaptic components), 1-D and 2-D gels were probed with antibodies to a number of membrane proteins that are known to be located at the presynaptic nerve terminal. Using this approach we were able to identify several proteins associated with presynaptic membrane complexes including i.) proteins involved in vesicular exocytosis including SNAP-25, syntaxin I, synaptotagmin I, and VAMP II; ii.) vesicular recruitment proteins including rabphilin, synaptophysin, and RIM; iii.) growth factor receptors including ERB-B2, ERB-B4, NGR-2, NGR-3, and TRKB; and iv.) synaptic organizational and signaling proteins including LAR, P2X receptor and CASK. Identified proteins are listed in table 2.3 and 2.4, and differences in their distribution between the P_2 and P_3 fractions, as well as between the different detergent solubilized fractions are indicated.

Three different patterns were exhibited by these protein separations i) proteins only isolated in either the hydrophobic fraction or hydrophilic fraction, ii) proteins common to both fractions but enriched in one compared to the other, and iii) differences observed between hydrophilic and hydrophobic fractions in terms of molecular weight or pI shifts that were unique to the different fractions. For example, VAMP II, a small single transmembrane domain protein, was isolated only in the hydrophobic fractions of both P_2 and P_3 fractions. Syntaxin I and many of the other proteins identified, demonstrated enrichment in the hydrophobic fraction, but were also found in the hydrophilic fractions.

A common characteristic among some of these proteins is that they typically contain multiple transmembrane domains. Finally, as an example of the third pattern, synaptophysin (shown in Figure 2.7), demonstrated a ubiquitous but varied pattern of bands between 50-75 kDa, although a 37 kDa band was present only in hydrophobic fractions.

Post synaptic membrane complexes isolated through differential centrifugation

Western blot analyses revealed that differential centrifugation and detergent fractionation of our neuromuscular junction enriched preparation resulted in the isolation of postsynaptic membrane proteins and protein complexes found at the neuromuscular junction. For instance, NGF/p75, a tyrosine kinase receptor that is located both pre- and post synaptically, demonstrated ubiquitous expression in both the P_2 and P_3 fractions and was mainly enriched in the hydrophilic fractions. In addition, two subunits of the nicotinic acetylcholine receptor, α4 and α7, were identified by western blot and were particularly enriched in the hydrophilic fraction of the P_3 preparation, while a 37 kDa band was completely isolated in the hydrophobic fraction of the P_3. MuSK, an acetylcholine receptor associated protein, is almost completely isolated in the P_3 preparation, but demonstrates only slight enrichment in the hydrophilic fraction. The two dimensional electrophoresis pattern of this protein (shown in Figure 2.6) demonstrates multiple linear spots that follow this same pattern of fractionation.

DISCUSSION

We utilized several different proteomic techniques in an effort to characterize neuronal proteins from a neuromuscular junction enriched preparation obtained from murine diaphragm. A combination of centrifugal and detergent fractionation was used to

generate a preparation concentrated in synaptic proteins. Initial results from MS-MS spectrometry, however, identified mostly highly abundant cytoplasmic and mitochondrial proteins. The small representation of synaptic proteins in this sample led to the utilization of western blot techniques to confirm the presence of synaptic proteins. Western blots of detergent fractionated P_2 and P_3 samples indicated interesting cellular protein arrangements.

Previous study of the specialized synapse of the mammalian neuromuscular junction has been limited primarily to histological and electrophysiological experimentation in whole tissue preparations. Although of considerable value, these approaches are somewhat tedious, labor intensive and time consuming. The ability to isolate a membrane enriched synaptosomal-like preparation from a mammalian neuromuscular tissue will permit greater scientific investigation of many physiological pathways associated with the neuromuscular junction. These include a variety of synaptic functions from electrochemical signaling and neurotransmitter release to neurotransmitter receptors and signaling pathways associated with muscular response. In the current study, western blot analyses of the mouse diaphragm preparation demonstrate that differential centrifugation can be used to isolate a synaptosomal-like preparation that demonstrates both pre- and postsynaptic protein components that comprise the neuromuscular junction.

The isolation and solubilization of membrane proteins for 2-DE followed by MS/MS identification has proved problematic at best. This is further complicated by the insoluble nature of the specialized interacting proteins which constitute the synaptic complex. To minimize these issues, we further fractionated our synaptic membrane

enriched preparation with non-ionic detergents. This treatment resulted in improved solubilization of some membrane bound proteins and detection of lower abundant proteins. However, an analysis of immunoblot patterns of two dimensional gels from detergent fractionated samples suggests incomplete partitioning for certain integral membrane or membrane-associated proteins.

One potential explanation for this may be the relative insolubility of proteins with a large number of transmembrane domains. Since detergent solubilization works best for proteins with less than four transmembrane domains, the presence of a larger number of domains such as those that constitute the acetylcholine receptor will likely result in the protein not being enriched into either fraction. Another interesting example is the P2X7 receptor; the P2X receptor isoforms P2X1 and P2X3 have been shown to exist as possible functional dimers and trimers within the cell membrane (Nicke et al., 1998). Therefore, the ~70 and ~150 kDa bands detected ubiquitously in all of the fractions may represent these multimeric functional units, while the smaller molecular weight band seen primarily in the P_2 and P_3 hydrophilic fraction may represent the monomer.

Membrane associated proteins such as MuSK, although largely partitioned into the hydrophilic fraction, also demonstrated incomplete fractionation. This may be the result of non-ionic detergent formation of mixed micelles. Within these mixed micelles, the proteins retain their physical/chemical structures. This allows the proteins to retain functionality; therefore, protein-protein interactions may occur in vitro that result in functionally associated proteins being pulled into one fraction or the other.

Differences in spot patterns (2-D) and band patterns (1-D) were evident in immunoblot comparisons of hydrophilic and hydrophobic fractions. There are a number of potential explanations for proteins demonstrating spots at different molecular weights and different pIs across fractions. First, spots or bands at different molecular weights may be the result of protein-protein interactions in which co-migration produces different mass sizes. For example, synaptophysin had a band at ~37 kDa that appeared strongly in both P_2 and P_3, but only in the hydrophobic fractions. Additionally, synaptophysin also demonstrated multiple bands between 50-75 kDa that were ubiquitous through all fractions. These larger molecular weight bands may represent a protein complex of synaptophysin with synaptobrevin that has been previously reported in brain extracts (Becher et al., 1999).

Second, since the proteins examined in this project are membrane or signaling proteins, it is likely that they are post-translationally modified. Modifications such as glycosylation and phosphorylation result in proteins exhibiting multiple isoelectric (ISE) points that are detectable on 2-D immunoblots. This can be seen with MuSK as horizontal, slightly linear spot patterns. These modifications may also control compartmentalization of proteins that results in movement between the plasma membrane and the cytoplasm or endosome.

Finally, detergent solubilization of membrane proteins may permit exposure of multiple antibody recognition sites while at the same time causing fragmentation of hydrophilic, cytoplasmically exposed loops of hydrophobic transmembrane domains. Each of these fragments may be recognized by the polyclonal antibody. It is plausible that this could result in multiple bands or spots of smaller size than the original protein.

Consistent with this hypothesis, LAR demonstrated a ~200 kDa band in non-fractionated samples, but, after fractionation, LAR demonstrated a 40 kDa band that was present ubiquitously in all fractions.

Proteomic techniques were originally developed and perfected for the identification of hydrophilic, highly abundant, cytoplasmic proteins, and are unreliable at best for the isolation and identification of membrane proteins. Membrane proteins tend to be extremely hydrophobic and demonstrate lower abundance. Large membrane proteins can form aggregates within acrylamide gels making them difficult to resolve by 2-DE. Enrichment and purification are important first steps towards successful proteomics of membrane proteins. In the current study, a combination of differential centrifugation and detergent fractionation enabled the isolation and identification of several low abundant proteins, including membrane proteins from a relatively insoluble synaptic protein matrix. Isolated proteins demonstrated different cellular functions ranging from energy production to synaptic transmission and were localized to several different subcellular compartments in addition to the plasma membrane. These results suggest that these enrichment and purification techniques, while valuable, yielded a still relatively complex protein sample. The complexity of this sample likely contributed to the lack of synapse specific protein identification by MS-MS. However, this same limitation was not encountered in western blot analyses which validated the enrichment of this synaptosomal-like preparation with proteins known to be associated with the neuromuscular junction. Further optimization of enrichment and purification techniques, as well as mass spectrometry, will be needed if proteomics is to be useful for the identification of low abundant membrane proteins.

REFERENCES

Becher A, Drenckhahn A, Pahner I, Margittai M, Jahn R, Ahnert-Hilger G. The synaptophysin-synaptobrevin complex: A hallmark of synaptic vesicle maturation. 1999; 19(6): 1922-1931.

Bordier C. Phase separation of integral membrane proteins in Triton X-114 solution. J Biol Chem 1981; 256(4): 1607-1607.

Cooper RL, Winslow CK Govind CK, Atwood HL. Synaptic structural complexity as a factor enhancing probability of calcium-mediated transmitter release. J. Neurophys. 1996; 75(6): 2451-2466.

Harlow ML, Ress D, Stoschek A, Marshall RM, McMahon UJ. The architecture of the active zone at the frog's neuromuscular junction. Nature 2001; 409: 479-484.

Ichimura T, Hashimoto PH. Structural components in the synaptic cleft captured by freeze-substitution and deep etching of directly frozen cerebellar cortex. J Neurocytol 1988; 17(1): 3-12.

Lehner I, Niehof M, Borlak J. An optimized method for the isolation and identification of membrane proteins. Electrophoresis 2003; 24(11): 1795-1808.

Lévêeque C,Hoshino T, David P, Shoji-Kasai Y, Leye K, Omori A, Lang B, El Far O, Sato K, Martin-Moutot N, Newson-Davis J, Takahashi M, Seagar MJ. The synaptic vesicle protein synaptotagmin associates with calcium channels and is a putative Lambert-Eaton myasthenic syndrome antigen. Proc Natl Acad Sci USA 1992; 89: 3625-3629.

Levitan IB, Mushynski WE, Ramirez G. Highly purified synaptosomal membranes from rat brain. J Biol Chem 1972; 247(17): 5376-81.

Mochida S, Sheng ZH, Baker C, Kobayashi H, Catterall WA. Inhibition of neurotransmission by peptides containing the synaptic protein interaction site of N-type Ca2+ channels. Neuron 1996; 17(4): 781-788.

Nicke A , Bäumert HG, Rettinger J, Eichele A, Lambrecht G, Mutschler E, Schmalzing G. $P2X_1$ and $P2X_3$ receptors form stable trimers: a novel structural motif of ligand-gated ion channels The EMBO Journal 1998; 17: 3016–3028.

O'Conner, VM, Shamotienko O, Grishin E, Betz H. On the structure of the 'synaptosecretosome.' Evidence for a neurexin/synaptotagmin/syntaxin/Ca^{2+} channel complex. FEBS Lett 1993; 326: 255-260.

Phillips GR, Huang JK, Wang Y, Tanaka H, Shapiro L, Zhang W, Shan WS, Arndt K, Frank M, Gordon RE, Gawinowicz MA, Zhao Y, Colman DR. The presynaptic particle web: ultrastructure, composition, dissolution, and reconstitution. Neuron 2001; 32(1): 63-77.

Stanley EF. Single calcium channels and acetylcholine release a presynaptic nerve terminal. Neuron 1993; 11(6): 1007-1011.

Szutowicz A, Frazier WA, Bradshaw RA. Subcellular localization of nerve growth factor receptors. Thirteen-day chick embryo brain. J Biol Chem 1976; 251(5): 1516-1523.

Table 2.1. MS/MS identification of spots enriched in either hydrophobic (H_1) or hydrophilic (H_3) fractions.

Spot ID	Protein name	Pubmed number	# peptides matched	Theoretical. M.W.	Protein location
H1-1	Heat Shock Protein Beta-1	P14602	5	27000	Cytoplasmic
	Hexokinase II	O08528	1	102500	Cytoplasmic
	Rab11b	gi49900	1	36400	Membrane Associated
H1-2	Heat shock Protein I	P14602	23	27000	Cytoplasmic
	Triosephosphate isomerase	P15711	5	26700	Cytoplasmic
	Desmin	P31001	2	35686	Cytoskeletal
H1-3	Glyceraldehyde-3-phosphate dehydrogenase	P16858	7	35800	Cytoplasmic
	Alpha crystallin B chain	P23927	3	20500	Cytoplasmic
	Glial fibrillary acidic protein	P03995	1	26400	Cytoskeletal

Table 2.1, continued.

Spot ID	Protein name	Pubmed number	# of peptides matched	Theoretical M.W.	Protein location
H1-4	Desmin	P31001	15	35686	Cytoskeletal
	Vitamin D binding Protein	P21614	1	26400	Cytoplasmic/actin associated
	Actin Gamma	P05271	2	41800	Cytoskeletal
	Transitional endoplasmic reticulum ATPase (Valosin containing)	Q08153	1	90100	Endoplasmic Reticulum
	Triosephosphate isomerase	P15711	5	26700	Cytoplasmic
H1-5	Glyceraldehyde-3-phosphate dehydrogenase	P16858	14	35800	Cytoplasmic
H3-1	Alpha crystallin beta	P23927	5	20100	Cytoplasmic
	Glyceraldehyde-3-phosphate dehydrogenase	Q8ECV2	3	34900	Cytoplasmic
H3-2	Alpha crystallin beta	P23927	5	20100	Cytoplasmic
	Glyceraldehyde-3-phosphate dehydrogenase	Q8ECV2	3	34900	Cytoplasmic

Table 2.2. Proteins identified by LC-MS-MS.

Mitochondrial proteins

Creatine kinase, sarcomeric mitochondrial precursor (Basic-type mitochondrial creatine kinase).
ATP synthase beta chain, mitochondrial precursor
ATP synthase alpha chain, mitochondrial precursor
Dihydrolipoyl dehydrogenase, mitochondrial precursor (Dihydrolipoamide dehydrogenase) (Glycine cleavage system L protein)
Pyruvate dehydrogenase E1 component alpha subunit, somatic form, mitochondrial precursor 2-oxoglutarate dehydrogenase E1 component, mitochondrial precursor (Alpha-ketoglutarate dehydrogenase)
Aconitate hydratase, mitochondrial precursor (Citrate hydro-lyase) (Aconitase)
Pyruvate dehydrogenase E1 component beta subunit, mitochondrial precursor
Aspartate aminotransferase, mitochondrial precursor (Transaminase A) (Glutamate oxaloacetate transaminase-2)
Propionyl-CoA carboxylase beta chain, mitochondrial precursor (PCCase beta subunit) (Propanoyl-CoA:carbon dioxide ligase beta subunit)
Dihydrolipoyllysine-residue acetyltransferase component of pyruvate dehydrogenase complex, mitochondrial precursor (Pyruvate dehydrogenase complex E2 subunit) (Dihydrolipoamide S- acetyltransferase component of pyruvate dehydrog
Electron transfer flavoprotein alpha-subunit, mitochondrial precursor (Alpha-ETF)
Isocitrate dehydrogenase
Short chain 3-hydroxyacyl-CoA dehydrogenase, mitochondrial precursor (HCDH) (Medium and short chain L-3-hydroxyacyl-coenzyme A dehydrogenase)
Citrate synthase, mitochondrial precursor
Fumarate hydratase, mitochondrial precursor (Fumarase)
Voltage-dependent anion-selective channel protein 1 (VDAC-1) (hVDAC1) (Outer mitochondrial membrane protein porin 1) (Plasmalemmal porin) (Porin 31HL) (Porin 31HM)
Cytochrome c1, heme protein, mitochondrial precursor (Cytochrome c-1).
Cytochrome c
Acyl-CoA dehydrogenase, long-chain specific, mitochondrial precursor (LCAD).
Stress-70 protein, mitochondrial precursor (75 kDa glucose regulated protein) (GRP 75) (Peptide-binding protein 74) (PBP74) (Mortalin) (MOT)

Cytoplasmic proteins

Beta enolase (2-phospho-D-glycerate hydro-lyase) (Muscle-specific enolase) (MSE). (Skeletal muscle enolase) (Enolase 3)
Creatine kinase, M chain (M-CK).
Fructose-bisphosphate aldolase A (Muscle-type aldolase) (Lung cancer antigen NY-LU-1).
Alpha crystallin B chain (Alpha (β)-crystallin) (Rosenthal fiber component) (Heat-shock protein beta-5) (HspB5)
Glyceraldehyde-3-phosphate dehydrogenase, liver (GAPDH).
UTP--glucose-1-phosphate uridylyltransferase 2 (UDP- glucose pyrophosphorylase 2) (UDPGP 2) (UGPase 2)
Fructose-bisphosphate aldolase C (Brain-type aldolase)
Glycogen phosphorylase, brain form
Glycogen phosphorylase, muscle form (Myophosphorylase)
Malate dehydrogenase, cytoplasmic

Table 2.2, continued.

L-lactate dehydrogenase B chain (LDH-B) (LDH heart subunit) (LDH-H).
T-complex protein 1, eta subunit (TCP-1-eta) (CCT-eta) (HIV-1 Nef interacting protein)
Glucose-6-phosphate isomerase (GPI) (Phosphoglucose isomerase) (PGI) (Phosphohexose isomerase) (PHI) (Neuroleukin) (NLK) (Sperm antigen-36) (SA-36)
Phosphoglycerate mutase 2 (Phosphoglycerate mutase isozyme M) (PGAM-M) (BPG-dependent PGAM 2) (Muscle-specific phosphoglycerate mutase)
Alpha-centractin (Centractin) (Centrosome-associated actin homolog) (Actin-RPV) (ARP1).
Fumarate hydratase, mitochondrial precursor (Fumarase)
Phosphoglucomutase (Glucose phosphomutase) (PGM)
Proteasome subunit alpha type 2 (Proteasome component C3) (Macropain subunit C3) (Multicatalytic endopeptidase complex subunit C3)
26S protease regulatory subunit 8 (Proteasome subunit p45) (p45/SUG) (Proteasome 26S subunit ATPase 5) (Thyroid hormone receptor interacting protein 1) (TRIP1)
T-complex protein 1, beta subunit (TCP-1-beta) (CCT-beta)
Glycogen debranching enzyme (Glycogen debrancher)
Proteasome subunit alpha type 6 (Proteasome iota chain) (Macropain iota chain) (Multicatalytic endopeptidase complex iota chain) (27 kDa prosomal protein) (PROS-27) (p27K)
Cytochrome c
Tubulin alpha-ubiquitous chain (Alpha-tubulin ubiquitous) (Tubulin K- alpha-1)
26S protease regulatory subunit 6A (TAT-binding protein 1) (TBP-1) (Proteasome subunit P50) Cylicin-1 (Cylicin I) (Multiple-band polypeptide I) (Fragment)
Myosin heavy chain, skeletal muscle, perinatal (MyHC-perinatal)
Myosin-binding protein C, slow-type (Slow MyBP-C) (C-protein, skeletal muscle slow-isoform).
26S proteasome non-ATPase regulatory subunit 3 (26S proteasome regulatory subunit S3) (Proteasome subunit p58)
Delta-aminolevulinic acid dehydratase (Porphobilinogen synthase) (ALADH)
26S proteasome non-ATPase regulatory subunit 13 (26S proteasome regulatory subunit S11) (26S proteasome regulatory subunit p40.5)
Tubulin beta-4 chain (Tubulin 5 beta) (Tubulin beta-4)
Proteasome subunit beta type 1 (Proteasome component C5) (Macropain subunit C5) (Multicatalytic endopeptidase complex subunit C5) (Proteasome gamma chain)
Aspartate aminotransferase, cytoplasmic (Transaminase A) (Glutamate oxaloacetate transaminase-1)
Proteasome subunit beta type 3 (Proteasome theta chain) (Proteasome chain 13) (Proteasome component C10-II)

Endoplasmic & sarcoplasmic reticular proteins

Sarcoplasmic/endoplasmic reticulum calcium ATPase 1 (Calcium pump 1) (SERCA1) (SR Ca (2+)-ATPase 1) (Calcium-transporting ATPase sarcoplasmic reticulum type, fast twitch skeletal muscle isoform) (Endoplasmic reticulum class 1/2 Ca (2+) ATPase)
Sarcoplasmic/endoplasmic reticulum calcium ATPase 2 (Calcium pump 2) (SERCA2) (SR Ca (2+)-ATPase 2) (Calcium-transporting ATPase sarcoplasmic reticulum type, slow twitch skeletal muscle isoform) (Endoplasmic reticulum class 1/2 Ca (2+) ATPase).
Transitional endoplasmic reticulum ATPase (TER ATPase) (15S Mg (2+)- ATPase p97 subunit) (Valosin-containing protein) (VCP).
Reticulon protein 2 (Neuroendocrine-specific protein-like 1) (NSP-like protein 1) (NSPLI)
Calsequestrin, skeletal muscle isoform precursor (Calsequestrin 1) (Calmitin)

Table 2.2, continued

Vesicular or plasma membrane proteins

Clathrin heavy chain 1 (CLH-17)
Leucyl-cystinyl aminopeptidase (EC 3.4.11.3) (Cystinyl aminopeptidase) (Oxytocinase) (OTase) (Insulin-regulated membrane aminopeptidase) (Insulin-responsive aminopeptidase) (IRAP) (Placental leucine aminopeptidase) (P-LAP).
Adenylyl cyclase-associated protein 1 (CAP 1).
Annexin A2 (Annexin II) (Lipocortin II) (Calpactin I heavy chain) (Chromobindin 8) (p36) (Protein I) (Placental anticoagulant protein IV) (PAP-IV).

Table 2.3. Table of western blots: Antibody & fractions tested.

Antibody	P2/H1 (*MW*)	P2/H3 (*MW*)	P3/H1 (*MW*)	P3/H3 (*MW*)
Synaptotagmin	+++ (*70*)	++ (*70*) ++ (*110*)	+ (*70*)	++ (*70*) + (*110*)
AChRα7	+ (*75*)	+++ (*75*)	+++ (*37*)	+ (*37*)
MuSK	+ (*37*)	+ (*37*)	++ (*37*)	+++ (*37*)
Neuregulin	++ (*50*) +++ (*75*) ++ (*250*)	++ (*50*)	++ (*50*) ++ (*100*)	+++ (*50*) +++ (*100*)
ERB-b2	++ (*25*) + (*170*)	+ (*25*) + (*75*) + (*170*)	+ (*25*) + (*75*) + (*170*)	+ (*75*) + (*170*)
ERB-b4	++++ (*25*)	++++ (*25*)	++++ (*25*)	++++ (*25*)
TRK-B	++ (*20*) + (*70*)	+ (*20*) ++ (*70*)	+ (*20*) + (*70*)	+ (*20*) ++ (*250*)
Synaptophysin	++ (*37*) + (*60*) +(70)	++(50) ++ (*60*) ++(70)	+++ (*37*) +(50) + (*60*)	+/- (*50*)
Syntaxin 1B	+++ (*67*)	++ (*67*)	+++ (*67*)	+ (*67*)
NGFRp75	+ (*50*)	++ (*50*)	+ (*50*)	+++ (*50*)
P2X7R	++ (47) +++ (*70*) ++ (*150*)	+++ (*47*) +++ (*70*) + (*150*)	+ (47) ++ (*70*) +++ (*150*)	+++ (47) +++ (*70*) +++ (*150*) +/- (250)
LAR	+++ (*40*)	+++ (*40*)	+++ (*40*)	+++ (*40*) ++ (*50*)
NGR-2	Not Visible	+ (*50*) + (*75*)	Not Visible	+ (*50*) + (*100*)
NGR-3	++ (*60*)	++ (*60*)	Not Visible	+ (*60*) + (*75*)
VAMP	+ (*17*)	Not Visible	+++ (*17*)	Not Visible
AP2	++ (*U/A*)	++ (*U/A*)	Not Visible	Not Visible

Note: All molecular weights are approximated by comparison to known molecular weight marker. Number of "+" indicates qualitative strength of visible band intensity; Numbers in () indicate MW of bands; U/A = Molecular weight not recorded.

Table 2.3, continued.

Antibody	P2/H1 (*MW*)	P2/H3 (*MW*)	P3/H1 (*MW*)	P3/H3 (*MW*)
SNAP-25	++ (*25*)	Not visible	Not visible	Not visible

Table 2.4. Additional proteins identified by western blot.

Antibody	P3	P2
Rim1	+	++
Dynamin	++	+
ACHE	+	+
CASK	++	Not tested
ERC-2	++	Not tested
α-β crystallin	+++	Not tested

Note: Number of "+" indicates qualitative strength of visible band intensity

Figure 2.1. Detergent solubilization protocol utilized for detergent fractionation. Phase separations performed after consecutive incubations at 4° and 37°C.

Figure 2.1. Detergent phase fractionation diagram.

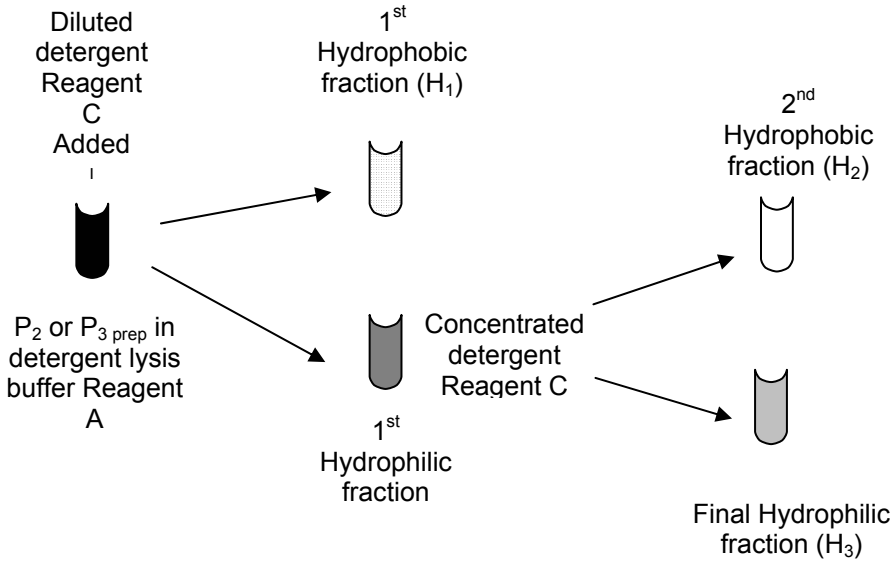

Figure 2.2. Two-dimensional gel of total P_3 sample from the neuromuscular junction enriched preparation of mouse diaphragm. Mouse diaphragm was fractionated through differential centrifugation into a final P_3 fraction. A 500 µg sample was then separated by 2-DE. Proteins separated on IPG strip 3-10 linear gradient.

Figure 2.2.

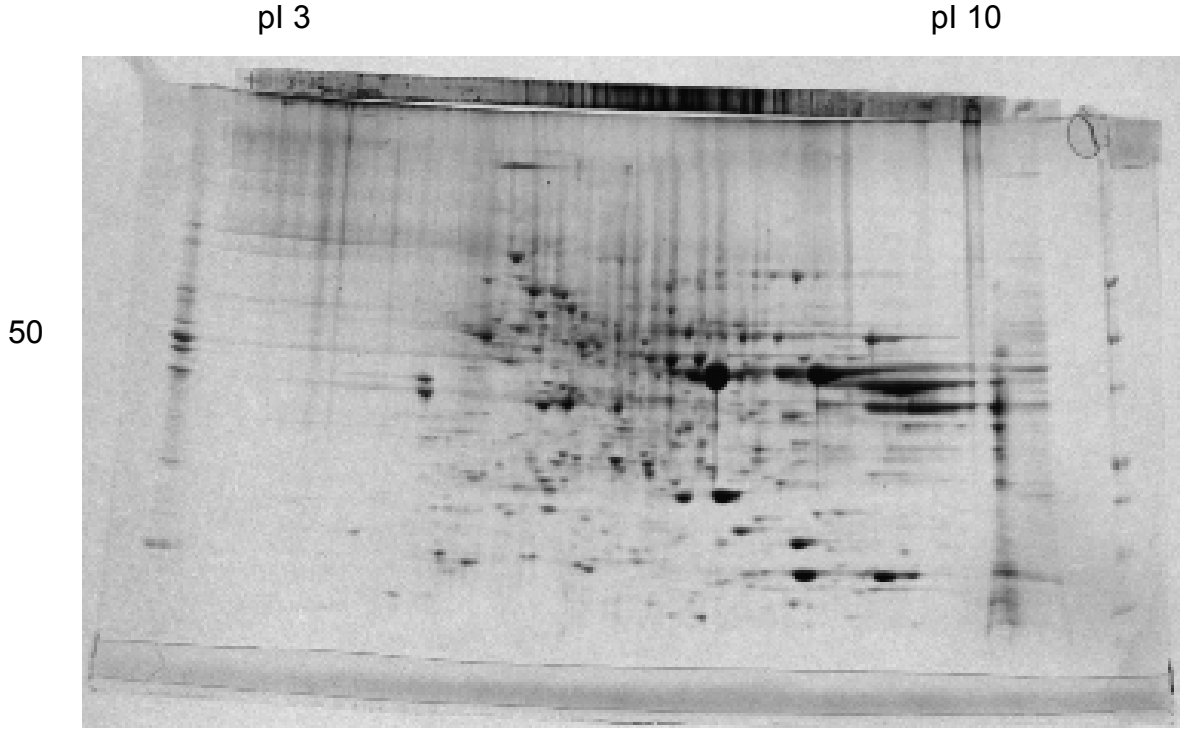

Figure 2.3A and 2.3B. Two dimensional gels of detergent fractionated P_3 samples. P_3 samples of mouse diaphragm (500 µg) were separated into hydrophobic (2.3A) and hydrophilic fractions (2.3B) through detergent phase partitioning. Proteins were then resolved utilizing 2-DE. Circled spots circled were submitted for MS-MS spectrometry identification.

Figure 2.3A.

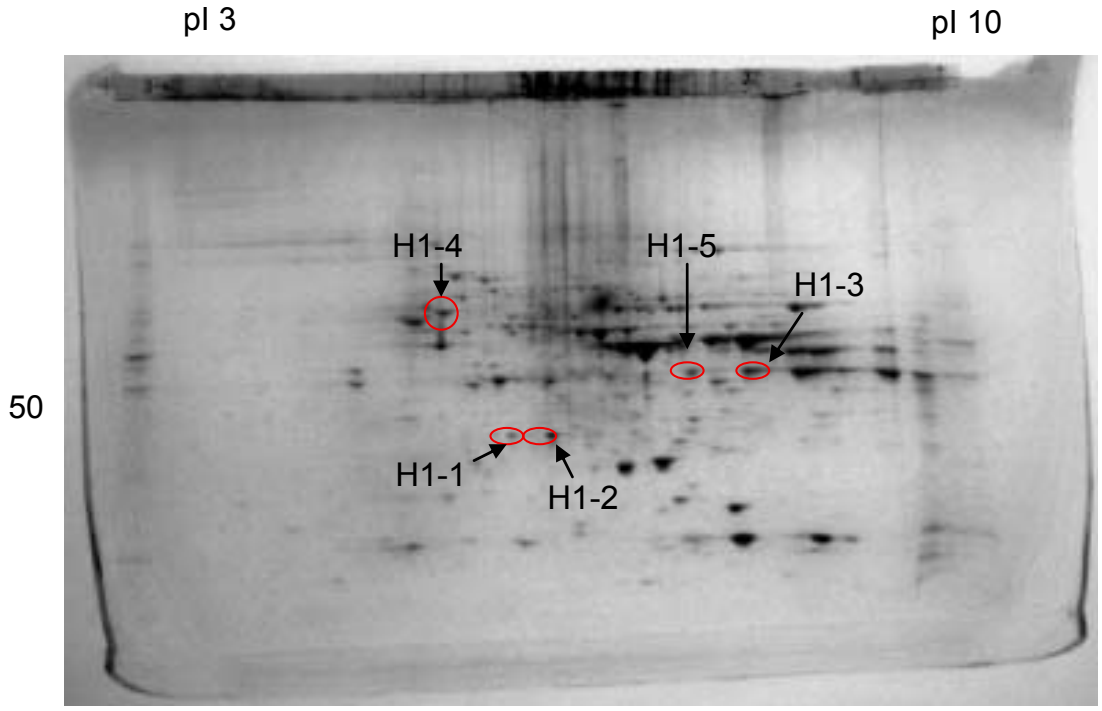

Figure 2.3B.

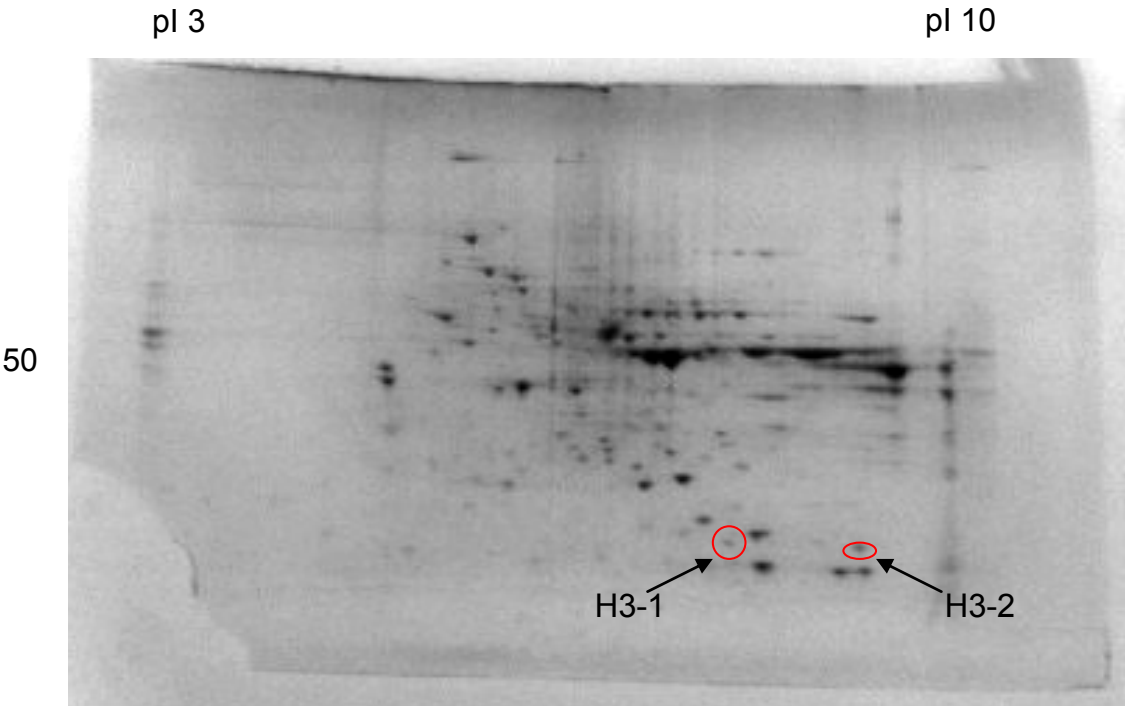

Figure 2.4. Two-dimensional gel of total P_2 sample from the neuromuscular junction enriched preparation of mouse diaphragm. Mouse diaphragm was fractionated through differential centrifugation into a final P_2 fraction. A 400 µg sample of this fraction was then separated by 2-DE. Proteins were separated on IPG strip 3-10 linear gradient.

Figure 2.4.

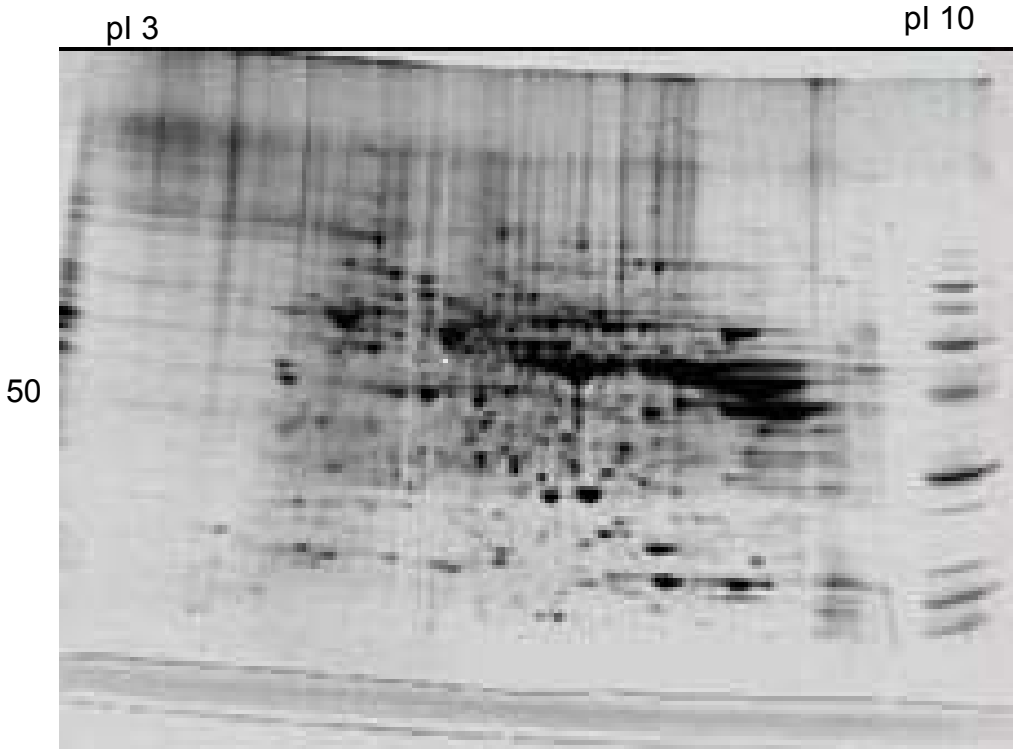

Figure 2.5A and 2.5B. Two dimensional gels of detergent fractionated P_2 samples. P_2 samples of mouse diaphragm (500 µg) were separated into hydrophobic (2.5A) and hydrophilic fractions (2.5B) through detergent phase partitioning. Proteins were then resolved utilizing 2-DE.

Figure 2.5A.

pI 3 pI 10

50

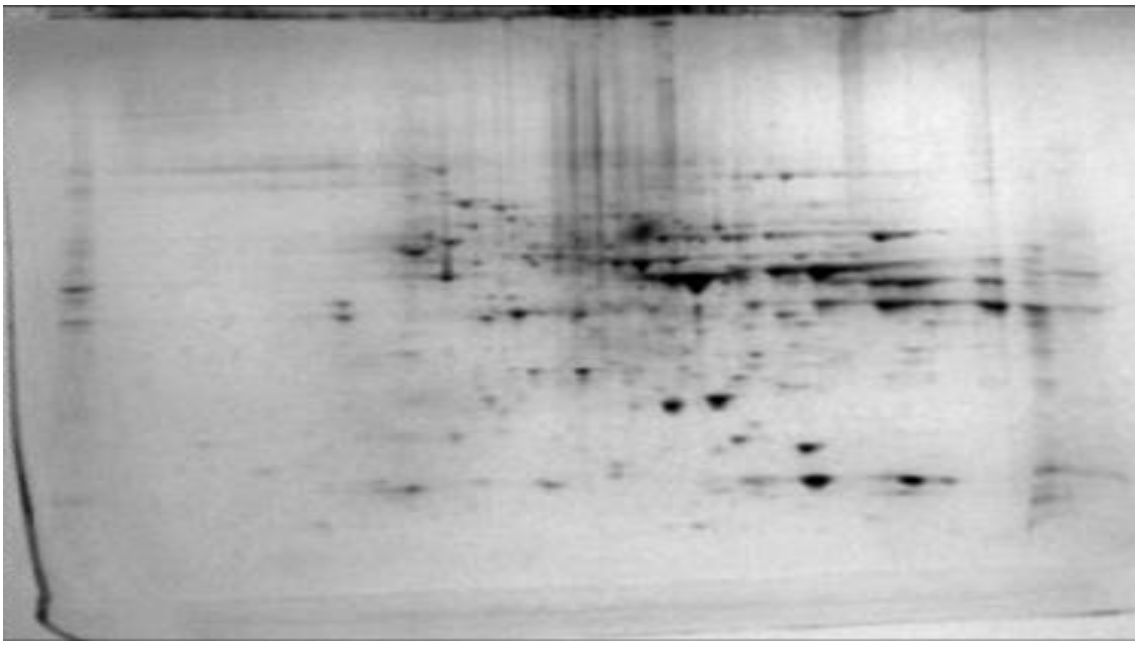

Figure 2.5B.

pI 3 pI 10

50

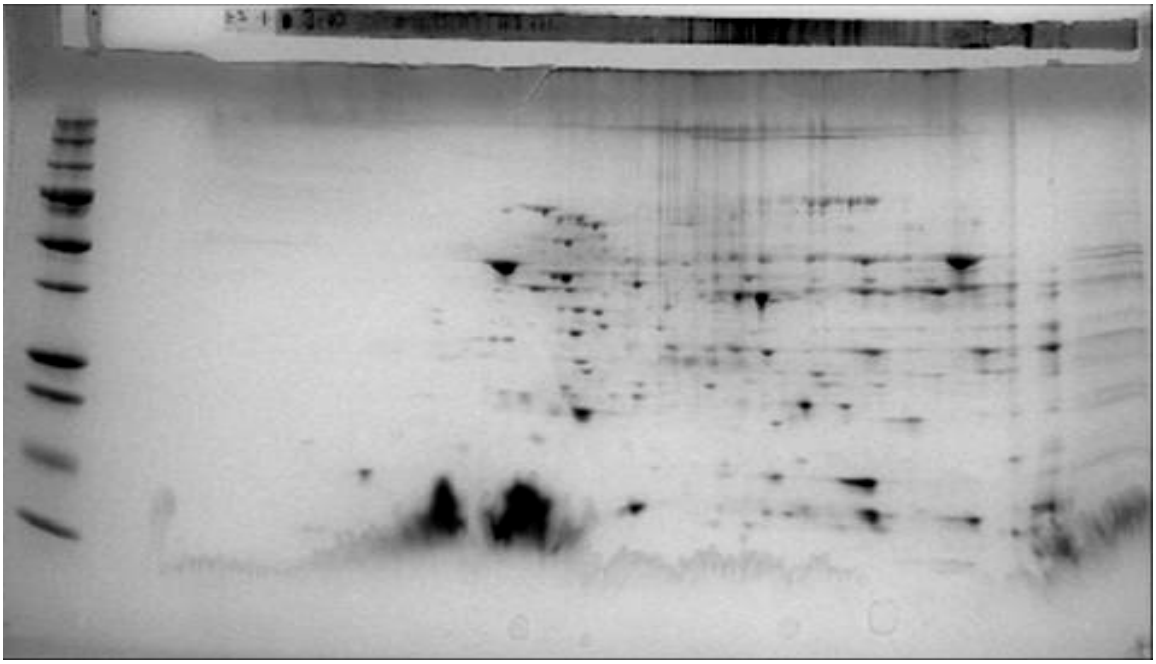

Figure 2.6. MuSK H_3 fractionation. 2-D electrophoresis of P_3 hydrophilic fraction. Linear patterned spots illustrate changes in pI possibly due to post-translational modifications.

Figure 2.6.

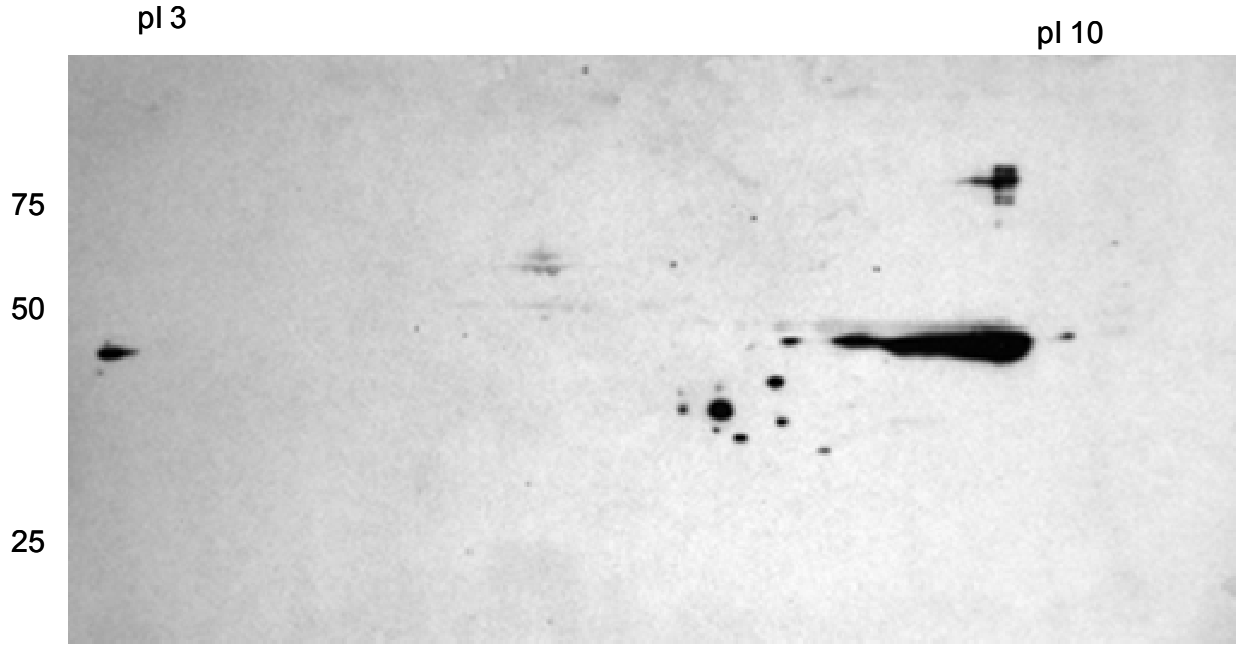

Figure 2.7. Detergent fractionation of P_3 and P_2 samples probed for synaptophysin (37kDa). This blot illustrates the higher molecular weight patterns, which may correlate to synaptophysin complexed with other proteins such as synaptobrevin.

Figure 2.7.

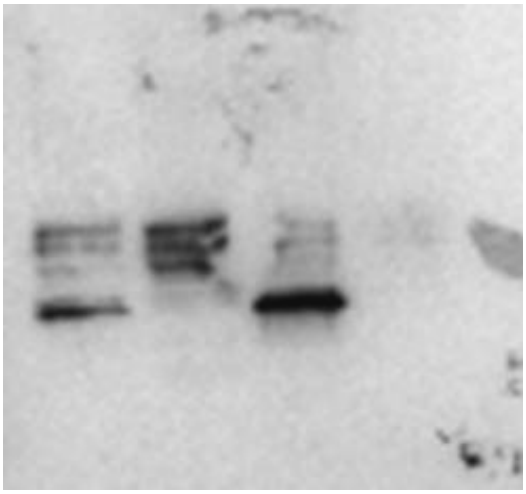

CHAPTER 3

THE USE OF PROTEOMIC TECHNIQUES TO ISOLATE AND IDENTIFY BOTULINUM TOXIN SEROTYPE A BINDING PROTEINS AT THE NEUROMUSCULAR JUNCTION[1]

[1] Parrott TM, Brooks PM, Vunnava A,Whelchel DD, Coffield JA. Manuscript to be submitted.

ABSTRACT

The overall goal of the studies reported in this chapter was to identify botulinum toxin serotype A (BoNT/A) binding proteins at the neuromuscular junction that could be investigated as potential toxin receptors in future studies. A combination of differential centrifugation and detergent phase partitioning was used to isolate synaptosomal fractions from diaphragm tissue. Affinity precipitation was utilized to investigate Botulinum serotype A protein-protein interactions in these membrane enriched fractions. Candidate binding proteins obtained through affinity precipitation were submitted for identification by tandem mass spectrometry (MS-MS). Results of MS-MS analyses were mixed with several protein identifications suggesting potential interactions of botulinum toxin (BoNT) with proteins localized to various intracellular compartments. However, the results did not yield specific identification of plasma membrane proteins. The potential reasons for this lack of plasma membrane protein identification were investigated and are discussed herein. In general, the findings suggest that even with the additional purification achieved by affinity precipitation, currently available proteomic methods employing mass spectrometry are inadequate to identify neuronal membrane proteins within a complex mixture.

INTRODUCTION

Botulinum toxin (BoNT), an extremely potent neurotoxin, is produced under anaerobic conditions primarily by the bacteria Clostridium botulinum. The cellular target of BoNT is the cholinergic nerve terminal of the peripheral nervous system, primarily the neuromuscular junction. Intoxication with BoNT causes botulism, an acute, afebrile disease characterized by a flaccid muscle paralysis due to inhibition of acetylcholine release. The toxin itself exists in seven distinct serotypes, A through G (see review by Collins and East, 1998). Each serotype is a specific protease with a distinct molecular target within the SNAP receptor (SNARE) complex, a protein complex required for membrane fusion. Cleavage of any of the three proteins that constitute this complex disrupts vesicular fusion, preventing neurotransmitter release from the synaptic vesicle (Link et al., 1994; Schiavo et al., 1992a, b; Blasi et a; 1993a; Schiavo et al., 1993a; Schiavo et al., 1994; Kalandakanond and Coffield, 2001). Death from botulism is due to respiratory paralysis. Simpson (1981) proposed a model of clostridial neurotoxin action in which toxin first binds to a serotype specific receptor, thought to be an integral plasma membrane protein, selectively located on the cholinergic nerve terminal. The toxin is then internalized through receptor-mediated endocytosis. Reduction of the disulfide bond linking the two primary chains of the toxin occurs in the endosome; the acidic conditions within the endosome promote the translocation of the toxin light chain to the cytosol, possibly through a pore formed by the toxin heavy chain in the endosomal membrane. The light chain then proceeds to cleave its serotype specific substrate.

The first plasma membrane constituents shown to bind BoNT were polysialogangliosides (Kitamura et al., 1980;; Kozaki, 1979; Bakry et al., 1991; Schengrund et al., 1991, Kozaki et al., 1998). These gangliosides, however, are unlikely to be the only toxin receptors because they are both widely distributed within the nervous system (i.e., non-selective) and reportedly bind toxin with low affinity (i.e., low potency). However, such binding may act to increase or facilitate the toxins exposure to a high affinity protein receptor site. Over the last fifteen years, a number of intriguing protein candidates has been proposed. In 1992, studies utilizing torpedo electric organ, a concentrated source of cholinergic nerve terminals, demonstrated binding of ^{125}I labeled toxin A and toxin A-gold complexes to a unidentified140 kDa protein (Blasi et al, 1992). Other studies utilizing brain synaptosomes have identified two different proteins that demonstrated ganglioside dependent binding to BoNT serotype A. In these initial binding experiments two separate proteins, one at ~80 kDa and the other at ~116 kDa were observed. These proteins were subsequently identified as adducin and synapsin (Schengrund et al., 1993, 1996). However, neither of these proteins have extracellular domains, making them unlikely candidates for toxin receptors.

Evidence from studies using both target and non-target tissues suggested that the synaptic vesicle proteins synaptotagmin I and II were functional binding proteins for botulinum toxin serotype B (BoNT/B; Nikishi et al., 1994; Nikishi et al., 1996a; NIkishi et al., 1996b). In support of this, concurrent studies reported that the n-terminus of synaptotagmin II was presented extracellularly during stimulus-evoked exocytosis (Angaut-Petit et al., 1995; 1998). However, other studies performed in brain

synaptosomes reported that serotypes A and E also bound to synaptotagmin I (Li and Singh, 1998). Very recently it was reported that serotype G also binds to synaptotagmin I and II in a phrenic nerve-hemidiaphragm preparation (Rummel et al., 2004). Collectively, these results are inconsistent with previous reports indicating that the pattern of toxin binding to cholinergic nerve terminals is serotype specific, and that intoxication with one serotype does not block intoxication with another (Black and Dolly 1986a;1986b). While these studies have demonstrated important concepts regarding toxin binding, further research is needed to address the relevance of these binding proteins to toxin action at its actual target site. To achieve this, the experimental model chosen must allow for the assessment of toxin activity. Therefore, it is imperative that characterization of BoNT binding proteins include studies that utilize functional assays in target tissues, particularly at the mammalian neuromuscular junction, which is the clinically relevant site of toxin action.

Recent research in our laboratory using electrophysiologic assessment of toxin-induced paralysis and substrate proteolysis has demonstrated the inability of synaptotagmin antibodies and synthetic peptides to antagonize BoNT/A activity at the murine neuromuscular junction. These data indicate that synaptotagmin I is unlikely to be the functional receptor for this particular toxin serotype. The overall goal of the studies reported in this chapter was to identify BoNT/A binding proteins at the neuromuscular junction that could be investigated as potential toxin receptors in future studies. To achieve this, we employed state of the art proteomic techniques.

Differential centrifugation and non-ionic detergent solubilization of the murine diaphragm preparation were used to obtain fractions that were enriched with pre- and

postsynaptic membrane and membrane associated proteins (previously discussed in chapter 2). Binding proteins were isolated from these membrane enriched fractions by affinity precipitation using agarose beads coupled with BoNT/A in a manner that exposed the toxin binding domain (toxin heavy chain). Candidate binding proteins, obtained using affinity precipitation, were submitted for identification through tandem mass spectrometry. The initial results of these studies were varied, necessitating several modifications in procedures that are discussed herein. In general, the findings suggest that even with the additional purification achieved by affinity precipitation, currently available proteomic methods employing mass spectrometry are inadequate to identify neuronal membrane proteins within a complex mixture.

METHODS

Tissue preparation and membrane protein enrichment

The protocols for these steps have been described in detail in the preceding chapter. Briefly, diaphragm tissue from 158 NIH Swiss mice were homogenized and processed to obtain neuromuscular junction enriched membrane fractions. Tissues were homogenized in 1mL of homogenizing buffer (EDTA 2 mM, Sucrose 250 mM, 2mM HEPES), then spun at 5,000 X g for 5 min to remove cellular debris. The supernatant was removed and spun at 10,000 X g for 10 min to remove nuclear debris. The resulting supernatant was spun a final time in order to obtain a synaptic membrane enriched preparation (P_3). This membrane-enriched preparation was fractionated with detergent using the Mem-Per Kit (Pierce Biochemical; Rockford, IL) to further solubilize and partition membrane proteins into enriched fractions.

Membrane fractionation and enrichment from rabbit

The diaphragms from two New Zealand White rabbits were homogenized and processed through the membrane enriched fraction. In short, each diaphragm was homogenized in 30 mL of homogenizing buffer (EDTA 2 mM, Sucrose 250 mM, 2 mM HEPES), then spun at 5,000 X g for 5 min to remove cellular debris. The supernatant was removed and spun at 10,000 X g for 10 min to remove nuclear debris. A 10 mL sample of the resulting supernatant was spun a final time in order to create a crude membrane preparation (P_3). These pellets were reconstituted with a total of 2.5 mL of lysis buffer. This membrane-enriched preparation was fractionated with detergent using the Mem-Per Kit (Pierce Biochemical; Rockford, IL) to further solubilize and partition membrane proteins into enriched fractions.

Affinity precipitation using amino-link beads

Affinity precipitation was performed with the Pierce Seize–X kit (Pierce Biochemical; Rockford, IL). Amino-link beads were chemically coupled with botulinum toxin serotype A (BoNT/A, 1µg/µL) through the amine terminus of the toxin light chain. This permitted the carboxyl terminus of the toxin heavy chain (containing the receptor binding site) to remain exposed. To achieve this, 1,500 µL of bead slurry were incubated with 1,500 µL of purified toxin or toxin complex (Metabiologics; Madison, WI) and 15 µL of sodium cyanoborohydride for 5 h. As a control, 1,500 µL of bead slurry were incubated with 1,500 µL of Dulbecco's Phosphate Buffered Saline (DPBS) at pH of 7.6 and 15 µL of sodium cyanoborohydride for 5 h. The beads were washed once with DPBS and once with a quenching buffer consisting of 1M Tris at pH of 7.0. Each set of beads was then incubated in 1,500 µL of quenching buffer and 15 µL of sodium

cynanoborohydride for an additional 30 min. After incubation, the beads were washed four times with 1M NaCl at pH of 7.0, then three times with DPBS. In initial experiments beads were incubated with ovalbumin, normal goat serum or quenched with a 1M glycine solution in an attempt to reduce non-specific binding in control beads.

Equal volumes of sample were added to control or toxin-coupled beads. Following 4 h incubation on a rotator at room temperature, the beads were spun to remove the unbound sample. The beads were then washed four times with DPBS containing 1% TRITON X-100 to remove non-specifically bound proteins. Bound proteins were eluted through 4 cycles utilizing 1 µL of elution buffer/1µL settled bead. Eluted proteins were then precipitated with acetone on ice for 1h and spun for 30 min at 12,000 X g. Acetone was removed and the pellet allowed to air dry.

Two-dimensional electrophoresis (2-DE)

2-DE was performed as previously described (Chapter 2). Coomassie stained gels were imaged and protein spots selected for further analysis. Gel spots were cored and submitted to Ohio State Proteomics facility for protein identification by electrospray ionization quadropole tandem mass spectrometer through peptide fingerprinting.

SDS-Page electrophoresis

Acetone precipitated pellets were solubilized in sample buffer with 5% mercaptoethanol. Samples were boiled (5 min), loaded onto 10-20% Tris-HCl precast gels (Bio-Rad; Hercules, CA) and resolved at 200 V for 55 minutes. Gels were washed once with TBS and then fixed for 1 h in methanol. Gels were then stained with colloidal coomassie blue overnight. The next day gels were destained in 25% methanol. Bands

of interest were excised from the gel and submitted to Ohio State Proteomics Facility for identification.

LC-MS-MS analysis

The mouse diaphragm elutions were subjected to acetone precipitation and the pellets were sent directly to Michigan State Proteomics Facility. Protein identification was performed utilizing nanospray LCQ XP ion-trap mass spectrometer.

RESULTS

Sample fractionation and 2-DE

Initial affinity precipitation experiments utilizing total (unfractionated) P_3 fractions demonstrated a significant degree of non-specific binding as illustrated in Figure 3.1A. Standard methods to reduce non-specific binding such as increased number of washes, washes with higher salt concentrations, or 1M glycine did not reduce significantly this background. The elutions resulting from these conditions are shown in Figure 3.1B. For this reason, it was necessary to further fractionate the membrane-enriched sample with detergent. Figure 3.1C illustrates the outcome of a precipitation using the hydrophobic fraction obtained by detergent separation of the P_3 sample. The non-specific binding observed in the control was reduced sufficiently by this treatment, enabling the determination of differences between toxin and control precipitations. Greater differences between these precipitations were evident when the more sensitive silver stain was used for detection as shown in Figure 3.2; however, initial MS screening for proteins determined that the quantity of protein in these silver stained spots was insufficient for identification. Thus, it was apparent that protein quantities detectable by the less sensitive Coomassie stain (µg quantities) were needed for MS analyses. To

achieve this, it was necessary to obtain tissue homogenates of approximately 40 mg total protein (96 mice), which were then fractionated by centrifugation and detergent separation, and processed through affinity precipitation. A comparison of matched control and toxin precipitated fractions indicated a number of differences, including differences in protein spot pattern, as well as differences in spot intensity. For example, differences in spot intensity were apparent for two closely apposed spots of approximately 25 kDa, with an increased intensity noted in the toxin precipitated hydrophobic (H_1) fraction (as shown in Figure 3.3B), when compared to controls of the same fractions (shown in Figure 3.3A). Other differences in spot pattern were discernable between 50-100 kDa and pI 8-10 between these same two gels. The elution from toxin precipitation of the hydrophobic H_2 fraction (Figure 3.4A) also demonstrated a strong spot pattern from pI 4-6, between 20 and 50 kDa, when compared with control H_2 fraction (not shown). One spot from the toxin precipitated hydrophilic fraction (shown in Figure 3.5A) differed from those in the control. Spots that differed between control and toxin precipitated fractions were submitted for further MS analyses.

Mass spectrometry identification of individual spots from mouse diaphragm

The results from the MS analyses are detailed in Tables 3.1 and 3.2. A total of 22 spots were submitted. Protein identification was variable with approximately 50% of the submitted spots identified. The two 25 kDa protein spots in the toxin precipitated fractions that appeared increased in intensity were both identified as α-β crystallin. A few of the spots were identified as hemagglutinin proteins and originated from the toxin preparation itself, since initial experiments utilized toxin complex rather than purified

toxin. These toxin associated components were not adequately removed by washing, but were removed during elution. Even with the increased load of protein in the starting sample, many of the smaller Commassie stained spots did not contain enough protein for MS identification.

In an effort to enhance identification of spots of interest in 2-D gels from the precipitated fractions, these gels were matched with gels from detergent fractionated P_3 samples that had not been subjected to affinity precipitation, and hence had a much greater protein content. Spots such as α-β crystallin were used as landmarks in this matching process. Matched spots of interest were cored from the non precipitated sample gels and submitted for MS identification. Utilization of this method increased the yield of spot identification slightly, with approximately 60% of the spots being identified. Interestingly, the majority of identified proteins originated from the hydrophilic fraction and were mainly cytoplasmic high abundant proteins (see Table 3.4).

Since only one spot out of four from the hydrophobic fraction was identified (Table 3.3), detergent interference was thought to be a factor. To address this possible interference, comparisons were also made to unfractionated P_3 gels shown in Figure 3.7. Proteins identified using this approach, are listed in Table 3.5. In general, while it was apparent that MS identification of proteins obtained by affinity precipitation was limited by protein load, it was also evident that plasma membrane proteins in particular were being excluded from MS identification.

One dimensional electrophoresis and rabbit diaphragm

Due to the technical limitations encountered with the mouse diaphragm tissue, it was clear that a different approach was needed. To further increase the protein in the

starting tissue, it was necessary to switch from the mouse to a much larger species, the rabbit. Further, because of the particular lack of membrane proteins in the MS data, it was suggested by the OSU Proteomics Facility that the 2-DE approach be abandoned in favor of 1-DE. The results of this approach are illustrated in Figures 3.8A and 3.8B for the hydrophobic fraction, and Figures 3.9A and 3.9B for the hydrophilic fraction. SDS-PAGE of each of the precipitated, fractionated rabbit P_3 samples demonstrated a few bands of greater intensity in the toxin precipitated fraction compared with control. All bands were excised and submitted, since 1-D bands contain multiple proteins, and differences in low abundant proteins between treatments may not be visualized. Approximately 50% of the bands from each treatment were identified. Details of the results of MS identification are found in Table 3.6 and 3.7. Since many of these identifications were based on small numbers of peptide fragments and low sequence coverage, other forms of protein identification will be necessary for confirmation.

MS analyses of affinity precipitation elutions

Because of the notable lack of plasma membrane proteins identified by MS in the mouse data, we decided to alter our approach somewhat by completely eliminating the gel electrophoresis step. Our primary concern was that hydrophobic proteins may actually be forming insoluble aggregates within the IPG strips. Utilizing this approach, the protein containing elutions from both control and toxin precipitations were submitted directly for MS identification. Proteins that were identified in the toxin exposed samples but not in control samples are listed in Table 2.7. Note that for two peptide sequences there are no protein matches.

DISCUSSION

The overall goal of the studies reported in this chapter was to identify BoNT/A binding proteins at the mammalian neuromuscular junction that could be investigated as potential toxin receptors in future studies. To achieve this, we employed state of the art proteomic techniques. Previous work on BoNT receptors has been limited to non-target tissues such as the CNS or cell lines (Li and Singh, 1998, Nishiki et al., 1994; 1996a; 1996b). This is understandable; since neuromuscular tissue preparations are quite complex and the ratio of neural to muscle protein is extremely low. Unfortunately, while this work has been highly informative, evidence from more traditional BoNT binding studies (Black and Dolly, 1986a; 1986b) suggest that binding within the CNS differs from that in the toxin target tissue, the neuromuscular junction. Thus, it is necessary that studies of BoNT binding and receptor identification be extended to the neuromuscular junction.

Over the past several decades, the mouse diaphragm muscle has been the tissue preparation of choice for much of the toxicological investigation of botululinum toxin action. This is due mainly to the exquisite sensitivity of the mouse to all of the toxin serotypes, as well as the unique anatomy of the diaphragm (thin, flat), and the organized pattern of neural innervation which makes visualization of the endplate regions reasonably easy. Because of this unique pattern of innervation, the diaphragm muscle has a much higher concentration of neuromuscular junction regions than other muscle. Careful isolation and preparation of the tissue results in a sample that is relatively high in neural protein compared with other muscle samples. Thus, to achieve the goal of this study, the mouse diaphragm tissue was used as the source of BoNT

receptor protein. Isolation of binding proteins from this tissue was performed by affinity precipitation. Identification of toxin binding proteins was performed by tandem mass spectrometry.

The results of the initial experiments of these proteomic studies revealed an unacceptable level of non-specific binding to the affinity precipitation beads. The most likely explanation for this was incomplete membrane solubilization resulting in the nonspecific binding of large protein complexes to the bead matrix. Subsequent modifications in the experimental protocol demonstrated that detergent fractionation of a complex tissue sample significantly reduced non-specific binding, revealing differences between control and toxin exposed samples. This was due most likely to the increased membrane solubilization and the resultant release of individual proteins. Triton-X 114, one of the components in the Pierce MemPer Kit, has been shown to be beneficial since its use results in micelle formation and separation of proteins, while allowing most of the proteins to maintain their confirmation and function. This was an important consideration in our work since we were interested in functional protein-protein interactions.

In the experiments involving two-dimensional electrophoresis, a number of differences between the toxin and control precipitations were evident in silver stained gels. However, in most instances, the proteins associated with these differences were not identifiable due to the reduced sensitivity of LC-MS-MS compared with silver stain. Increasing the starting protein amount prior to affinity precipitation resulted in an increase in the eluted protein that was detectable by Coomassie stain. Unfortunately, this rather significant increase in protein resulted in only a minimal increase in MS-MS identification. A few spots yielded single peptide fragments that did not match to a

specific protein, even when matched to the best possible match generated by programs such as MASCOT. Termed 'one hit wonders', due to only a single peptide match, these matches have been archived for further analysis if future experiments demonstrate their continued presence.

Matching of protein spots from affinity precipitation samples with those from P_3 and P_2 fractions resulted in the identification of previously unidentified spots. Several of these identifications were informative in that they matched to conserved regions recognized as cell signaling domains including: a protein kinase, a tyrosine phosphatase, and a Src domain. Since these matches were to single peptides of conserved regions, specific protein identification was unlikely. However, it is notable that these conserved signaling domains are found in plasma membrane or membrane associated proteins.

In general, however, identification of membrane protein was variable, with only a few spots identified as subcellular organelle membrane proteins such as those associated with mitochondria, endoplasmic reticulum, or endosomes. This coupled with the fact that only approximately 50% of the submitted protein spots were identified suggested that we needed to increase the amount of starting protein used in the affinity precipitation assays. In addition, current research in membrane proteomics indicates that 2-DE of membrane proteins may be undesirable due to their tendency to precipitate at their pI and form insoluble aggregates. Altering the experimental protocol by using rabbit diaphragm muscle and single dimension SDS-PAGE did not significantly improve the results. For instance, only single peptide matches were made for most protein identifications. Further, for each gel band examined, significant matches resulted for

only a single protein, usually a protein of high abundance. This was surprising since examination of 2-D gels reveals many protein spots. These results indicate that this methodology, while increasing the number of peptide hits did not result in a significant increase in reportable protein identification, nor did it result in any type of reasonable identification of plasma membrane proteins. It should be noted however, that these findings were complicated by the fact that the rabbit database is relatively incomplete compared to that of the mouse. The impact of an incomplete protein database on our findings is illustrated by the observation that of most of the identified proteins consisted of highly abundant enzymes of metabolism found in the cytoplasm. Although these proteins are associated mainly with muscle, their association with neural tissue can not be ruled out.

There were similarities in the protein identification between mouse and rabbit. Two abundant cytoplasmic proteins identified included the chaperone protein α-β crystallin and glyceraldehyde 3-phosphate dehydrogenase (GAPDH). The identification of GAPDH in both species was intriguing in that it was localized to spots that were extremely different in pI. One spot was located at pI ~5 and the other at ~8. Differences in pI are reported to correspond to differences in protein localization as well as function. The GAPDH protein identified at the more alkaline pI is thought to be glycosylated and membrane bound. Interestingly, functional studies have demonstrated a role for the glycosylated form of GAPDH in membrane fusion (see review by Sirover, 1999).

Several cellular functions have been ascribed to the crystallins; the majority of which pertain to the maintenance of protein conformation and function under conditions

of cellular stress such as heat or an acidic pH. Small heat shock proteins have also been implicated in apoptosis, as well as in the ubiquination-proteosome pathways. While crystallins exist in skeletal muscle associated with the cytoskeleton, α-β crystallin is ubiquitously expressed, and is also found in neural tissue. In particular, small heat shock proteins tend to interact with intermediate filament proteins. Neuronal filament proteins have demonstrated roles in axonal sprouting during initial neurite outgrowth, or during regeneration. Neuronal cytoskeletal proteins may also be associated with synaptic organization, including the transport of organelles such as synaptic vesicles.

The increased amount of α-β crystallin in the toxin affinity precipitation samples may offer some interesting insight into toxin transport. As stated previously, BoNT is thought to be internalized through receptor mediated endocytosis. These endosomes will likely not only contain the receptor, but other endosomal associated proteins including neurofilament and neurofilament associated proteins. Eluted samples from the toxin precipitations may include non-specific proteins that remain associated with the receptor in the membrane. In addition, the endosomal associated crystallin may interact with the toxin heavy chain domain as a chaperone, keeping the light chain properly folded as it is translocated from the endosome to the cytosol. Obviously, further research is necessary to determine whether the potential interactions of BoNT/A with α-β crystallin revealed here have any functional significance in membrane translocation, or if it is merely an artifact of endosomal protein isolation.

As indicated earlier, there were several peptides that corresponded to conserved domains of different functional groups of membrane proteins. These peptide fragments, however, did not offer enough sequence coverage to identify specific proteins or to be

confidently reported. Interestingly, a number of neurospecific proteins are associated with these protein domain families. For instance, a peptide sequence for the MAGUK family of proteins was identified in both toxin precipitated samples of mouse diaphragm that were not subjected electrophoresis, as well as in protein spots cored from 2-D gels of total P_3 samples that had been matched to corresponding gels of toxin precipitated samples. The MAGUK proteins, especially PSD 95 on the postsynaptic side and CASK on the presynaptic side, have been implicated in a role for structural organization of the active zone. These proteins have three different protein-protein interaction domains including a calmodulin domain, SH3 domain, and a PDZ domain, enabling multiple interactions to form a protein scaffold at the synapse. Other single peptide matches of interest included an annexin precursor protein and a weak match to a domain corresponding to FGF protein. Annexins are membrane proteins that are associated with calcium binding and cell-cell interactions. Annexins demonstrate isoform specificity among cell types, with isoform two demonstrating a possible role in lipid raft formation and exocytosis of dense core vesicles (Chasserot-Golaz et al., 2005). The FGF proteins are growth factor proteins that are found in several different cell types. They have been shown to demonstrate many functions including a possible role in neurogenesis. Similarly, another weak peptide match corresponding to the Ig-like domain of Siglec proteins represents another interesting prospective membrane protein. The Siglecs are typically identified in leukocytes and neural tissue, and are involved in cellular interactions. One neurospecific Siglec protein of great interest, known as myelin associated glycoprotein, reportedly binds to the same family of complex

trisialogangliosides on the axon as does BoNT, and interacts with the Nogo receptors to inhibit neurite growth.

Although some rather intriguing peptide matches were made suggesting the potential for the interaction of BoNT/A with plasma membrane cell signaling proteins, as well as endosomal chaperone proteins, the overall results of these proteomic studies were somewhat disappointing. Most membrane protein matches were limited to single peptide matches of conserved protein domains. Significant, multiple peptide matches were found only for highly abundant or cytoplasmic proteins. We are at a loss to explain why easily detectable Coomassie stained spots should yield so little identification. While there was little difference in the proteins identified in the hydrophobic versus the hydrophilic fractions, identification from the hydrophobic fraction appeared to be more sporadic. The latter may be explained by the recent suggestion from at least one proteomics facility that even minute amounts of detergent in a sample may interfere with MS-MS, decreasing the success of protein identification. Clearly, state of the art proteomic methods are 'state of the art' only for a limited number and types of proteins, e.g. highly abundant, cytoplasmic proteins from non-complex samples. Proteomics of membrane proteins remains in its infancy. Thus, studies to identify membrane receptors in complex tissues will need to employ other methods in addition to proteomics.

REFERENCES

Angaut-Petit D, Molgo J, Faille L, Juzans P, Seager MJ, Takahashi M. Mouse motor nerve terminal immunoreactivity to synaptotagmin II during sustained quantal transmitter release. Brain Res 1995; 681: 213-217.

Angaut-Petit D, Molgo J, Faille L, Juzans P, Takahashi M, Incorporation of synaptotagmin II to the axolemma of botulinum type A-poisoned mouse motor endings during enhanced quantal acetylcholine release. Brain Res 1998; 797: 357-360.

Bakry N, Kamata Y, Simpson LL. Lectins from Triticum Vulgaris and Limax Flavus are universal antagonists of botulinum neurotoxin and tetanus toxin. J Pharmacol Exp Ther 1991; 258: 830-836.

Black JD, Dolly O. Interaction of ^{125}I-labeled botlinum neurotoxins with nerve terminals. I. Ultrastructural autoradiographic localization and quantitation of distinct membrane acceptors for types A and B on motor nerves. J Cell Biol 1986a; 103: 521-534.

Black JD, Dolly O. Interaction of ^{125}I-labeled botlinum neurotoxins with nerve terminals. II. Autoradiographic evidence for its uptake into motor nerves by acceptor mediated endocytosis. J Cell Biol 1986b; 103: 535-544.

Blasi J, Chapman ER, Link E, Binz T, Yamasaki S, De Camilli P, Sudhof TC, Niemann H, Jahn R. Botulinum neurotoxin A selectively cleaves the synaptic protein SNAP-25. Nature 1993a; 365: 160-163.

Blasi J, Egea G, Castiella MJ, Arribas M, Solsona C, Richardson PJ, Marsal J. Binding of botulinum neurotoxin to pure cholinergic nerve terminals isolated from the

electric organ of torpedo. J Neural Transm Gen Sect 1992; 90: 87-102.

Chasserot-Golaz S, Vitale N, Umbrecht-Jenck E, Knight D, Gerke V, Bader, MF. annexin 2 promotes the formation of lipid microdomains required for calcium-regulated exocytosis of dense-core vesicles. Mol Biol Cell 2005; 16(3): 1108-1119.

Collins MD, East AK. Phylogeny and taxonomy of the food borne pathogen Clostridium botulinum and its neurotoxins. J Appl Microbiol 1998; 84: 5-17.

Der Perng M, Wen SF, van den IJssel P, Prescott AR, Quinlan RA. Desmin aggregate formation by R120G α-B-crystallin is caused by altered filament interactions and is dependent upon network status in cells. Mol Biol Cell 2004; 15(5): 2335-2346.

Kalandakanond S, Coffield JA. Cleavage of intracellular substrates of botulinum toxin A, C, and D in a mammalian target tissue. J Pharmacol Exp Ther 2001; 296: 749-755.

Kitamura M, Iwamori, M, Nagai Y. Interaction between Clostridium botulinum neurotoxin and gangliosides. Biochem Biophys Acta 1980; 62: 328-335.

Kozaki S, Kamata Y, Watari S, Nishiki T, Mochida S. Ganglioside Gt1b as a complementary receptor component for Clostridium botulinum neurotoxins. Microbial Pathogenesis 1998; 25: 91-99.

Kozaki S. Interactions of botulinum toxin A, B, and E derivative toxins with synaptosomes of rat brain. Naunyn-Scmiedebergs Arch Pharmacol 1979; 308: 67-70.

Li L, Singh, BR. Isolation of synaptotagmin as a receptor for types A and E botulinum neurotoxin and analysis of their comparative binding using a new microtiter plate

assay. J Nat Toxins 1998; 7: 215-226.

Link E., Blasi J, Chapman, ER, Edelmann L, Baumeister A, Binz T, Yamasaki S, Neimann H, Jahn R. Tetanus and botulinal neurotoxins: Tools to understand exocytosis in neurons. Adv Second Messenger Phosphoprotein Res 1994; 29: 47-58.

Nikishi T, Kamata Y, Nemoto Y, Omori A, Ito T, Takashi M, Kozaki S. Identification of the protein receptor for clostridium botulinum type B neurotoxin in rat brain synaptosomes. J Biol Chem 1994; 269: 10498-10503.

Nikishi T, Tokuyama Y, Kamata Y, Nemoto T, Yoshida A, Sekiguchi M, Takahashi M, Kozaki S. Binding of botulinum type B neurotoxin to chinese hamster ovary cells transfected with rat synaptotagmin I cDNA. Neurosci Lett 1996b; 208: 105-108.

Nikishi T, TokuyamaY, Kamata Y, Nemoto Y, Yoshida A, Sato K., Sekiguchi M, Takahashi M, Kozaki S. The high affinity binding of clostridium botulinum type B neurotoxin to synaptotagmin I associated with gangliosides Gt1b/Gd1a. FEBS Lett 1996a; 378: 253-257.

Rummel A,KarnathT,Henke T,Bigalke H, Binz T. Synaptotagmins I and II act as nerve cell receptors for botulinum neurotoxin G. J Biol Chem 2004; 279(29): 30865-30870.

Schengrund CL, DasGupta B, Hughes CA, Ringler NJ. Ganglioside-induced adherence of botulinum and tetanus neurotoxins to adducin. J Neurochem 1996; 66(6): 2556-2561.

Schengrund CL, Dasgupta BR, Ringler NI. Binding of botulinum and tetanus neurotoxins to ganglioside GT1b and derivatives thereof. J Neurochem 1991; 57:

1024-1032.

Schengrund CL, DasGupta BR, Ringler NJ. Ganglioside GD3 enhances adherence of botulinum and tetanus neurotoxins to bovine brain synapsin. Neurosci Letters 1993; 158: 159-162.

Schiavo G, Benfenati F, Poulain B, Rossetto O, Polverino De Laureto P, Dasgupta BR, Montecucco C. Tetanus and botulinum-B neurotoxins block neurotransmitter release by proteolytic cleavage of synaptobrevin. Nature 1992; 359: 832-835.

Schiavo G, Rosseto O, Benfenati F, Poulain B, Montecucco C. Tetanus and botulinum neurotoxins are zinc proteases specific for components of the neuroexocytosis apparatus. Ann NY Acad Sci 1994; 710: 65-67.

Schiavo G, Rosseto O, Catsicas S, Delaureto PP, Dasgupta, BR, Benefenati F, Montecucco C. Identification of the nerve terminal targets of botulinum neurotoxin serotype-A, serotype-D, and serotype-E. J Biol Chem 1993a; 268: 23784-23787.

Schiavo G, Rosseto O, Santucci A, Dasgupta BR, Montecucco C. Botulinum neurotoxins are zinc proteins. J Biol Chem 1992b; 267: 23479-23787.

Schiavo G, Shone D, Rossetto O, Alexander FCG, Montecucco CL. Botulinum neurotoxin serotype-F is a zinc endopeptidase specific for VAMP/synaptobrevin. J Biol Chem 1993b; 268: 11516-11519.

Simpson LL, Coffield JA, Bakry N. Inhibition of vacuolar adensosine triphosphatase antagonizes the effects of clostridial neurotoxins but not phospholipase A2 neurotoxins. J Pharmacol Exp Ther 1994; 269: 256-262.

Simpson LL. The origin, structure, and pharmacological activity of botulinum toxin.

Pharmacol Rev 1981; 33: 155-188.

Sirover MA. New insights into an old protein: The functional diversity of mammalian glyceraldehyde-3-phosphate dehydrogenase. Biochimica et Biophysica Acta 1999; 1432: 159-184.

van Ermengem E. Classics in infectious diseases. A new anaerobic bacillus and its relation to botulism. E. Van Ermengem. Originally published as “Ueber einen neuen anaeroben bacillus und seine beziehungen zum botulismus” in Zeitschrift Fur Hygeine Und Infektionskrankheiten 1897; 26: 1-56. Rev Infect Dis 1979; 1: 701-719.

Table 3.1. Identification of spots selected from control precipitation of H_1 detergent fraction illustrated in Figure 3.3A.

Spot ID	Protein ID	Pubmed number	# peptides matches	Theoretical M.W.	Protein Location
H1 Ctl A	**Dihydrolipoamide S-Acetyltransferase precursor**	165608128	4	59047	Mitochondria
H1 Ctl B	**Muscle glycogen phosphorylase**	gi|6755256	3	97225	Cytoplasm
	Unnamed protein product (sequence similarity to DNA polymerase)	gi|26352896	1	*	Ribosome

Proteins in bold represent significant matches
* Information not available

Table 3.2. Identification of spots selected from toxin precipitation of H_1 detergent fraction illustrated in Figure 3.3B and 3.4A.

Spot ID	Protein ID	Pubmed number	# peptides matched	Theoretical M.W.	Protein location
H1-5 Tox E	**Putative Clostridium Botulinum HA-17**	gi|33321090	4	17023	Toxin associated
	Unknown mouse protein similar to tensin (conserved Protein tyrosine phosphatase catalytic domain)	gi|26354643	1	68720	Binds actin filaments
	Lobe homolog-like (AKT1 substrate 1 (proline-rich))	gi|21312878	1	27466	Cytoplasm
	Syntaxin 5 conserved t-SNARE complex subunit	gi|7110528	1	34117	Plasma Membrane
H1-6 Tox F	**Cryab protein**	gi|14789702	4	20056	Cytoplasm/ Nuclear/ membrane
H1-7 Tox G	**Cryab protein**	gi|14789702	6	20056	Cytoplasm/ nuclear/ membrane
H1-18 Tox R	**Non-toxin haemagglutinin HA17 [Clostridium botulinum]**	gi|33321090	3	17023	Toxin Associated
H1-19 Tox S	**Non-toxin haemagglutinin HA70 [Clostridium botulinum]**	gi|33321094	4	71207	Toxin Associated

Proteins in bold represent significant matches

Table 3.3. Identification of selected spots from matched H_1 hydrophobic P_3 fraction illustrated in Figure 3.5.

H1-9	**Creatine kinase, muscle**	gi|6671762	15	43018	Cytoplasm
	Pyruvate dehydrogenasase E1 alpha 1 subunit	gi|57657	3	43169	Cytoplasm
	Glyceraldehyde-3-phosphate dehydrogenase	gi|51772343	1	41295	Cytoplasm
	Immunoglobulin heavy chain variable region	gi|27762553	1	Fragment	Cytoplasm

Table 3.4. Identification of selected spots from matched H_3 hydrophilic P_3 fraction illustrated in Figure 3.6.

Spot ID	Protein ID	Pubmed Number	# peptides matched	Theoretical M.W.	Protein location
H3-1	**ATP 5b protein**	gi|23272966	20	56632	Mitochondria
H3-2	**Pdhb protein**	gi|12805431	4	34814	Mitochondria
H3-4	**Creatine kinase, muscle**	gi|6671762	19	43018	Cytoplasm
	Glycine-, glutamate-, thienylcyclohexyl-piperidine binding protein	gi|57657	2	45818 (frag)	Ribosome
	Pyruvate dehydrogenase E1 alpha form 1 subunit	gi|57657	1	43169	Cytoplasm
	Unnamed protein similar to Tesk2 protein kinase	gi|26343415	1	63470	Cytoplasmic
	GAS2-related protein	gi|51828694	1	72417	Cytoskeletal-Associated
	Similar to Lysosome-associated membrane glycoprotein 1 precursor	gi|12835945	1	45647	Lysosomal/ Integral to membrane
	Spectrin alpha chain, brain	gi|17380501	1	167533	Cytoskeletal/ membrane
	Olfactory receptor Olr421 conserved domain g-protein receptors	gi|47577341	1	35247	Plasma membrane
	Huntingtin Disease (HD) protein	gi|438807	1	344690	Cytoplasm
H3-5	**Albumin 1**	gi|26341396	7	64961	Cytoplasm
	Creatine kinase	gi|203480	3	33252	Cytoplasmic
	Similar to HEF-like protein Src homology 3 domains	gi|28488800	1	87144	Cytoplasmic/ tyrosine kinase

Proteins in bold represent significant matches

Table 3.5. Identification of selected spots from matched P_3 sample illustrated in Figure 3.7

Spot ID	Protein ID	Pubmed number	# peptides matched	Theoretical M.W.	Protein location
A-1	**Unnamed protein product proteasome (prosome, macropain) subunit, alpha type 1**	gi|26353732	4	29448	Cytoplasmic/ nuclear
	Membrane protein, palmitoylated 2 (MAGUK p55 subfamily member 2) conserved SH3 domain guanylate kinase Lin7-1 Associated protein	gi|7710062	1	77229	Membrane Associated
A-2	**Cryab protein**	gi|14789702	12	64961	Cytoplasmic
	KIAA0406-like protein Structure ARM superfamily	gi|14193703	2	120765	Unknown
	Similar to glyceraldehyde-3-phosphate dehydrogenase (phosphorylating)	gi|51766433	2	24480	Cytoplasmic

Proteins in bold represent significant matches

Table 3.6. Identification of 1D bands of rabbit P_3 hydrophobic fraction precipitations as illustrated in Figure 3.8A and 3.8B.

Spot ID	Protein ID	Pubmed Number	# peptides matched	Theoretical M.W.	Protein location
B 4C	**Alpha β-crystallin**	gi|57580	3	19945	Cytoplasm/ Membrane Associated
B 4T	**Alpha β-crystallin**	gi|57580	5	19945	Cytoplasm/ Membrane Associated
	Similar to tensin (conserved protein tyrosine phosphatase catalytic domain)	gi|26354643	1	68720	Binds to actin filaments
B 5T	**Glyceraldehyde-3-phosphate-dehydrogenase**	gi|56188	3	35725	Cytoplasm/ Membrane Bound
	Lysosomal membrane glycoprotein A	gi|293692	1	41480	Lysosome
B 6T	Glyceraldehyde-3-phosphate dehydrogenase, muscle	P00354	1	35853	Cytoplasm/ Membrane Bound
	Annexin A13	Q99JG3	1	35768	Membrane Bound
	Myosin-binding protein C, slow-type	Q00872	1	128214	Cytoplasm
B 7C	**Glyceraldehyde-3-phosphate dehydrogenase (phosphorylating**)	gi|49435	2	35725	Cytoplasm
	Annexin A13	Q99JG3	1	35768	Membrane
B 7T	**Glyceraldehyde-3-phosphate dehydrogenase (phosphorylating)**	gi|49435	4	35725	Cytoplasm
B 8C	**Fructose-bisphosphate aldolase**	gi|68184	3	39187	Mitochondria
B 8T	Fructose-bisphosphate aldolase	gi|68184	1	39187	Mitochondria

Proteins in bold represent significant matches

Table 3.6, continued.

Spot ID	Protein ID	Pubmed Number	# peptides matched	Theoretical M.W.	Protein location
B 8T	Glutamate receptor, ionotropic kainate 4 precursor	Q99JG3	1	35768	Membrane
B 9C	**Creatine kinase, M chain**	gi|125307	6	43085	Cytoplasm
	Gamma-actin	gi|178045	1	25862	Cytoskeletal
B 11C	**Pyruvate kinase M**	gi|551295	3	57824	Cytoplasm
B 12C	**Glycogen phosphorylase b**	gi|231300	13	95801	Cytoplasm
B 9C	**Creatine kinase, M chain**	gi|125307	6	43085	Cytoplasm
	Gamma-actin	gi|178045	1	25862	Cytoskeletal
B 11C	**Pyruvate kinase M**	gi|551295	3	57824	Cytoplasm
B 12C	**Glycogen phosphorylase b**	gi|231300	13	95801	Cytoplasm

Proteins in bold represent significant matches

Table 3.7. Identification of 1D bands of rabbit P_3 hydrophilic fraction precipitations as illustrated in Figure 3.9A and 3.9B.

Spot ID	Protein ID	Pubmed number	# peptides matched	Theoretical M.W.	Protein location
A 2T	**Unnamed protein product hemoglobin, beta adult major chain**	gi|12846616	3	15768	Cytoplasm
	Glyceraldehyde-3-phosphate dehydrogenase	gi|31645	1	36031	Cytoplasm
	Alpha-globin	gi|49900	2	15076	Cytoplasm
A 3T	**Alpha β-crystallin**	gi|57580	3	19945	Cytoplasm/ Membrane Associated
A 5T	Glyceraldehyde-3-phosphate dehydrogenase (phosphorylating)	gi|12846616	1	35686	Cytoplasm/ Membrane bound
	Disks large homolog DLG2 MAGUK p55 subfamily member 2	gi|2135005	1	64572	Membrane Associated
	Similar to FGFR-like protein	gi|57084699	1	154021	Membrane protein
	Unknown mouse Protein similar to sulfide quinone reductase	P00354	1	35853	Mitochondria
A 6T	Glyceraldehyde-3-phosphate dehydrogenase, muscle	P00354	1	35853	Cytoplasm/ Membrane bound
	Annexin A13	Q99JG3	1	35768	Membrane bound
	Myosin-binding protein C, slow-type	Q00872	1	128214	Cytoskeletal/ Muscle
A 7T	Glyceraldehyde-3-phosphate dehydrogenase, muscle	P00354	1	35853	Cytoplasm/ Membrane bound
	Stromelysin-1 precursor	P28863	1	53908	Matrix metallo-proteinase
	Potential phospholipid-transporting ATPase IF	Q9N0Z4-00-00-00	1	133363	Membrane

Proteins in bold represent significant matches

Table 3.7, continued.

Spot ID	Protein ID	Pubmed number	# peptides matched	Theoretical M.W.	Protein location
	Chromogranin A precursor	Q9XS63	1	49832	Secretory granules neuroendocrine
A 9T	Glyceraldehyde-3-phosphate dehydrogenase, muscle	P00354	1	35853	Cytoplasm/ Membrane bound
	mKIAA0938 protein similar to neuron navigator		1	34108	Microtubule Associated
A 10T	Fructose-bisphosphate aldolase A	P00883	1	39187	Cytoplasm
A 11T	**Creatine kinase, M chain**	P00563	3	43085	Cytoplasm
	Cullin homolog 5 Ca-mobilizing receptor VACM-1	Q9D5V5	1	90916	Membrane
	Transient receptor potential vanilloid type 1	gi|39983005	1	94941	Membrane
	Glutamate receptor, ionotropic kainate 4 precursor	Q00872	1	128214	Membrane
	ATPase, Ca^{2+} transporting, type 2C, member 1	gi|28461195	2	104712	Membrane Ubiquitous (Sarcoplasmic reticulum, endosomal
	Sialic acid binding Ig-like lectin 10 precursor (Siglec-10)	Q96LC7-02-00-00	1	fragment	Membrane
A 14T	Keratin, type II cytoskeletal 1	gi|1346343	3	65978	Cytoskeletal/contaminant
	Pyruvate kinase	Q96LC7-02-00-00	1	57681	Cytoplasm

Proteins in bold represent significant matches

Table 3.8. Proteins identified directly from toxin precipitations of mouse P_3 not subjected to electrophoresis.

Protein ID	# peptides matched
Myosin regulatory light chain-like	3
No description	1
No description	1
Myosin light chain 1 atrial/fetal isoform	1
Major vault protein	1
Transitional endoplasmic reticulum ATPase	1
Actin cytoplasmic 2 gamma actin	1
Serum deprivation Response	1

Figure 3.1A. One dimensional SDS-PAGE gels of protein precipitations from toxin coupled (lane 1) and control beads (lane 2). Protein bands are visualized with Silver Stain.

Figure 3.1B. Control bead precipitation (lane 1) compared with treatments with high salt washes (lane 2), and high salt washes and 1M glycine quenching treatment (lane 3).

Figure 3.1C. Reduction of non-specific binding due to detergent fractionation. Protein precipitations from toxin coupled (lane 1) and control beads (lane 2) exposed to the second hydrophobic fraction.

Figure 3.1A.

1 2

Figure 3.1B.

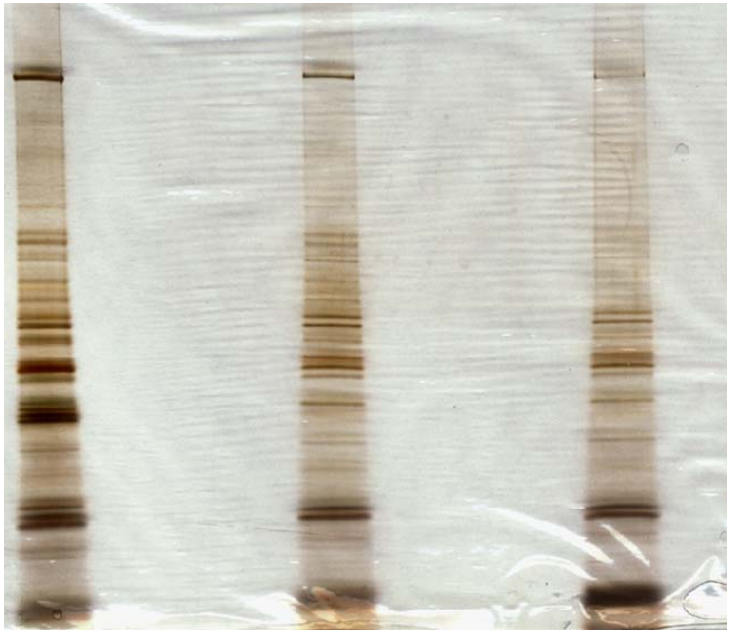

1 2 3

Figure 3.1C.

1 2

Figure 3.2. Detergent fractionation of P_3 into 2 hydrophobic (H_1, H_2) and 1 hydrophilic (H_3) fractions. Each fraction was split equally by volume and exposed to toxin coupled or control beads. 2-DE gels stained with silver stain. A) toxin H_1 fraction B) control H_1 C) toxin H_2 fraction D) control H_2 fraction E) toxin H_3 fraction F) control H_3 fraction. Linear pI 3-10, left to right. Differences are present between toxin and control in all sets at ~37-50 kDa and between pI 3-5.

Figure 3.2.

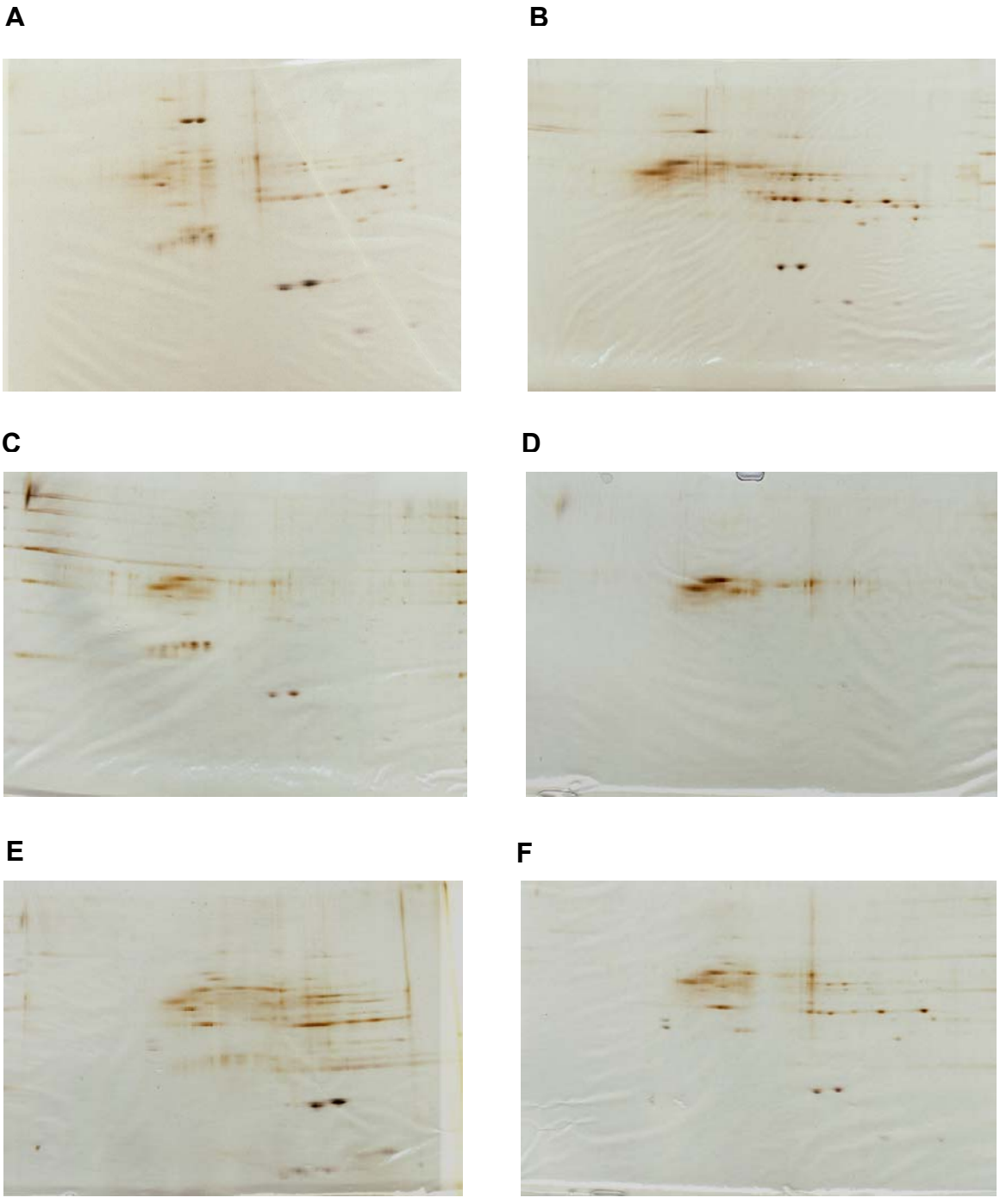

Figure 3.3A. Two-dimensional electrophoresis of control precipitation of H_1 detergent fraction. Coomassie Stain. Labels in bold represent proteins identified by LC-MS-MS. See Table 3.1 for identifications.

Figure 3.3B. Two-dimensional electrophoresis of toxin precipitation of H_1 detergent fraction. Coomassie Stain. Spots 5, 6, 7, 16 were identified by LC-MS-MS. See table 3.2 for identifications. Remaining spots yielded either no results or peptides with no matches.

Figure 3.3A.

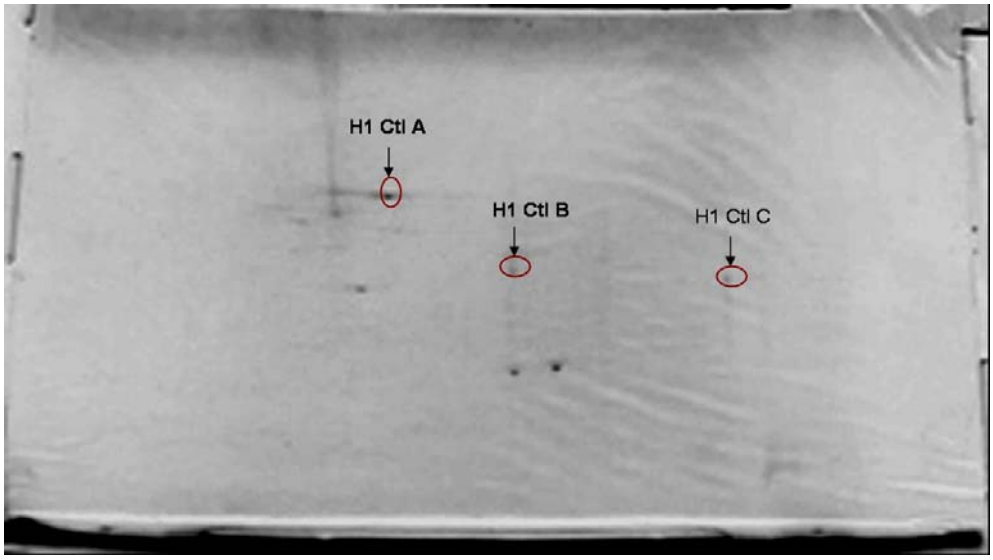

Figure 3.3B.

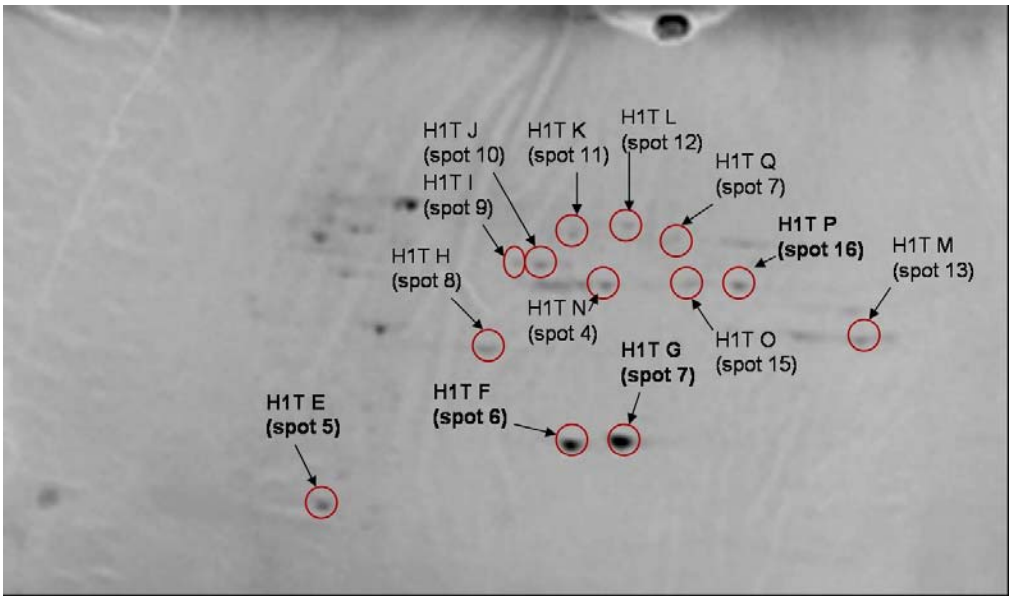

Figure 3.4A. Two dimensional electrophoresis of toxin precipitation of H_2 detergent fraction. Only spots 18, 19 yielded identifications.

Figure 3.4B. Two dimensional electrophoresis of toxin precipitation of H_3 hydrophilic fraction. None of the submitted spots yield identifications.

Figure 3.4A.

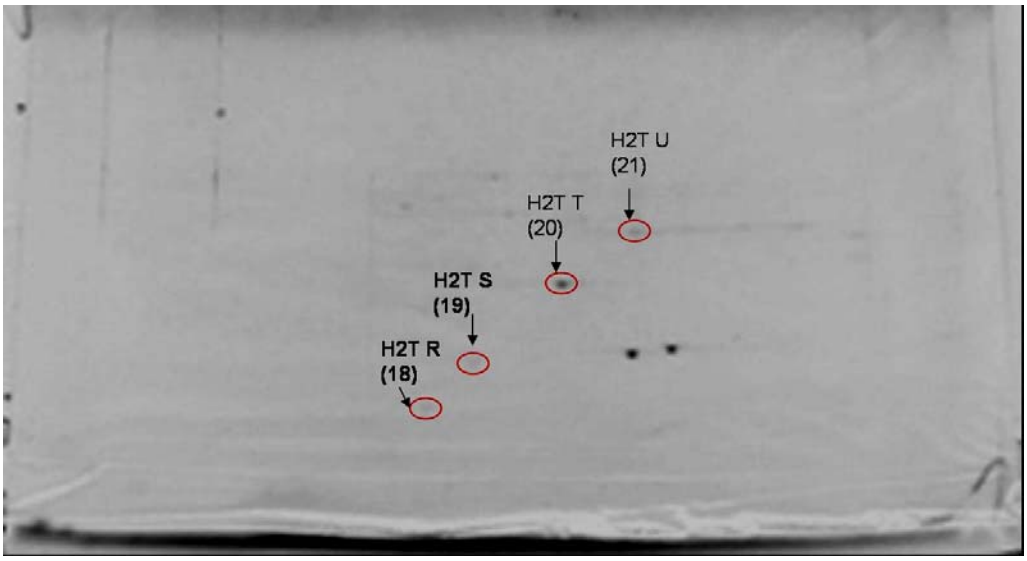

Figure 3.4B.

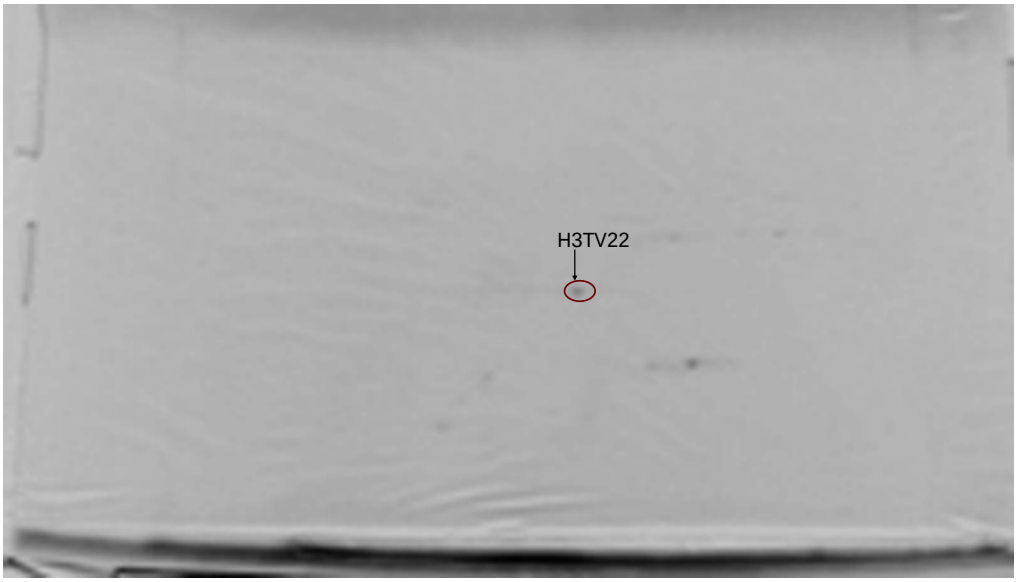

Figure 3.5. Matching of H_1 detergent fraction from total P_3 (lower gel) with toxin precipitation of H_1 detergent fraction (upper gel) utilizing spots at 25 kDa as landmarks (red circles). Matched spots of interest (arrows) were extracted from total P_3 H_1 fraction (lower gel). See Table 3.5 for details.

Figure 3.5.

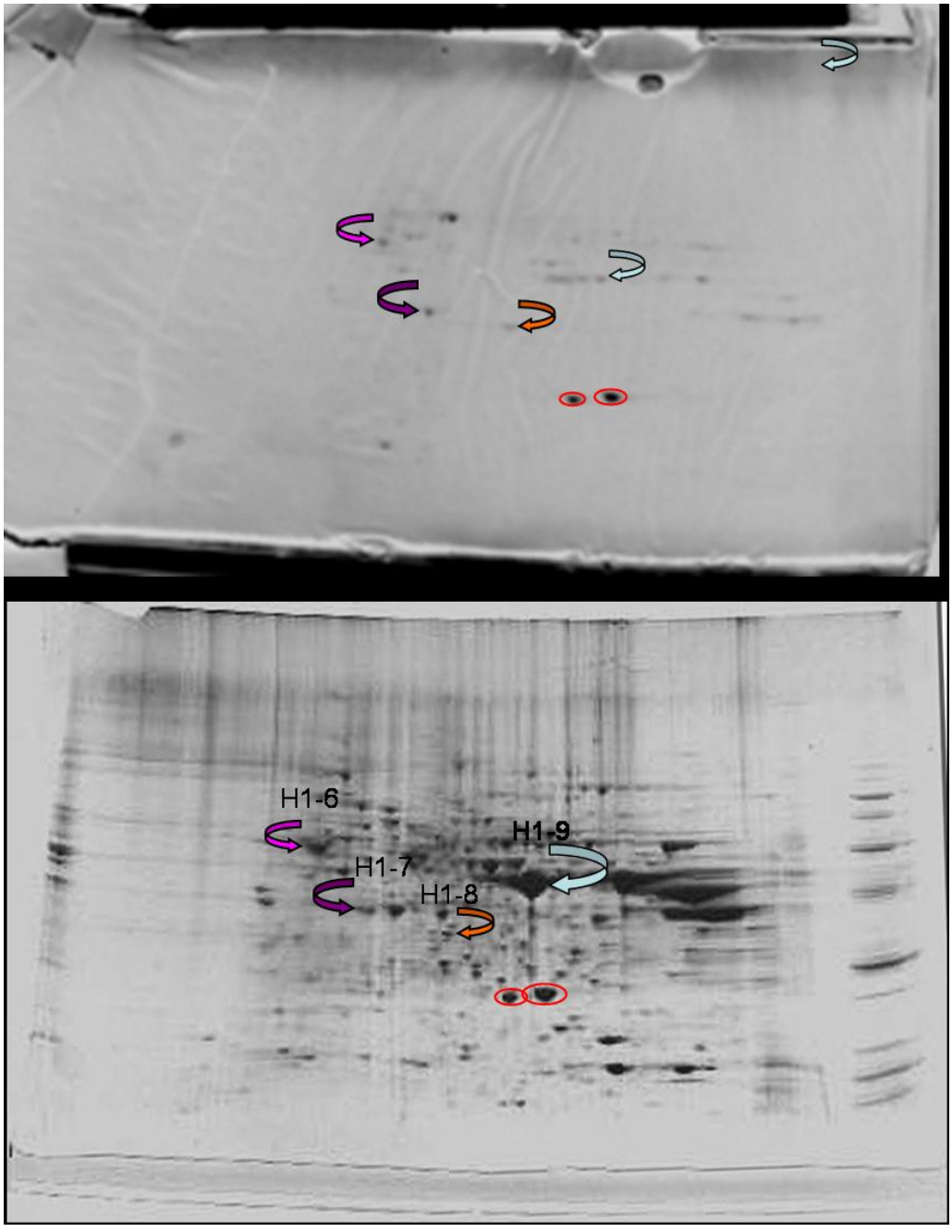

Figure 3.6. H_3 hydrophilic fraction from total P_3 that has been matched to toxin precipitation of H_3 detergent fraction. Spots marked with arrows represent those that demonstrated a visible difference in toxin elution gels. Spots were excised from total P_3 H_3 hydrophilic fraction. See Table 3.4 for protein identifications.

Figure 3.6.

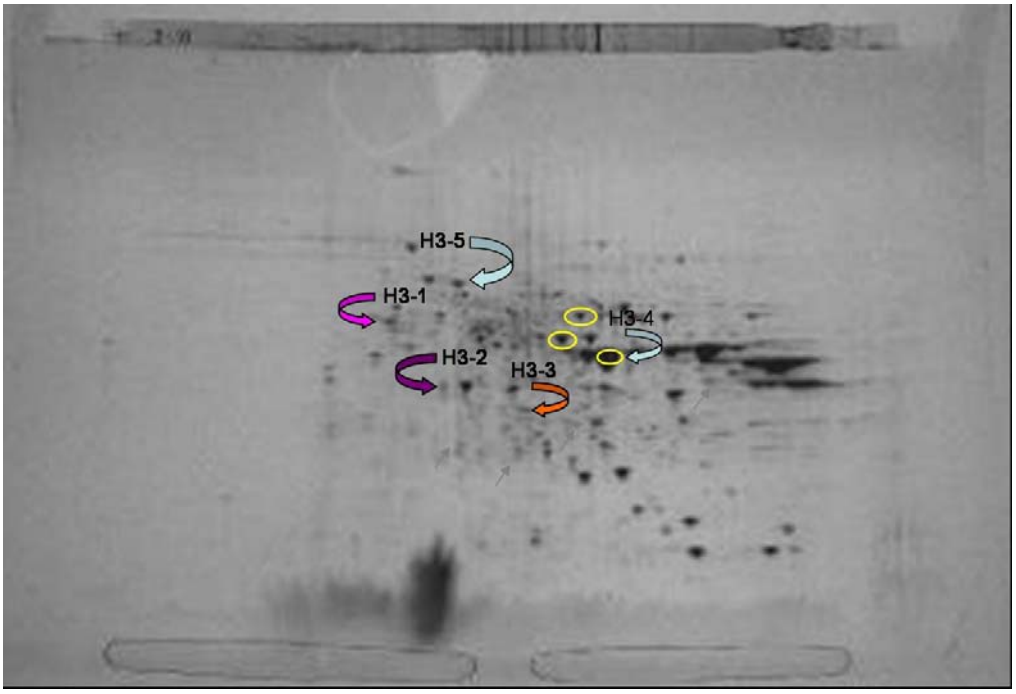

Figure 3.7. Spots that were visibly increased in toxin precipitations were matched to gels of non detergent fractionated total P_3 utilizing similar spot patterns as landmarks. Matched spots (labeled and circled) were excised and sent for LC-MS identification. See Table 3.5 for protein identifications.

Figure 3.7.

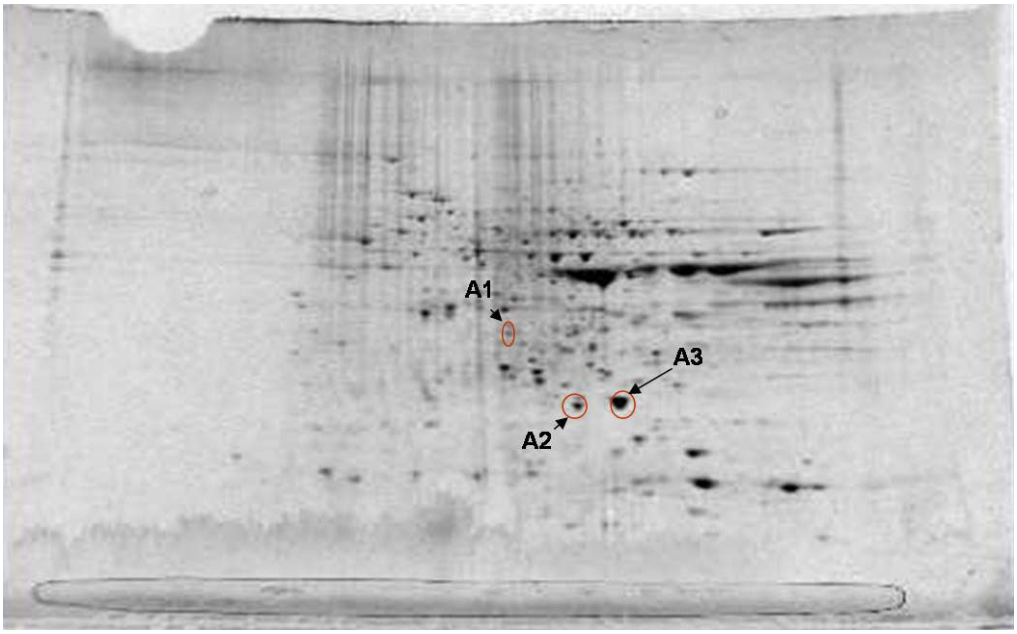

Figure 3.8A and 3.8B. Gels from 1D SDS-PAGE of rabbit diaphragm. Precipitations utilized the hydrophobic P_3 fraction. A) Control elution; B) Toxin elution. All labeled bands were excised and submitted for LC-MS-MS.

Figure 3.8A.

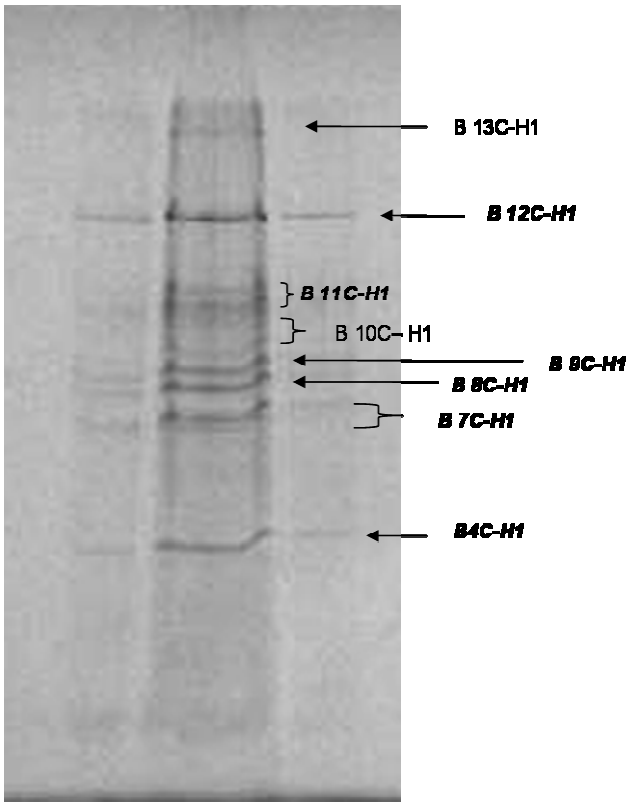

Figure 3.8B.

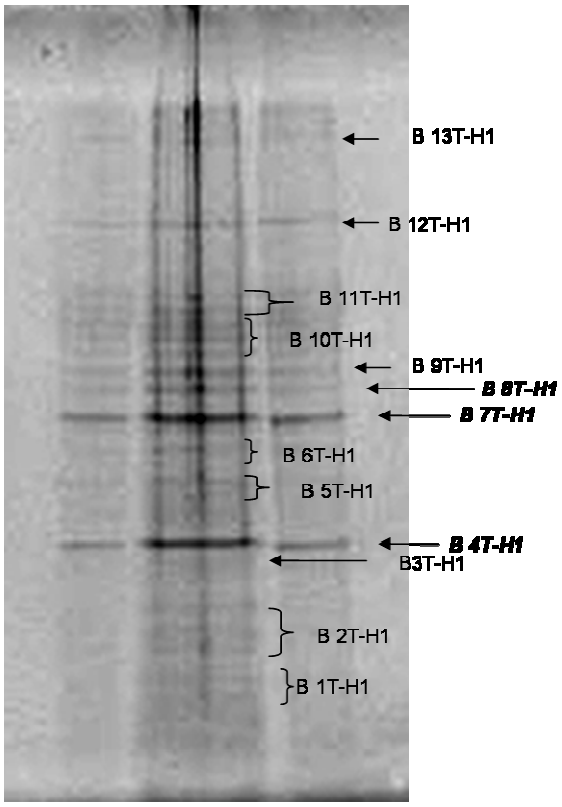

Figure 3.9A and 3.9B. Gels from 1D SDS-PAGE of rabbit diaphragm. Precipitations utilized the hydrophilic P_3 fraction. A) Control elution; B) Toxin elution. All labeled bands were excised and submitted for LC-MS-MS.

Figure 3.9A.

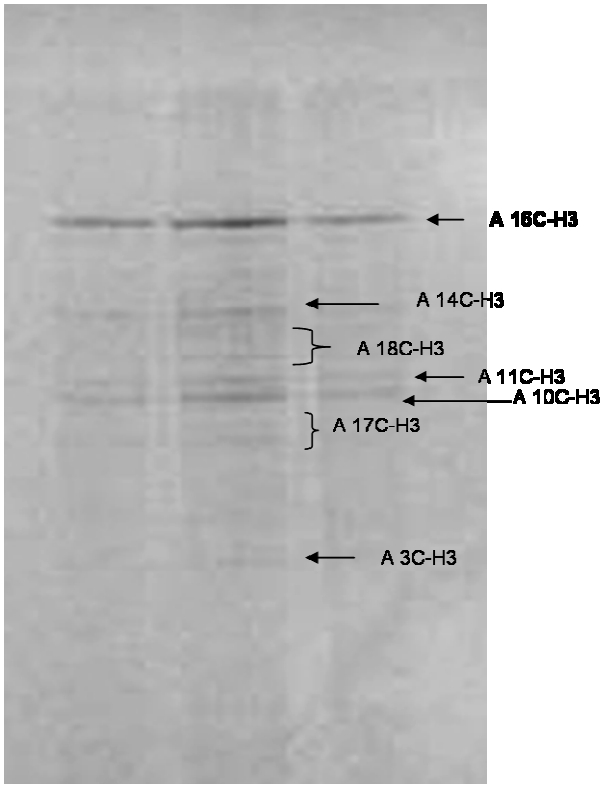

Figure 3.9B.

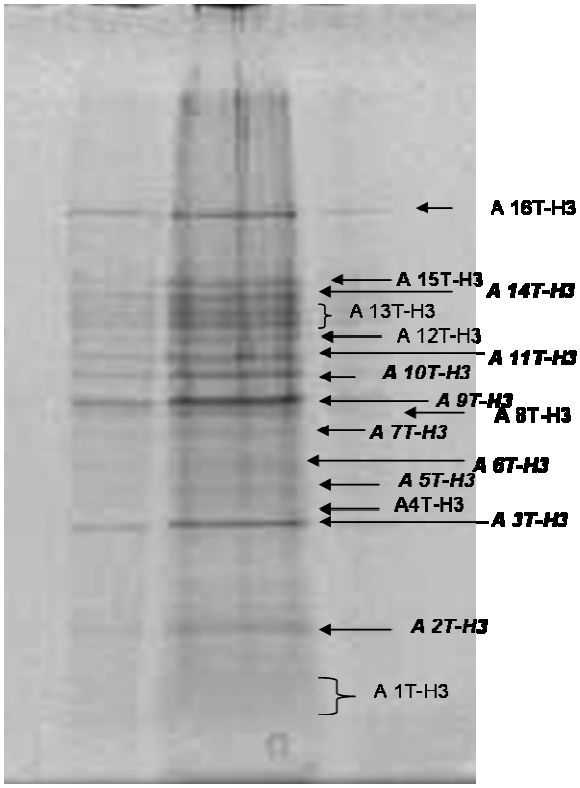

CHAPTER 4

IDENTIFICATION OF TWO GROWTH FACTOR RECEPTORS THAT DEMONSTRATE BINDING TO BOTULINUM TOXIN SEROTYPE A[1]

[1] Parrott TM, Baxter VZ, Kellock K, Coffield JA. Manuscript to be submitted

ABSTRACT

It has been well documented that muscles treated with botulinum toxin serotype A (BoNT/A) demonstrate the formation of functional sprouts from poisoned nerve terminals. This neurite outgrowth seems to be unique to BoNT/A and BoNT/D, leading to an intriguing possibility that binding of toxin to its receptor may result in cytoskeletal rearrangement and subsequent neurogenesis. Recent mass spectrometry data obtained from BoNT/A affinity precipitation of mouse diaphragm performed in our laboratory matched peptides to several protein domains that are conserved among different growth factor receptors. Therefore, in the current study, affinity precipitated preparations were probed with antibodies to several growth factor receptors that are thought to be expressed on cholinergic nerve terminals. Through this approach, two separate proteins that demonstrate toxin binding were identified: Nogo-66 receptor isoform 2 and Fibroblast growth factor isoform III. Both of these proteins are known to interact with complex gangliosides and to participate in lipid raft signaling. Further elucidations of the functionality of their interactions with botulinum toxin have yet to be explored.

INTRODUCTION

It is well documented that Botulinum toxin serotype A (BoNT/A) causes flaccid muscle paralysis through a proposed mechanism involving cleavage of the SNARE fusion complex protein SNAP-25. Therapeutic use of BoNT/A under the trade name BOTOX was given FDA approval in 1989 to treat strabismus and other spasticity disorders. More recently, it was also approved for the treatment of wrinkles (Jankovic and Brin, 1997). This treatment is only temporary, however, with the clinical benefit ranging from 2-6 months. This transient response is thought to be due to the ability of BoNT/A to induce the formation of functional sprouts from the poisoned nerve terminal. Several studies have demonstrated the formation of nerve sprouts in muscles treated with BoNT/A, and the presence of these functional sprouts corresponds to the subsequent improvement in muscle function (Angaut-Petit et al., 1990, de Paiva et al., 1999, Juzans et el., 1996). With the exception of serotype D, which has no clinical utility in human medicine, the ability of BoNT/A to stimulate neurite outgrowth appears to be unique among the toxin serotypes. It is, therefore, intriguing to consider the possibility that binding of BoNT/A to its nerve terminal receptor not only initiates toxin internalization, but, it may also induce cytoskeletal reorganization and subsequent neurogenesis. This possibility would then suggest that the serotype specific receptor for BoNT/A may have the characteristics of a growth factor receptor.

Recent mass spectrometry data obtained from BoNT/A affinity precipitations performed in our laboratory matched peptides to several protein domains that are conserved among different growth receptors, including: leucine-rich repeat domains, Ig-like domain, tyrosine kinase domain, and an FGFR-like protein. Unfortunately, specific

protein identifications could not be made because these matches resulted in weak proteomic scores. In the studies presented in this chapter, information from the previous proteomic analyses was used to identify likely growth factor receptor proteins that contain the conserved domains. Affinity precipitations using BoNT/A coupled beads were performed as previously described. The resultant elutions were then probed for selected growth factor receptor proteins using standard Western blot techniques. Through this process selective enrichment of two growth factor receptor proteins, Nogo-66 receptor 2 (NgR2) and Fibroblast growth factor III (FGFR3) was demonstrated. This enrichment was observed in different subcellular fractions obtained through differential centrifugation followed by detergent phase partitioning. Since both NgR2 and FGFR3 are reported to interact with complex gangliosides and to associate with lipid rafts, these results suggest that the serotype specific, high affinity toxin receptor for BoNT/A may exist as a protein array within a lipid raft domain of the nerve terminal membrane.

MATERIALS AND METHODS

Tissue preparation and membrane protein enrichment

The protocols for these steps have been described in detail in the preceding chapters. Briefly, diaphragm tissues from NIH Swiss mice were homogenized and processed to obtain neuromuscular junction enriched membrane fractions. Tissues were homogenized in 1mL of homogenizing buffer (EDTA 2 mM, Sucrose 250 mM, 2 mM HEPES), then spun at 5,000 X g for 5 min to remove cellular debris. The supernatant was removed and spun at 10,000 X g for 10 min to remove nuclear debris. The resulting supernatant was spun a final time in order to obtain a synaptic membrane

enriched preparation (P_3). This membrane-enriched preparation was fractionated with detergent using the Mem-Per Kit (Pierce Biochemical; Rockford, IL) to further solubilize and partition membrane proteins into enriched fractions.

Preparation of toxin and control beads

Amino-link beads (Seize–X kit; Pierce Biochemical, Rockford, IL) were coupled with BoNT/A through the toxin amine terminus following the protocol described in the preceding chapter.

Affinity precipitation

Equal volumes of sample were added to control or toxin-coupled beads. Following 4 h incubation on a rotator at room temperature, the beads were spun to remove the unbound sample. The beads were then washed four times with DPBS containing 1% TRITON X100 to remove non-specifically bound proteins. Bound proteins were eluted through 4 cycles utilizing 1 µL of elution buffer/1µL settled bead. Eluted proteins were then precipitated with acetone on ice overnight and spun for 15 min at 12,000 X g. Acetone was removed and the pellet allowed to air dry.

SDS-Page electrophoresis

Acetone precipitated pellets were solubilized in sample buffer containing 5% mercaptoethanol. Samples were boiled, loaded onto 4-20% Tris-HCl precast gels (Bio-Rad; Hercules, CA), and run at 200 V for 55 minutes. Resolved proteins were transferred to methanol treated PVDF membranes (Hybond; Amersham Life Science, Inc Arlington Height, IL). Membranes were blocked in 3% nonfat powdered milk diluted in TBS (milk-TBS) for 2 h. Following 4 washes in TBS, membranes were incubated in primary antibodies to selected growth factor receptor proteins according to the

manufacturers' recommendations. Membranes were allowed to warm and then washed 4 times in TBS. Horseradish peroxidase conjugated secondary was added to the membranes for 1 h at 25°C. Protein bands were detected with enhanced chemiluminescence (ECL^+; Amersham Life Science). Membranes were then exposed to hyper-film-ECL for times adequate to visualize bands.

Antibodies

Polyclonal rabbit antibodies to NgR2 1:200, NgR3 1:200 (Alpha Diagnostic; San Antonio, TX); FGFR3 1:800 (Sigma-Aldrich; St. Louis MO); TRK-B 1:800, LAR 1:400, ERB-B2 1:400, ERB-B4 1:300 (Santa Cruz; Santa Cruz, CA); Goat anti-rabbit horseradish peroxidase conjugated secondary antibody (Biosource; Camarillo CA) was used at a 1:7500 dilution.

Rho A assay

Activated Rho A was isolated using a rhotekin bead affinity binding kit (Upstate; Charlottesville, VA). Diaphragm tissues were extracted from mice (n=6/replicate) and hemisected. Each hemidiaphragm was washed 3 times in PBS, and then incubated in either PBS alone or in PBS plus BoNT/A (1 μg/μl) or MAG, for 30 min at room temperature. In some experiments the tissues were preincubated in toxin for 10 min prior to the addition of MAG. After 30 min, diaphragms were washed in ice cold PBS, homogenized on ice in a 1X Mg^{2+} containing lysis buffer (Upstate; Charlottesville, VA) with a polytron homogenizer and spun at 10,000 X g for 10 min. Supernatants were then assayed for protein by the modified Lowery method. 1.5 mg of protein/treatment was incubated with 38 μl of Rhotekin coated beads (Upstate). After 45 min, beads were spun out of the supernatant and washed 3 times in Mg^{2+} containing lysis buffer. The

beads were then boiled in 30 µl of sample buffer containing 0.5% mercaptoethanol for 5 min. Boiled samples were spun and the supernatant was added to Criterion 4-20% Tris-HCl gels (Bio-Rad) and resolved for 1 h at 200 V. Proteins were then transferred to methanol treated PVDF membranes at 100 V for 30 min. Following washes with TBS, membranes were blocked in 3% milk-TBS overnight at 4°C. Blocked membranes were washed twice in TBS and then incubated in anti-RhoA (Santa Cruz; Santa Cruz, CA) diluted 1:500 in 1% milk-TBS for 1 h. After several washes, membranes were incubated in goat anti-rabbit (Bio-Source; Camarillo, CA) diluted 1:7500 in 1% milk-TBS for 1 h. Detection of protein bands was performed as described above. Densitometric analysis of bands was performed using Quantity One Software (Bio-Rad). Statistical analyses were done with GraphPad InStat software.

RESULTS

Growth factors tested for specific binding to botulinum toxin A

Control and toxin affinity precipitations were probed with antibodies to six growth factor receptors. These receptor proteins were chosen because they demonstrated some specificity to the nerve terminal, or because previous research indicated possible involvement with BoNT/A (Fernández-Salas et al,. 2005). The results of this experiment are shown in Table 4.1. Of the six receptors tested, two demonstrated selective interaction with BoNT/A.

Selective interaction of NgR2 with botulinum toxin serotype A

In initial immunoblots of non-detergent fractionated P_2 and P_3 samples probed for NgR2, differences were noted between the elutions from toxin and control precipitations. These differences included increases in the immunoreactive signal of a

~75 kDa band in the P_3 toxin sample (Figure 4.1A), and the detection of immunoreactive bands at ~50 and ~28 kDa in the P_2 toxin samples that were not present in the corresponding control (Figure 4.1B). A variable amount of background signal was observed in control elutions. This was likely due to the occurrence of non-specific protein interactions with the control beads. To minimize these nonspecific interactions, P_2 and P_3 samples were further solubilized and fractionated by detergents prior to incubation with toxin coupled or control beads. As illustrated in Figure 4.2, it is apparent that the P_2 fractions yielded a greater degree of background than the P_3 fractions, and that the H_1 hydrophobic fractions demonstrated higher background than the H_3 hydrophilic fractions. However, on closer inspection differences were observable. Notably, an increased immunoreactive signal at ~75 kDa was detected consistently in the P_2 hydrophilic fraction, while variable differences were observed in this same signal in the P_3 fractions.

Selective interaction of FGFR3 with botulinum toxin serotype A

In initial immunoblots of non-detergent fractionated P_2 and P_3 samples probed for FGFR3, a few specific bands were observed in the P_3 elution sample from toxin precipitations (see Figure 4.3A) that were not present in control elutions. The detection of these bands, of approximately 110 kDa and >250 kDa, was inconsistent between experimental replicates. Immunoblots of non-detergent fractionated P_2 samples revealed no discernable differences between toxin and control elutions (see Figure 4.3B). Detergent fractionation, to reduce non-specific interactions, resulted in reproducible detection of the ~110 kDa and 250 kDa band in the P_3 hydrophobic

fraction, and an increased signal at ~50 kDa that alternated between hydrophobic and hydrophilic fractions (shown in Figure 4.4).

The effects of botulinum serotype A on RhoA activation in mouse diaphragm

Recent evidence suggests that myelin associated glycoprotein (MAG) may interact with NgR2 as a functional ligand in the CNS. These same studies reported that the interaction of MAG with Nogo receptors, including NgR2, leads to the activation of the small GTPase RhoA in CNS neurons. This activation of RhoA resulted in the blockade of neurite outgrowth, most likely through an interaction with the actin cytoskeleton. Thus, preliminary experiments were performed to investigate the functional significance of the interaction of BoNT/A with the NgR2. An affinity precipitation kit was utilized to selectively isolate GTP bound RhoA (activated RhoA) from control and toxin treated diaphragm samples. This assay demonstrated a increased amount of variability between experiments. This variability may be a result of non-specific binding seen in previous bead affinity assays (see chapter 3). Figure 4.5A illustrates the results of initial activation experiments using BoNT/A at 3 doses (1, 10, 100 µg/ml). Densitometric analysis of the RhoA-GTP signal revealed an increase of 94.8% in RhoA activation at the lowest dose when compared with control, and a decrease in activation at the higher doses (42.8%, 47.7% respectively). However, nonparametric analysis of variance (Kruskal-Wallis test) indicated that the differences between doses were not statistically significant ($p = 0.3744$). Figure 4.6B illustrates the results of Rho activation by MAG at 3 doses (0.1, 1, 10 µg/ml). Somewhat unexpectedly, densitometric analysis of the MAG data revealed a decrease in activated RhoA at all three doses with the lowest dose yielding the greatest reduction (88.1%) in

the activated RhoA compared with control. Analysis of variance to test the statistical significance of these findings could not be done because of the low sample number in the two lower dose groups. However, Dunn's multiple comparisons test demonstrated that the difference between control and the highest dose group (10 μg/ml) was not statistically significant ($p > 0.05$). Finally, to further investigate the interaction between BoNT and NgR2, the ability of BoNT to antagonize the effect of MAG on RhoA activation was examined. The results of these data, presented in Figure 4.7, demonstrate that the inhibition of RhoA activation by MAG illustrated in the preceding figure was reduced in the presence of BoNT/A by approximately 19%. Statistical analysis indicate that the difference between these two groups was not significant ($p = 0.4000$ Mann-Whitney test).

DISCUSSION

Serotype A interactions with growth factor receptors

The results of previous affinity precipitation experiments with BoNT/A demonstrated weak MS-MS identification of conserved receptor regions including tyrosine kinases, leucine rich repeat domains, Ig-like domains and an FGFR -like domain. In the current study, immunoblots from control and toxin affinity precipitated samples were screened for several growth factor receptors that are expressed on nerve terminals and reportedly contain these conserved domains. In addition, screening for an FGF receptor isoform recently reported to demonstrate affinity for BoNT/A in PC12 cells was also performed (Fernandez-Salas et al., 2005). The results of these screens revealed differential precipitation of two receptors NgR2 and FGFR3 by toxin coupled beads compared with control beads. The selective precipitation of these proteins was

reproducible, even with the variable background signal detected in control precipitations. These results suggest that NgR2 and/or FGFR3 may participate in the binding of BoNT/A to the nerve terminal at the mouse neuromuscular junction.

NgR-2 receptors and Rho GTPases

Neural regeneration is severely limited within the CNS. Three biological factors thought to be responsible for this limitation include Nogo-A, oligodendrocyte-myelin glycoprotein (OMgp), and MAG (Schwab, 1990). Nogo-66 receptors (NgR) are expressed broadly in the CNS, including in the cell bodies of projection neurons, the gray matter of spinal cord and in myelinated axons (Laurén et al., 2003). Three isoforms of NgR (1, 2, and 3) have been characterized, and reportedly share similar structural motifs. These include eight leucine rich repeat domains capped on both ends with unique cysteine rich regions, and a unique carboxyl teminus sequence linked to an glycosylphosphatidylinosital (GPI) anchor (McGee and Strittmater, 2003).

Neuronal responses to MAG are regulated by both development and location. For instance, MAG deficient mice demonstrate axon degeneration and reduced fiber diameter (Pan et al., 2002). In the PNS, MAG acts to promote nerve growth in the dorsal root ganglion of rat pups up to post natal day 4, after which MAG inhibits nerve growth (Mukhopadhyay et al., 1994). MAG has been shown to bind to NgR2 through interactions with complex gangliosides such as GT1b. Since NgR2 is a GPI linked protein, its signaling activity is mediated by the formation of a complex with other transmembrane proteins including TAJ/Troy, and Lingo-1 (Park et al., 2005). The binding of MAG to NgR2 and the interactions with this complex activates Rho A, a small GTPase, by increasing the amount of GTP bound RhoA. Activation of RhoA leads to

downstream regulation and activation of ROCK which ultimately results in growth cone collapse. An interaction of clostridial toxins with Rho GTPAses is not unfounded, a number of other clostridial toxins including, toxin A and B (*Clostridium difficile*) as well C3 toxins produce effects via Rho GTPases (Just et al., 1995a; 1995b). In particular, C3 toxin has been shown to inhibit Rho A, while activating the Ras GTPases RAC and Cdc42 leading to axonal regeneration (Kozma et al., 1997).

An in vitro assay to measure RhoA activation was utilized in preliminary experiments to determine the functional significance of the interaction of BoNT/A with NgR2. Unfortunately, the results of these preliminary studies are inconclusive, due to the low number of samples tested, and the high variability of the assay. However, a few interesting observations were notable. Contrary to what had been reported in a majority of studies, MAG appeared to decrease RhoA activation in our neuromuscular preparation, and this effect was most pronounced at the lowest dose tested. BoNT appeared to produce biphasic responses, with a pronounced effect opposite that of MAG at the lowest dose, and responses similar to MAG at the higher doses. Further, preincubation of the preparation with toxin appeared to reduce the response to MAG, although again this was not statistically significant.

The finding that the most pronounced effects for both toxin and MAG appeared to be at the lowest doses is difficult to interpret. A recently published study that examined the time course of RhoA activation may shed some light on this finding (Hunter et al., 2003). In this study the activation of RhoA by TNF-α in cultured smooth muscle cells, began within 1 min and peaked at 15 min, returning towards baseline over the next 45 min. In the current study, only a single time point of 30 min was examined, based on a

range of time points reported in the MAG literature. It is possible that by looking only at this later time point the peak responses of RhoA at the higher doses of MAG and toxin were missed. Additional studies using larger sample sizes and appropriate sampling times will be needed to clarify these findings.

FGFR3 receptors

The FGF receptors are tyrosine kinase receptors with extracellular regions containing immunoglobulin-like domains (Johnson et al., 1990). It has been demonstrated that these receptors interact with cell surface heparin sulfate proteoglycans to exhibit biological activity (Yayon et al., 1991; Rapraeger et al., 1991). FGFRs are expressed as multiple isoforms that recognize different ligands through changes in their extracellular domain brought about by alternative splicing (Tiki et al., 1992). FGFR3 is ubiquitously expressed in several different tissues including not only the PNS but also bone, brain, and kidney. Its function in these tissues may be quite diverse. In several studies it has been reported that FGFR3 may be involved in apoptotic cell death, while an inverse response has been noted in myeloma cells, where increased expression of FGFR3 resulted in decreased apoptosis and cellular proliferation (L'hŏte and Knowles, 2005). A recent study examining axonal development after nerve injury, reported that FGFR3 deficient mice demonstrated a lack of neuronal loss that typically occurred in wild type mice, although the axons were developmentally smaller in diameter. This suggests a potential role for FGFR3 in axonal development (Jungnickel et al., 2004). Functional assays of FGFR3 were not performed in the current study.

NgR2 and FGFR3: Possible toxin receptors

The possible role that each of these growth factor receptors plays in the selective binding and internalization of BoNT/A merits consideration. First, if FGFR3 is ubiquitously expressed in several different tissues, and BoNT/A demonstrates selective binding to cholinergic nerve terminals, how could this selectivity be generated? One possibility may be that the selectivity is conferred by interactions with specific proteoglycans on the nerve terminal membrane. Binding of ligands to FGFRs requires low affinity binding to these cell surface molecules (Yayon et al., 1991; Rapraeger et al., 1991). Secondly, the selectivity may be conferred by binding to NgR2 itself, since its expression is much more limited than FGFR3.

NgR2, a GPI-anchored protein requires an interaction with another transmembrane protein in order to generate an intracellular signal (Fujitani et al., 2005). GPI-anchored proteins have been shown to localize to lipid rafts, as have complex gangliosides and downstream components of FGFR3 signaling (see review by Kasahara and Sanai, 2000; see review by Tsui-Pierchala et al., 2002; Neithhammer et al., 2002; see review by Pike, 2005). Complex gangliosides such as GT1b, the same ganglioside that has been shown to bind BoNT/A with low affinity, have been shown to regulate binding to growth factor receptors, including FGFR3 and NgR2. Thus, binding of the BoNT/A may be mediated by recruitment of one or more of these receptors into lipid rafts, that may result not only in clathrin mediated endocytosis but also activation of other cell signaling pathways resulting in neurogenesis. These interactions would lend support to the intriguing theory by Montecucco, Rossetto, and Schiavo (2004) that toxin

A binds to an array of proteins, with the common links being complex gangliosides and lipid raft signaling.

REFERENCES

Angaut-Petit D, Molgó J, Comella JX, Faille L, Tabti N. Terminal sprouting in mouse neuromuscular junctions poisoned with botulinum type A toxin: Morphological and electrophysiological features. Neuroscience 1990; 37: 799-807.

Comella JX, Molgó J, Faille L. Sprouting of mammalian motor nerve terminals induced by in vivo injection of botulinum type-D and the functional recovery of paralyzed neuromuscular junctions. Neurosci Lett 1993; 153: 61-64.

de Paiva A, Meunier FA, Molgó J, Aoki JR, Dolly JO. Functional repair of motor endplates after botulinum toxin type A poisoning: Biphasic switch of synaptic activity between nerve sprouts and their parent terminals. Proc Natl Acad Sci USA 1999; 96: 3200-3205.

Fernández-Salas E, Garay PE, Iverson C, Malik SZ, Steward LE, Aoki KR. Identification of FGFR3 as a putative receptor for botulinum neurotoxin type A uptake in neuronal cells. International Conference on Botulinum and Tetanus Toxins 2005; Abstract 29.

Fujitani M, Kawai H, Proia RL, Kashiwagi A, Yasuda H, Yamashita T. Binding of soluble myelin-associated glycoprotein to specific gangliosides induces the association of $p75^{NTR}$ to lipid rafts and signal transduction. J Neurochem 2005; 94:15-21.

Hunter I, Cobban J, Vandenabeele P, Macewan DJ, Nixon GF. Tumor necrosis factor-α-induced activation of RhoA in airway smooth muscle cells: role in the Ca^{2+} sensitization of myosin light $chain_{20}$ phosphorylation. Mol Pharmacol 2003; 63: 714-721.

Jankovic J, Brin MF. Botulinum toxin: Historical perspective and potential new indications. Muscle Nerve 1997; Suppl 6: S129-45.

Johnson DE, Lee PL, Lu J, Williams LT. Diverse forms of a receptor for acidic and basic fibroblast growth factors. Mol Cell Biol 1990; 10: 4728-4736.

Jungnickel J, Gransalke K, Timmer M, Grothe C. Fibroblast growth factor receptor 3 signaling regulates injury related effects in the peripheral nervous system. Mol Cell Neurosci 2004; 25: 21-29.

Just I, Wilm M, Selzer J, Rex G, von Eichel-Streiber C, Mann M, Aktories K. The enterotoxin from Clostridium difficile (ToxA) monoglucosylates the Rho proteins. J Biol Chem 1995a; 270(23): 13932-13936.

Just I, Selzer J, Wilm M, von Eichel-Streiber C, Mann M, Aktories K. Glucosylation of Rho proteins by Clostridium difficile toxin B. Nature 1995b; 375(6531): 500-503.

Juzans P, Comella JX, Molgó J, Failee L, Angaut-Petit D. Nerve terminal sprouting in botulinum type A treated mouse levator auris longus muscle. Neuromusc Disord 1996; 6 (3): 177-185.

Kasahara K, Sanai Y. Functional roles of glycosphingolipids in signal transduction via lipid rafts. Glycoconjugate Journal 2000; 17: 153-62.

Kozma R, Sarner S, Ahmed S, Lim L. Rho family GTPases and growth cone remodelling: Relationship between increased complexity induced by Cdc42Hs, Rac1, and acetylcholine and collapse induced by Rho A Lysophosphatidic acid. Mol and Cell Biol1997; 17 (3): 1201-1211.

L'hŏte CG, Knowles MA. Cell responses to FGFR3 signaling: growth, differentiation, and apoptosis. Exp Cell Res 2005; 304: 417-431.

Laurén J, Aireksinen MS, Saarma M, Timmusk T. Two novel mammalian Nogo receptor homologs differentially expressed in the central and peripheral nervous system. Mol Cell Neurosci 2003; 24: 581-594.

Mcgee AW, Strittmater SM. The Nogo-66 receptor: Focusing myelin inhibition of axon regeneration. Trends Neurosci 2003; 26 (4): 193-198.

Miki T, Bottaro DP, Fleming TP, Smith CL, Burgess WH, Chan AM, Aaronson SA. Determination of ligand binding specificity by alternative splicing: Two distinct growth factor receptors encoded by a single gene. Proc Natl Acad Sci U.S.A. 1992; 89 (1): 246-50.

Montecucco C, Rossetto O, Schiavo G. Presynaptic receptor arrays for clostridial neurotoxins. Trends Microbiol 2004; 12 (10): 442-446.

Mukhopadhyay G, Doherty P, Walsh FS, Crocker PR, Filbin MT. A novel role for myelin-associated glycoprotein as an inhibitor of axonal regeneration. Neuron 1994; 13 (3): 757-767.

Niethammer P, Delling M, Sytnyk V, Dityatev A, Fukami K, Schachner M. Cosignaling of NCAM via lipid rafts and the FGF receptor is required for neuritogenesis. J Cell Biol 2002; 157(3): 521-532.

Pan B, Fromholt SE, Hess EJ, Crawford TO, Griffin JW, Sheikh KA, Schnaar RL. Myelin-associated glycoprotein and complementary axonal ligands, gangliosides, mediate axon stability in the CNS and PNS: neuropathology and behavioral deficits in single- and double-null mice. Exp Neurol 2005;195 (1): 208-217.

Park JB, Yiu G, Kaneko S, Wang J, Chang J, He XL, Garcia KC, He Z. A TNF receptor family member, TROY, is a coreceptor with Nogo receptor in mediating the inhibitory activity of myelin inhibitors. Neuron 2005; 45 (3): 345-51.

Pike LJ. Growth factor receptors, lipid rafts and caveolae: An evolving story. Biochimica et biophysica atca 2005; (In press).

Rapraeger AC, Krufka A, Olwinn BB. Requirement of heparin sulfate for bFGF-mediated fibroblast growth and myoblast differentiation. Science 1991; 252 (5013): 1705-1708.

Reuss B, von Bohlen und Halbach O. Fibroblast growth factors and their receptors in the central nervous system. Cell Tissue Res 2003; 313: 139-157.

Schwab ME. Myelin associated inhibitors of neurite growth and regeneration in the CNS. Trends Neurosci1990; 13 (11): 452-456.

Tsui-Pierchala BA, Encinas M, Milbrandt J, Johnson EM. Lipid rafts in neuronal signaling and function. Trends Neurosci 2002; 25(8): 412-416.

Venkatesh K, Chivatakarn O, Lee H, Joshi PS, Kantor DB, Newman BA, Mage R, Rader C, Giger RJ. The Nogo-66 receptor homolog NgR2 is a sialic acid dependent receptor selective for myelin associated glycoprotein. J Neurosci 2005; 24 (4): 808-822.

Yayon A, Klagsbrun M, Esko JD, Leder P, Ornitz DM. Cell surface, heparin-like molecules are required for binding of basic fibroblast growth factor to its high affinity receptor. Cell 1991; 64 (4): 841-848.

Table 4.1. Growth factor receptors tested for toxin binding.

Antibody	P_3 Toxin	P_3 control	P_2 Toxin	P_2 control	S_1 Tox	S_1 Control
LAR					++	++
TRK-B	++	++	++	++	++	+++
ERB-B2	++	++	++	++	+++	+++
ERB-B4	++	++	++	++	++	++
NgR2	+++/+ (73,75)	+/++ (75)*	+ (78) + (75) ++ (65) + (30)*	+ (75)* + (65)*		
FGFR3	+ (50) ++ (75) + (100-120) ++ (250)*	+ (50) ++ (75)	+++ (50) + (75) + (100)	+++ (50) + (75) +/- (100)		

*Denotes bands that demonstrated variable amounts of binding

Figure 4.1A and 4.1B. Initial pull-downs utilizing non-detergent fractionated P_3 (Figure 4.1A), and P_2 (Figure 4.1B) demonstrated variable differences between toxin and control beads when blots were probed with antibodies to NgR2. Molecular weights (kDa) are denoted on the left of each blot. Affinity precipitations of each unfractionated P_2 or P_3 sample are illustrated for comparison due to potential differences in protein localization (see Chapter 2).

Figure 4.1A

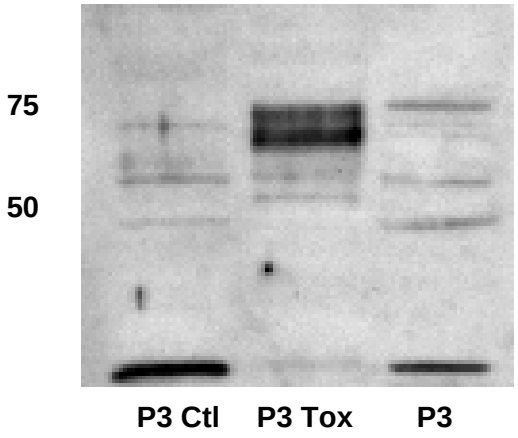

Figure 4.1B.

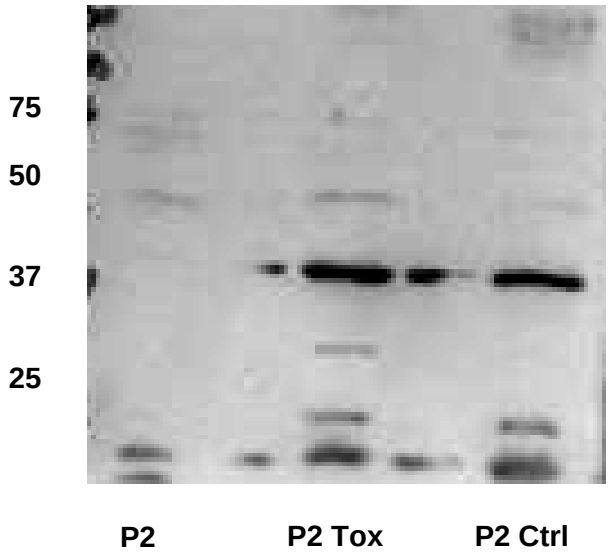

Figure 4.2. Fractionated P_2 and P_3 fractions into Hydrophobic (H_1) and hydrophilic fractions (H_3) utilizing detergent phase separation. These fractions were then incubated with either botulinum toxin coupled beads or uncoupled control beads. Membranes probed with anti-NgR2 demonstrated increased binding of a 75 kDa band in the P_2 H_3 band in toxin coupled beads (n=3). Other bands, such as the 37 kDa in P_2 H_1, were not reproducible.

Figure 4.2.

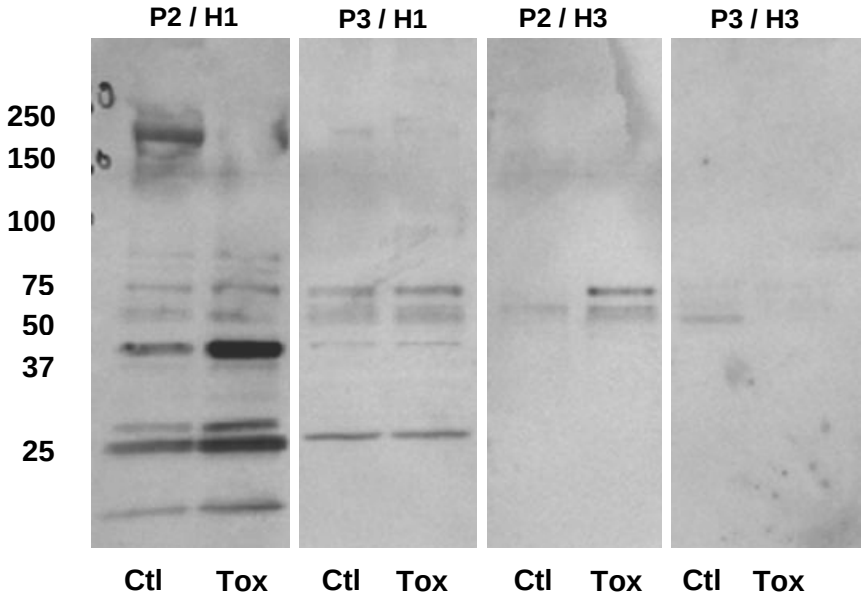
P2 / H1
P3 / H1
P2 / H3
P3 / H3
250
150
100
75
50
37
25
Ctl
Tox
Ctl
Tox
Ctl
Tox
Ctl
Tox

Figure 4.3A and 4.3B. Initial affinity precipitations utilizing non-detergent fractionated P_3 (Fig 4.3A) and P_2 (Fig 4.3B) exposed to toxin and control beads demonstrated variable differences when blots were probed with antibodies to FGFR3. Affinity precipitations of each unfractionated P_2 or P_3 sample are illustrated for comparison due to potential differences in protein localization (see Chapter 2).

Figure 4.3A.

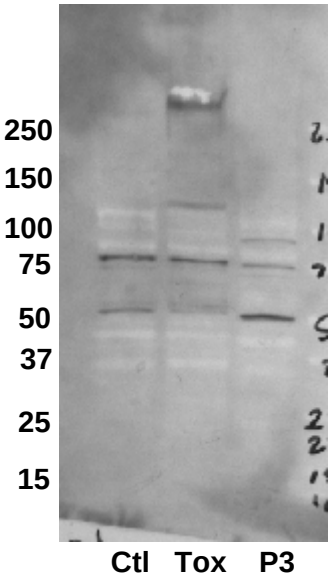

Figure 4.3B.

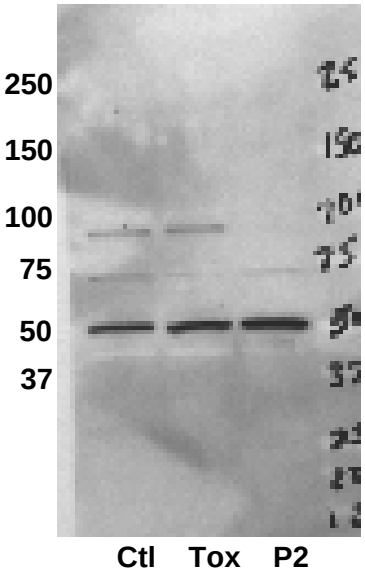

Figure 4.4. Fractionated P_2 and P_3 samples into Hydrophobic (H_1) and hydrophilic fractions (H_3) utilizing detergent phase partitioning. These fractions were then incubated with either botulinum toxin coupled beads or uncoupled control beads. Membranes probed with anti-FGFR3, demonstrated variably increased immunoreactive signal at ~45 kDa in toxin precipitated samples. In this particular blot weak bands at ~100 and 250 kDa were observed that may correlate to previous bands in assays utilizing non-detergent fractionated specimens. Detection of these bands was inconsistent between experiments.

Figure 4.4.

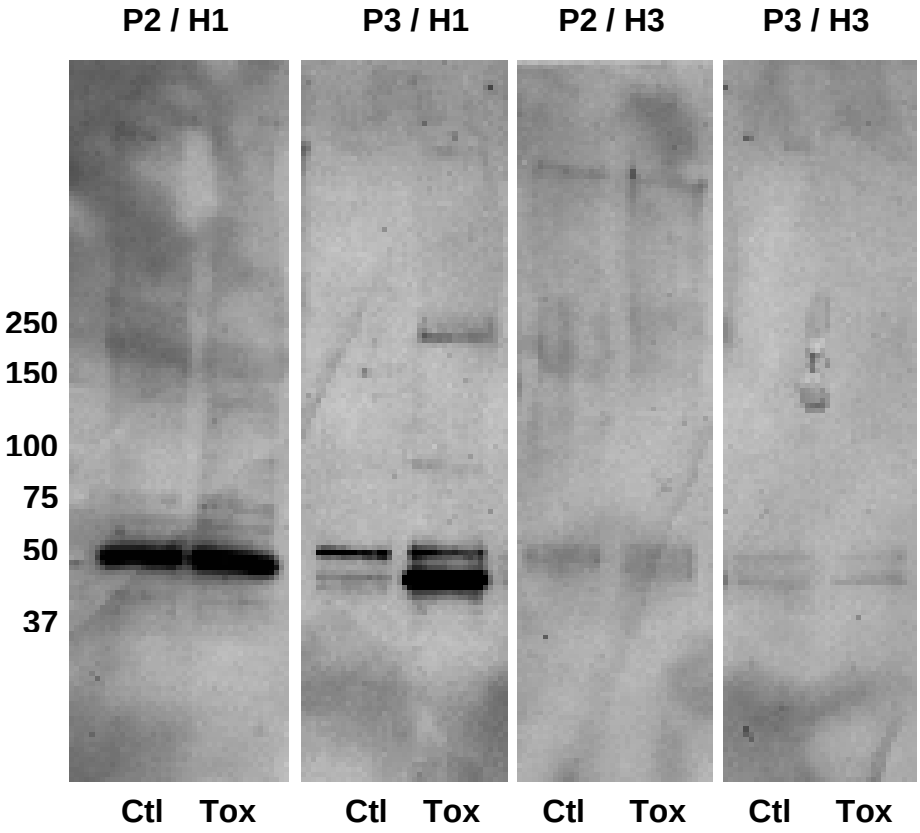
P2 / H1
P3 / H1
P2 / H3
P3 / H3
250
150
100
75
50
37
Ctl
Tox
Ctl
Tox
Ctl
Tox
Ctl
Tox

Figure 4.5A and 4.5B. Graph of RhoA activation following incubation in BoNT/A (4.5A) or MAG (4.5B). Diaphragm preparations were incubated for 30 min in BoNT/A or MAG and then processed for RhoA-GTP affinity precipitation. The x-axis denotes the 3 doses (μg/ml) tested. A minimum of 3 replicates per dose were analyzed, with the exception of MAG doses 1 and 10 where there were 2 replicates each. RhoA activation was measured by densitometric analysis of immunoblots probed with anti-RhoA. Data are represented as a percent of control mean densitometry (± SEM).

Figure 4.5A.

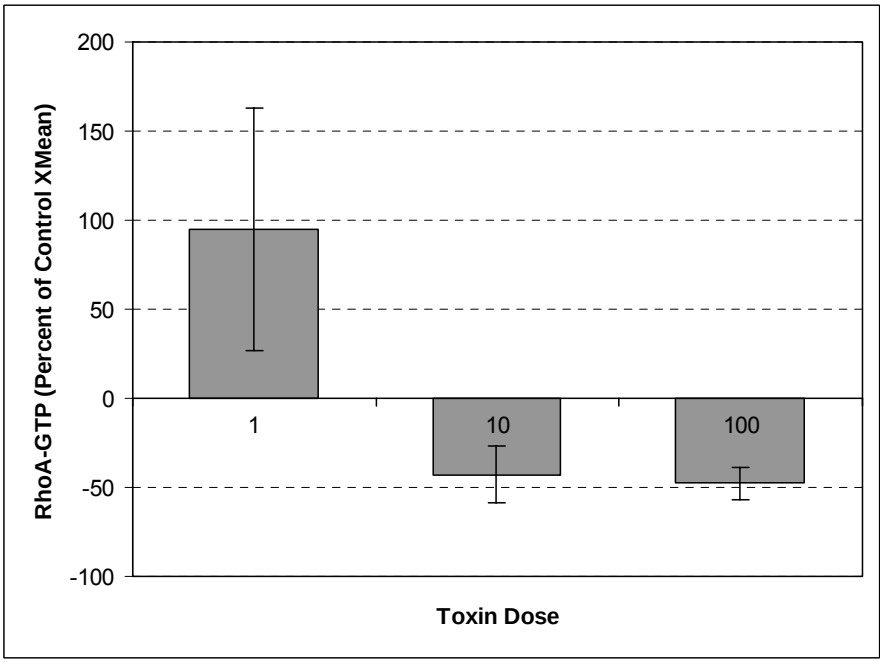

Figure 4.5B.

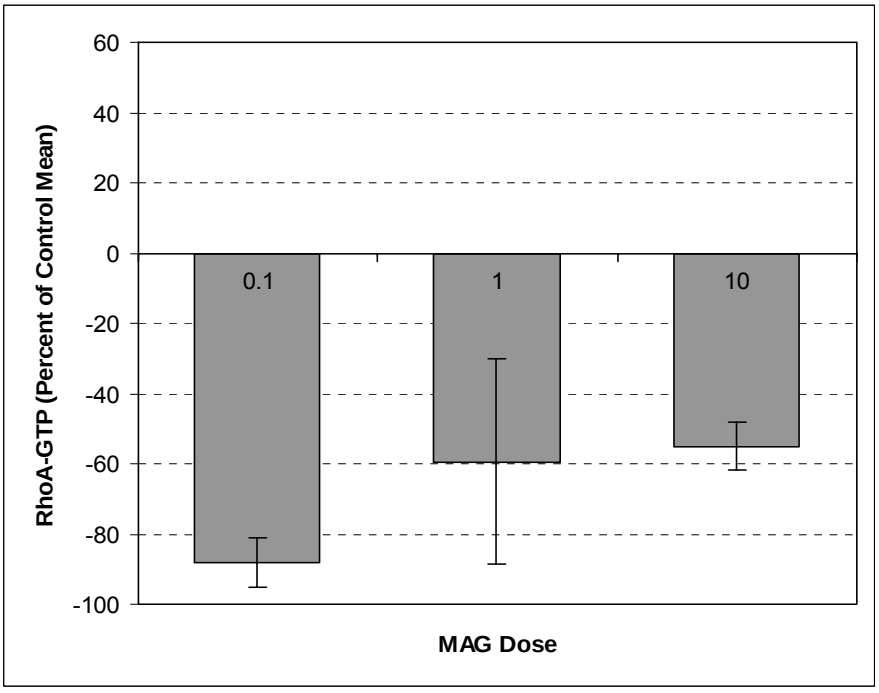

Figure 4.6. Graph of RhoA activation following incubation in MAG only or MAG plus BoNT/A. Diaphragm preparations were preincubated for 10 min in BoNT/A (100 µg/ml) followed by 30 min in MAG (10 µg/ml) and then processed for RhoA-GTP affinity precipitation. Three replicates per treatment were analyzed. RhoA activation was measured by densitometric analysis of immunoblots probed with anti-RhoA. Data are represented as a percent of control mean densitometry (± SEM).

Figure 4.6.

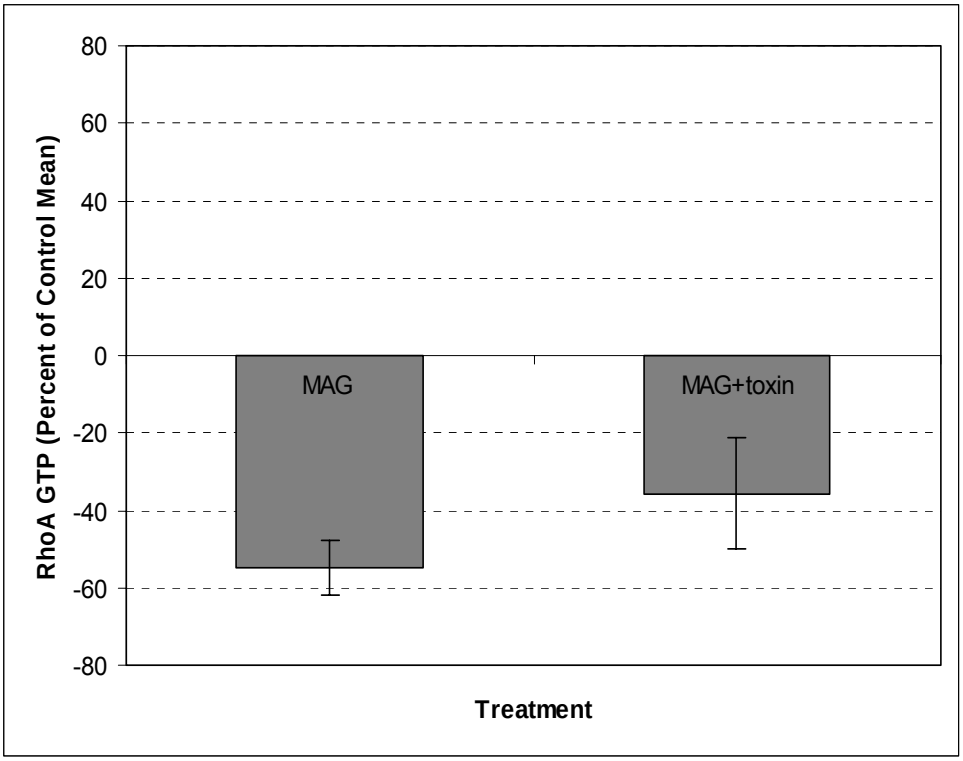
80
60
40
20
0
-20
-40
-60
-80
RhoA GTP (Percent of Control Mean)
MAG
MAG+toxin
Treatment

CHAPTER 5

CONCLUSION

Botulinum toxin serotype A (BoNT/A) causes flaccid muscle paralysis by inhibiting vesicular release of acetylcholine at synapses in the peripheral nervous system (PNS). This occurs through zinc dependent proteolytic cleavage of the SNAp REceptor complex (SNARE) protein SNAP-25. Cleavage of this protein is thought to inhibit the assembly of functional fusion machinery, thereby inhibiting membrane fusion and neurotransmitter release. Simpson (1986) proposed a four step process of toxin action which begins with toxin binding to a high affinity cell surface receptor, followed by internalization through receptor mediated endocytosis. Subsequently, the proteolytic light chain of the toxin translocates across the endosomal membrane and cleaves SNAP-25 (Blasi et al., 1993a; Schiavo 1993a; 1993b).

The identity of the high affinity cell surface receptor has long been in question. Efforts to identify this receptor have been unsuccessful so far, although information regarding many of its characteristics has been collected. First, the high affinity receptor works in tandem with a low affinity ganglioside receptor, possibly as a receptor complex, although the exact relationship is unknown (van Heyningen, 1974a; 1974b; Kitamura et al., 1980; Bakry et al., 1981). Second, this receptor complex may be lipid raft associated, since treatment of nerve cells with cholesterol depleting agents has been shown to inhibit toxin binding (Herreros et al., 2001). Third, the high affinity receptor is both serotype specific and selective for cholinergic nerve terminals (Burgen et al., 1949; Black and Dolly 1986a; 1986b). Fourth, several different proteins have been postulated as receptor candidates, all identified in nontarget tissues by different protein association studies (Schengrund et al., 1993; 1996; Blasi et al., 1992; Li and Singh, 1998). These associations have since demonstrated little functional activity, but can be extrapolated

to show that the toxin may be highly promiscuous in *in vitro* type assays. The ultimate goal of this dissertation was to identify the high affinity receptor for BoNT/A in a physiological relevant target tissue. To achieve this goal, a number of different proteomic approaches were employed to examine toxin protein-protein interactions in the neuromuscular junction-enriched mouse diaphragm.

Synaptosomal proteomics

In previous work in our laboratory, a synaptic membrane preparation from mouse diaphragm was developed to study toxin substrates (Kalandakanond and Coffield, 2001). However charecterization of this preparation as synaptosome-like had not been performed. Hence, we began a study to characterize the proteins in our preparation to determine if this was a synaptosomal preparation. Utilizing mass spectrometry, we characterized a predominance of cytoskeletal and mitochondrial proteins, a few endosomal proteins, but very few neuronal specific proteins. Western blots of these preparations demonstrated the presence of several active zone, SNARE fusion machinery, and post synaptic proteins. Therefore, we are confident that our preparation does represent proteins present at the synaptic cleft.

Initial proteomic studies of the mouse diaphragm synaptic membrane preparation revealed a variable, but unacceptably large, amount of nonspecific binding in affinity precipitation assays using uncoupled amino-link beads. After testing a number of different methods to reduce this nonspecific binding, we hypothesized that the cause was large portions of incompletely solubilized membrane that were binding to the beads through protein interactions. We further hypothesized that the variability was likely due to the amount and type of protein complexes within these segments of bound

membrane. In retrospect, this was not surprising considering the complexity of muscle tissue and the fact that affinity precipitation protocols are developed primarily for cells in culture. Given these concerns, we pursued other methods that would further reduce the complexity of our sample as well as improve protein solubilization. Phase partitioning using temperature sensitive detergents was chosen to fractionate the synaptic membrane preparation into hydrophobic and hydrophilic membrane protein fractions. The procedure chosen used a detergent that forms micelles which allows proteins to retain function during solubilization. Since we were studying functional protein- protein interactions, this was an important consideration.

Botulinum toxin serotype A protein-protein interactions

This dissertation began with a description of the journey of BoNT/A from gut entry to target cell intoxication in an effort to demonstrate how little is known about how toxin moves across cell barriers. Efforts to identify receptors in gut epithelium have not generated any potential candidates, and there is still discussion as to what component of the toxin actually participates in toxin binding and uptake. Since pure toxin has been shown to cross the gut epithelial barrier, what role, if any, do hemagglutinins and non-hemaglutinin components play except in protection of the toxin from enzymatic proteolysis? Does this indicate a role for the pure toxin in functional binding of proteins in the gut epithelial cells, and if so, what proteins are involved in movement of toxin across the barrier. What, if any, protein(s) does the toxin bind to when it is carried through the vascular endothelial cells, especially since some reports regarding macromolecular movement suggest that it may be a function of receptor mediated actin rearrangement to create leaks in the membrane. What protein(s) does the toxin bind to

at the cholinergic nerve terminal membrane, and are binding and receptor mediated internalization the only functional response of that binding? What protein interactions occur during translocation of the light chain through the endosome? Finally, what protein(s) does the toxin interact with as part of the cleavage of SNAP-25, are there proteins involved in targeting the toxin to its substrate?

Obviously, not all of the potential protein interactions revealed by the studies in this dissertation represent an interaction of BoNT/A with its cell surface receptor. In fact, many of the proteins identified are cytoplasmic with no known association with the nerve terminal membrane. Rather, as the questions posed above suggest, it is quite plausible that many of these proteins may eventually be shown to participate in toxin trafficking at multiple levels. For example, the isolation and identification of small heat shock proteins in association with BoNT/A supports the possibility that these proteins are involved in chaperoning the light chain across the endosomal membrane. The strong increase in the membrane associated isoform of GAPDH may be interpreted in a number of ways, especially since there are so many roles being identified for this protein including membrane fusion (Laschet et al., 2004; Tisdale et al., 2004). Although it is too ubiquitous of a protein to be a nerve cell receptor, GAPDH might serve as a receptor for movement of toxin across other membranes. The identification of ubiquitin proteins, while not required for activation and translocation, may suggest that BoNT/A, demonstrates some evolutionary binding characteristics of other AB toxins which require the ubiquitin pathway to escape from the endosome. While it is beyond the scope of this dissertation, these findings of multiple toxin protein-protein interactions

indicate the need for further studies in this arena to clarify the potential role of these proteins in toxin trafficking.

Growth factors and neurogenesis

BoNT/A has demonstrated an ability to induce neurogenesis in tissues that have been intoxicated (Angaut-Petit et al., 1990, de Paiva et al., 1999, Juzans et el., 1996). This response does not seem to be induced by decreased muscle stimulation since this response has not been documented with serotype B treatment. This suggests that the binding of BoNT/A to its high affinity receptor may directly or indirectly activate neurogenesis. It was intriguing then that several conserved domains found in a number of growth factor receptors were identified by MS/MS in toxin affinity precipitations .To pursue this further, the more sensitive Western blot methodology was used to screen precipitated elutions against several known nerve growth factor receptors that are present in the PNS. Through this effort, two different receptors were found to be selectively enriched in certain fractions when exposed to toxin. The significance of this selective enrichment is that it suggests that the toxin interacts with certain proteins only when they are present in one cellular compartment versus another. This further suggests that the toxin may recognize and bind selectively to proteins that only exhibit certain post-translational modifications or compartmentalization.

It was somewhat unexpected that BoNT/A demonstrated specific interactions with two very different growth factor receptor proteins NgR2 and FGFR3. This 'dual' binding may be significant in that NgR2 is a GPI linked protein that is selectively expressed in the PNS and requires an associated signal protein to produce a cellular response; while FGFR3 is non-selectively expressed in many tissues, including the

nervous system, and contains a tyrosine kinase domain. It is possible that these proteins may act as co-receptors. The common thread between these two proteins is that they are both thought to be lipid raft associated, and both have demonstrated interactions with complex gangliosides including the low affinity botulinum toxin receptor GT1b (see review Kasahara and Sanai, 2000; review by Tsui-Pierchala et al. 2002 ; Neithhammer et al., 2002). A plausible sequence of events may be the following. BoNT/A first binds to the low affinity receptor GT1b, which then acts to compartmentalize NgR2 and FGFR3 into functional microdomains forming a receptor complex or array within the membrane that promotes more efficient toxin binding and internalization (Montecucco et al., 2004). In this scheme, NgR2 provides the specificity for the PNS, while FGFR3 and GT1b provide the signal for internalization. Binding of BoNT/A to the NgR2 may lead to a reduction in MAG binding, either directly through competitive blockade or indirectly as a consequence of internalization of the entire toxin receptor complex. The impact of this on RhoA activation would lead to an equilibrium shift in RAC-1, with corresponding changes in the actin cytoskeleton regulating neurogenesis. An interaction of BoNT/A with FGFR3 may lead to activation of several possible pathways including MAPK activation, protein kinase C, or phosphotidyl inositol. Further, since the 78 kDa FGFR3 fragment that bound BoNT/A has been shown to be a degraded form of the receptor, it is possible that this interaction occurs during internalization (Pandit et al., 2002). This mechanism may be used to target the toxin for degradation in the ubiquitin pathway.

With identification of NgR2 as a possible binding protein, we attempted to determine whether treatment of tissues with BoNT/A altered RhoA activity. Since MAG

is the proposed ligand for NgR2 in the PNS, comparisons between MAG activation of RhoA and toxin were pursued. This effort was complicated by the fact that there are no published studies of MAG activity in tissue preparations, only cells in culture; nor are there published works reporting MAG dose-response properties. Although the results from these preliminary studies were inconclusive due to the small sample size and the variability of the RhoA assay, a couple of interesting observations were noted. First, the direction of the effect of the low dose of MAG on RhoA activity was opposite from that generally reported in the literature for the adult CNS. Second, the effect of the low dose of BoNT/A on RhoA activity was opposite that of MAG. These opposing effects are intriguing to consider in light of the differing capacities of the CNS and PNS for regeneration and the ability of BoNT/A to promote neurogenesis.

Future studies

Future research will be needed to determine definitively whether NgR2 and/or FGFR3 participate in the serotype specific binding of BoNT at the neuromuscular junction. Studies to address optimization of the RhoA assay in neuromuscular tissue will be required, including a more thorough examination of MAG dose response properties. Similar studies should be done using in vitro assays to measure downstream effectors of FGFR3 activation. Future research should also include electrophysiologic assessment of the potential antagonism of toxin induced paralysis and substrate proteolysis by ligands such as MAG and/or fibroblast growth factor. In addition, proteomic studies should be extended to purified motor neuronal populations to minimize the methodological problems encountered in the more complex neuromuscular preparation. Collectively, these studies have the potential to either

confirm the proteomic findings presented here or to identify other potential receptor candidates.

REFERENCES

Angaut-Petit D, Molgó J, Comella JX, Faille L, Tabti N. Terminal sprouting in mouse neuromuscular junctions poisoned with botulinum type A toxin: Morphological and electrophysiological features. Neuroscience 1990; 37: 799-807.

Bakry N, Kamata Y, Simpson LL. Lectins from Triticum Vulgaris and Limax Flavus are universal antagonists of botulinum toxin and tetanus toxin. J Pharmacol Exp Ther 1991; 258: 830-836.

Black JD, Dolly O. Interaction of ^{125}I-labeled botlinum neurotoxins with nerve terminals. II. Autoradiographic evidence for its uptake into motor nerves by acceptor mediated endocytosis. J Cell Biol 1996b; 103: 535-544.

Black JD, Dolly O. Interaction of ^{125}I-labeled botlinum neurotoxins with nerve terminals. I. Ultrastructural autoradiographic localization and quantitation of distinct membrane acceptors for types A and B on motor nerves. J Cell Biol 1986a; 103: 521-534.

Blasi J, Chapman ER, Link E, Binz T, Yamasaki S, De Camilli P, Sudhof TC, Niemann H, Jahn R. Botulinum neurotoxin A selectively cleaves the synaptic protein SNAP-25. Nature 1993a; 365: 160-163.

Blasi J, Egea G, Castiella MJ, Arribas M, Solsona C, Richardson PJ, Marsal J. Binding of Botulinum neurotoxin to pure cholinergic nerve terminals isolated from the electric organ of Torpedo. J Neural Transm Gen Sect 1992; 90: 87-102.

Burgen ASV, Dickens F, Zatman LJ. The action of botulinum toxin on neuromuscular junction. J Physiol 1949; 109: 10-24.

de Paiva A, Meunier FA, Molgó J, Aoki JR, Dolly JO. Functional repair of motor endplates after botulinum toxin type A poisoning: Biphasic switch of synaptic activity between nerve sprouts and their parent terminals. Proc Natl Acad Sci USA 1999; 96: 3200-3205.

Herreros J, Ng T, Schiavo G. Lipid rafts act as specialized domains for tetanus binding and internalization into neurons. Mol Biol Cell 2001; 12: 2947-2960.

Juzans P, Comella JX, Molgó J, Failee L, Angaut-Petit D. Nerve terminal sprouting in botulinum type A treated mouse levator auris longus muscle. Neuromusc Disord 1996; 6 (3): 177-185.

Kalandakanond S, Coffield JA. Cleavage of intracellular substrates of botulinum toxin A, C, and D in a mammalian target tissue. J Pharmacol Exp Ther 2001; 296: 749-755.

Kasahara K, Sanai Y. Functional roles of glycosphingolipids in signal transduction via lipid rafts. Glycoconjugate Journal 2000; 17: 153-162.

Kitamura M, Iwamori M, Nagai Y. Interaction between clostridium botulinum neurotoxin and gangliosides. Biochem Biophys Acta 1980; 62: 328-335.

Laschet JJ, Minier F, Kurcewicz I, Bureau MH, Tottier S, Jeanneteau F, Griffon N, Samyn B, Van Beeumen J, Louvel J, Sokoloff P, Pumain R. Glyceraldehyde-3-phosphate dehydrogenase is a $GABA_A$ receptor kinase linking glycolysis to neuronal inhibition. J Neuro 2004; 24(35): 7614-7622.

Li L, Singh BR. Isolation of synaptotagmin as a receptor for types A and E botulinum neurotoxin and analysis of their comparative binding using a new microtiter plate assay. J Nat Toxins 1998; 7: 215-226.

Montecucco C, Rossetto O, Schiavo G. Presynaptic receptor arrays for clostridial neurotoxins. Trends in Microbiol 2004; 12(10): 442-446.

Niethammer P, Delling M, Sytnyk V, Dityatev A, Fukami K, Schachner M. Cosignaling of NCAM via lipid rafts and the FGF receptor is required for neuritogenesis. J Cell Biol 2002; 157(3): 521-532.

Pandit SG, Govindra P, Sasse J, Neame PJ, Hassell JR. The fibroblast growth factor, FGFR3, forms gradients of intact and degraded protein across the growth plate of developing bovine ribs. J Biochem 2002; 361: 231-241.

Schengrund CL, DasGupta B, Hughes CA, Ringler NJ. Ganglioside-induced adherence of botulinum and tetanus neurotoxins to adducin. J Neurochem 1996; 66(6): 2556-2561.

Schengrund CL, DasGupta BR, Ringler NJ. Ganglioside GD3 enhances adherence of botulinum and tetanus neurotoxins to bovine brain synapsin. Neurosci Letters 1993; 158: 159-162.

Schiavo G, Rosseto O, Catsicas S, Delaureto PP, DasGupta BR, Benefenati F, Montecucco C. Identification of the nerve terminal targets of botulinum toxin serotype A, serotype D, and serotype E. J Biol Chem 1993a; 268: 23784-23787.

Schiavo G, Santucci A, Dasgupta BR, Mehta PP, Jontes J, Benfanati F, Wilson MC, Montecucco C. Botulinum neurotoxins A and E cleave SNAP-25 at distinct COOH terminal peptide bonds. FEBS Lett 1993b; 335: 99-103.

Simpson LL. The origin, structure, and pharmacological activity of botulinum toxin. Pharmacol Rev 1981; 33: 155-188.

Tisdale EJ, Kelly C, Artalejo CR. Glyceraldehyde-3-phosphate dehydrogenase interacts with rab2 and plays an important role in endoplasmic reticulum to Gogi transport exclusive of its glycolytic activity. J Biol Chem 2004; 279(52): 54046-54052.

Tsui-Pierchala BA, Encinas M, Milbrandt J, Johnson EM. Lipid rafts in neuronal signaling and function. Trends Neurosci 2002; 25(8): 412-416.

van Heynigan WE, Miller PA. The fixation of tetanus toxin by ganglioside. J Gen Microbiol 1974a; 24: 107-119.

van Heynigan WE. Gangliosides as membrane receptors for tetanus toxin, cholera toxin and serotonin. Nature 1974b; 249: 415-417.